



ACIBADEM MEHMET ALI AYDINLAR UNIVERSITY
INSTITUTE OF HEALTH SCIENCES

**THEORETICAL AND EXPERIMENTAL STUDIES ON THE
STRUCTURE AND DYNAMICS OF THERMOSTABLE
ENZYMES IN NON-AQUEOUS MEDIA**

MOHAMED GAMAL MOHAMED ABEL AZIZ SHEHATA
PH.D. THESIS

DEPARTMENT OF MEDICAL BIOTECHNOLOGY

SUPERVISOR

Assoc. Prof. Dr. Emel Timuçin

ISTANBUL-2021



ACIBADEM MEHMET ALI AYDINLAR UNIVERSITY
INSTITUTE OF HEALTH SCIENCES

**THEORETICAL AND EXPERIMENTAL STUDIES ON THE
STRUCTURE AND DYNAMICS OF THERMOSTABLE
ENZYMES IN NON-AQUEOUS MEDIA**

MOHAMED GAMAL MOHAMED ABDEL AZIZ SHEHATA
PH.D. THESIS

DEPARTMENT OF MEDICAL BIOTECHNOLOGY

SUPERVISOR
Assoc. Prof. Dr. Emel Timuçin

ISTANBUL-2021

DECLARATION

I declare that this thesis work is my own work, I had no unethical behavior at any stages from the planning to the writing of the thesis, I obtained all the information in this thesis in accordance with academic and ethical rules, I cited all the information and comments that were not obtained with this thesis work, and I provided resources in the list of references. I also declare that there was no violation of any patents and copyrights during the study and writing of this thesis.

22.11.2021

Mohamed Gamal Mohamed Abdel Aziz Shehata

PREFACE AND ACKNOWLEDGMENTS

Firstly, I would like to express my sincere gratitude to my advisor Assoc.Prof. Emel Timuçin for her continuous support, patience, motivation, and immense knowledge. Her guidance helped me in all the time of research and writing of this thesis. I could not have imagined having a better advisor and mentor for my Ph.D. study.

My sincere thanks also go to Prof. Uğur Sezerman whose office door was always open for me whenever I ran into a trouble or needed help. I also would like to thank Assoc.Prof. Günseli Bayram Akçapınar and Asst. Prof. Perinur Bozaykut Eker for being in my thesis committee and for their insightful comments and discussions during my thesis progress meetings.

I also wish to convey my gratitude to my host researchers during my Ph.D., Dr. Alessandro Venturini at the Italian National Research Council in Italy, Prof. Marcel Swart and Prof. Silvia Osuna at Girona University in Spain, and Prof. Bert de Groot and Dr. Wojciech Kopec at Max Planck Institute for Biophysical Chemistry in Germany.

I would also like to thank my friends; Prof. Rania Morsi, Dr. Aişe Ünlü, Dheeraj Prakaash, Christian Seitz, Ismail Erol, Sümeyye Akçelik, and Dr. Farzaneh Jalalypour.

A special thanks to my parents. Words cannot express how grateful for all of the sacrifices that you've made on my behalf. Your prayer for me was what sustained me thus far.

A very special gratitude goes to my wife, friend and my strength Nour Alnajjarine for her love, patience, and support. I shall always love you till infinity and beyond.

Lastly, I want to thank me for believing in me, for doing all this hard work, for having no days off, for never quitting, for always being a giver and trying to give more than I receive, for trying to do more right than wrong, and for just being me at all times.



TABLE OF CONTENTS

DECLARATION.....	iii
PREFACE AND ACKNOWLEDGMENTS.....	iv
TABLE OF CONTENTS.....	vi
LIST OF ABBREVIATIONS AND SYMBOLS	viii
LIST OF FIGURES	x
LIST OF TABLES	xv
ÖZET.....	1
ABSTRACT	2
1 INTRODUCTION.....	3
2 BACKGROUND	6
2.1 Biocatalysis: A very Long History and A promising Future	6
2.2 Lipases.....	7
2.2.1 Background.....	7
2.2.2 Structure	8
2.2.3 Reactions	9
2.2.4 Catalytic mechanism.....	10
2.2.5 Interfacial activation.....	10
2.2.6 Selectivity	11
2.2.7 Lipases in industry	13
2.2.8 Thermoalkalophilic lipases.....	16
2.3 Lipases in Non-aqueous Media	18
2.3.1 Lipases in organic solvents.....	18
2.3.2 Lipases in deep eutectic solvents.....	23
2.3.3 Lipases in surfactants	28
3 MATERIALS AND METHODS	33
3.1 Computational Methods	33
3.1.1 Structures.....	33
3.1.2 Systems generation.....	33
3.1.3 Data analysis and visualization.....	36
3.2 Experimental Methods	36
3.2.1 BTL2 lipase expression and purification	36
3.2.2 Lipase activity assays	37
3.2.3 Lipase stability assays.....	37

4	RESULTS	38
4.1	Lipase in Organic Solvents.....	38
4.1.1	Stability of lipase backbone in organic solvents	40
4.1.2	Fluctuations of lipase backbone in organic solvents	41
4.1.3	Compactness of lipase structure in organic solvents	43
4.1.4	Solvent accessible surface area of lipase structure in organic solvents...	44
4.1.5	Essential dynamics analysis of lipase in organic solvents.....	45
4.1.6	Correlation of lipase motions in organic solvents	45
4.1.7	Stability of lipase catalytic machinery in organic solvents.....	46
4.1.8	Stability of the lipase critical salt bridges in organic solvents	50
4.1.9	Interactions between lipase and organic solvents	52
4.1.10	Conformational change of Phe17 in organic solvents.....	53
4.1.11	Experimental validation of lipase stability in organic solvents.....	54
4.2	Lipase in deep eutectic solvents	57
4.2.1	Stability of lipase backbone in different reline formulations.....	59
4.2.2	Flexibility of lipase backbone in different reline formulations.....	60
4.2.3	Compactness of lipase structure in different reline formulations	62
4.2.4	Solvent accessible surface area of lipase in reline formulations	63
4.2.5	Essential dynamics of lipase in different reline formulations	64
4.2.6	Contact maps analysis of lipase in different reline formulations	65
4.2.7	Identification of lipase regions stabilized in reline.....	68
4.2.8	Stability of lipase catalytic machinery in reline formulations	70
4.2.9	The effect of water and temperature on lipase-reline interactions.....	74
4.2.10	The effect of hydration level on reline nanostructure.....	76
4.3	Lipase in sodium dodecyl sulfate	83
4.3.1	Stability of lipase backbone in SDS	85
4.3.2	Compactness of lipase structure in SDS.....	87
4.3.3	Investigation of lipase dynamics in SDS	88
4.3.4	Investigation of SDS-induced lipase interfacial activation.....	94
4.3.5	Investigation of lipase-SDS interactions.....	99
4.3.6	Effect structural dimerization on lipase stability in SDS	107
5	DISCUSSION	109
5.1	Lipase in Organic Solvents.....	109
5.2	Lipase in Deep Eutectic Solvents	112
5.3	Lipase in Sodium Dodecyl Sulfate	116
6	CONCLUSION.....	120
7	REFERENCES.....	122
8	CURRICULUM VITAE.....	138

LIST OF ABBREVIATIONS AND SYMBOLS

ΔG	Gibbs Free Energy
μM	Micromolar
μS	Microsecond
\AA	Angstrom
COM	Center of Mass
DCCM	Dynamic Cross Correlation Maps
DES	Deep Eutectic Solvents
ED	Essential Dynamics
FS	Femtosecond
$G.CM^{-3}$	Gram per Cubic Centimeter
G/L	Gram per Litre
K	Kelvin
KDA	kilodalton
M	Molar
MD	Molecular Dynamics
MG	Milligram
ML	Milliliter
NM	Nanomolar
NPT	Isothermal–Isobaric Ensemble
NS	Nanoseconds
NVT	Canonical ensemble
PC	Principal Component
PCA	Principal Component Analysis
PDB	Protein Data Bank
Q1	Fraction of Native Contacts
RDF	Radial Distribution Function
RG	Radius of Gyration
RMSD	Root Mean Square Deviation
SASA	Solvent Accessible Surface Area
SDS	Sodium Dodecyl Sulfate

V/V Volume/Volume
W/V Weight/Volume



LIST OF FIGURES

Figure 1. Two different views of the aligned crystal structures of the closed (1KU0) and the open (2W22) conformations of thermoalkalophilic lipases. The lid domain is coloured in blue. The β -flap region is coloured in red. Top panel shows the top side of the catalytic cleft and bottom panel shows the top view of the cleft.	38
Figure 2. Pairwise sequence alignment of the closed and open states of lipase.	39
Figure 3. RMSD analysis of the open and closed conformations of lipase in different solvents.....	40
Figure 4. RMSF analysis of the open and closed conformations of lipase in different solvents.....	41
Figure 5. Flexibility of the open and closed states of lipase at 450 K.	42
Figure 6. Rg analysis of the open and closed conformations of lipase in different solvents.....	43
Figure 7. SASA analysis of the open and closed conformations of lipase.	44
Figure 8. Essential dynamics of lipase conformations in different solvents.....	45
Figure 9. DCCMs of lipase conformations in different solvents.	46
Figure 10. Distances between the catalytic triad of lipase at 310 K.	47
Figure 11. Rg of the catalytic machinery of lipase conformations in different solvents.	48
Figure 12. Distances between the catalytic triad of lipase at 450 K.	49
Figure 13. Stability of the open conformation critical salt bridges.....	51
Figure 14. RDF analysis between the center of mass of lipase and solvent molecules.	52
Figure 15. Change in residue Phe17 side chain conformation in different solvents..	53
Figure 16. Effect of different organic solvents on BTL2 lipase activity.	56
Figure 17. Snapshots of the equilibrated systems before MD simulations. The circled illustrations represent a closed-up view of a licorice representation of the solvent molecules (choline: cyan, urea: blue, chloride: yellow, and water: red).....	58

Figure 18. RMSD of lipase backbone atoms. (A) and (B) shows simulations replicates. For all figures, the reference structure was set as the last frame of the equilibrium simulation. (water: blue, 8M Urea: red, pure reline: black, water:reline (30:70): green, water:reline (70:30): orange).....	59
Figure 19. Pairwise RMSD plots of lipase backbone C-alpha atoms. (A) and (B) shows 310 and 373 K simulations respectively. For both subfigures, top and bottom panels show open and closed conformations, respectively	60
Figure 20. RMSF analysis of lipase backbone in different reline formulations. (A) and (B) show replicate simulations.....	61
Figure 21. Rg analysis of lipase backbone in different reline formulations.	62
Figure 22. Change of lipase SASA analysis of in different reline formulations.....	63
Figure 23. Scree plots of the PCA of production trajectories showing the first five principal components.	64
Figure 24. Plots of the top two principal components. Top panel indicates the closed structure and bottom panel indicates the open structure. the red color represents 310 K simulations and black color represents high 373 K simulations.....	65
Figure 25. Contact map analysis of lipase at 310 K. Blue points indicates the initial contacts that were lost after the simulations while red points indicate those that formed after simulations.	66
Figure 26. Contact map analysis of lipase at 373 K.....	67
Figure 27. Residue contribution to the first two principal components. The shaded regions corresponding to the β -flap domain, N terminal, and the lid region mark the highest contributions.	69
Figure 28. Reduced trajectory of the 310 K simulations. N-terminal region (purple), B-flap domain (red) and the lid region (blue).	70
Figure 29. Reduced trajectory of the 373 K simulations. N-terminal region (purple), B-flap domain (red) and the lid region (blue).	70
Figure 30. Rg of the catalytic machinery of lipase.	71
Figure 31. Distances between the catalytic triad C-alpha atoms at 310 K.....	72
Figure 32. Distances between the catalytic triad C-alpha atoms at 373 K.....	73
Figure 33. COM-RDF analysis of lipase and solvents.....	74
Figure 34. Number water molecules in close contact with any of the catalytic site. .	75

Figure 35. Number urea molecules in close contact with any of the catalytic site. ...	76
Figure 36. COM-RDF analysis of reline molecules around the open conformation at (A) 310K and (B) 373 K.	77
Figure 37. COM-RDF analysis of reline molecules around the closed conformation at (A) 310K and (B) 373 K.	78
Figure 38. Atomic RDF analysis of reline components.	79
Figure 39. Normalized hydrogen bonds count between urea and choline.	80
Figure 40. Normalized hydrogen bonds count between urea and chloride.	81
Figure 41. Normalized hydrogen bonds count between urea and urea.	81
Figure 42. Normalized hydrogen bonds count between urea and water.	82
Figure 43. Normalized hydrogen bonds count between lipase and reline.	82
Figure 44. Snapshots of the MD systems were shown after 10 ns of equilibration. Water oxygen: blue CPK, SDS: licorice (C: tan, S: yellow, O: red), open lipase backbone: blue cartoon, closed lipase backbone: red cartoon.	84
Figure 45. All-to-all RMSD plots of lipase backbone atoms in different SDS concentrations. For both subfigures, top and bottom panels show close and open conformations, respectively.	86
Figure 46. Rg (solid lines, left y axis) and SASA (dotted lines, right y axis) (blue-298 K, red-373 K) analyses of all systems.	88
Figure 47. RMSF analysis based on C α fluctuations throughout 2 μ s. The lid domain and its neighboring β -flap is shaded by purple and orange respectively.	89
Figure 48. Residue loading onto the first two principal components (pcs) obtained from PCA. The lid domain and its neighboring β -flap is shaded by purple and orange respectively.	89
Figure 49. Scree plots showing the variance explained by the first 5 pcs for all systems.	90
Figure 50. Reduced trajectory of the highly fluctuating two regions that are shaded in purple (the lid domain) and in orange (β -flap domain). The time dependence of the trajectory is color-scaled; 0-white, 2 μ s-black. The crystal structures are illustrated with the two highly fluctuating regions in surface representation. Top two rows indicate the open lipase systems and the bottom two show the closed systems. Arrows used to indicate the ordered lid movements comparable to those during activation.	91

Figure 51. Time-dependent change in the first two pcs, (B) Scatterplots of the first two pcs (x,y; pc1, pc2), (C) Representative conformations showing the initial and the final conformations that were obtained as the snapshots of the time-points shown by colored vertical lines in (A) and dots in (B). Red color indicates the start of the simulation and the blue color the end of the simulation.	93
Figure 52. Fraction of native contacts analysis.	94
Figure 53. Catalytic Tunnels determined in (A) The Crystal structure of the open and closed conformations, (B) Simulated systems at 298K, (C) Simulated Systems at 373K. Structures showing non-catalytic tunnels were shaded in grey.	96
Figure 54. Number of SDS molecules occupied within the catalytic cleft.	98
Figure 55. The distribution of the number of SDS contacts (< 5 Å) with the entire lipase, the lid domain (169-239) and the β-flap (270-320) were illustrated by box-plots for (A) the open and (B) closed conformations. For both (A) and (B), top panel shows the absolute number of SDS atom contacts and the bottom panels shows the number of SDS molecules.	100
Figure 56. Structural visuals extracted from every 660 ns. Protein structures were rendered by surface views while SDS molecules were rendered by VdW spheres (C: tan, S: yellow, O: red)	100
Figure 57. Number of SDS contacts with protein. Bars in yellow show number of SDS head contacts; bars in brown shows SDS tail contacts.	102
Figure 58. Snapshots of SDS assemblies from SDS simulations at 373K in the absence of lipase	102
Figure 59. Snapshots from every 200 ns of simulations of (A) 20-SDS and (B) 180-SDS containing systems were visualized. Lipase structures were rendered by surface representation, SDS molecules were shown by its headgroup (S: yellow, O: red) and tail (C: tan). For clarity waters and ions were not shown.	103
Figure 60. COM-RDF analysis of protein and SDS (left) and SDS-SDS (right). ...	104
Figure 61. Analysis of hydrogen bonds formed between SDS and lipase; left Y-axis shows raw count of hydrogen bonds while right Y-axis shows normalized hydrogen bonds count	106
Figure 62. RMSF analysis of chain A of 1KU0 lipase in monomeric state simulation (black) and in dimeric state simulation (blue).	108
Figure 63. Comparison of hydrophobic content of bulky amino acids (W, F, Y) between CALB and thermoalkalophilic lipase structures.	115

Figure 64. Comparison of the β -flap domain flexibility in 1KUO and 2DSN lipases.
..... 118



LIST OF TABLES

Table 1. Details of lipase simulated systems in organic solvents.	34
Table 2. Details of lipase simulated systems in deep eutectic solvents.	34
Table 3. Details of lipase simulated systems in sodium dodecyl sulfate	35



ÖZET

Termokararlı enzimlerin susuz ortamlardaki yapı ve dinamikleri üstüne teorik ve deneysel çalışmalar

Termoalkalofilik lipazlar, çok yönlü reaksiyonları kataliz edebilen endüstriyel potansiyele sahip termostabil enzimlerdir. Bu enzimlerin sulu olmayan ortamlarda nasıl davrandığının anlaşılması, kimya endüstrisindeki uygulamalarını güçlendirilmesine ve zorlu endüstriyel koşullar için kararlı lipaz varyantlarının akılcı tasarımına katkıda bulunabilir. Buna dayanarak, bu tez çalışmasında, sulu olmayan ortamlardaki termoalkalofilik lipazlarla ilgili üç ayrı çalışmaya yer verilmiştir. İlk olarak, organik çözücülerin lipaz aktivitesi ve stabilitesi üzerine olan etkisi araştırıldı. Kısaca, moleküler dinamik (MD) simülasyonları ile, polar çözücülerin düşük sıcaklıkta lipaz dinamiklerini iyileştirdiği, polar olmayan çözücülerin ise yüksek sıcaklıklarda lipazı önemli ölçüde stabilize ettiği gösterildi. Bu gözlemler, düşük sıcaklıkta polar çözücülerde yüksek lipaz aktivitesi ve yüksek sıcaklıkta polar olmayan çözücülerde geliştirilmiş termostabilite olarak belirlenmiştir. İkinci olarak, derin ötektik çözücülerdeki (DES'ler) su içeriğinin lipaz yapısı üzerindeki etkileri incelenmiştir. MD simülasyonları ile, saf DES'in lipazı yüksek oranda stabilize ettiği, DES'e su ilavesinin ise lipaz dinamiklerini iyileştirdiği gösterilmiştir. Özellikle, yüksek oranda sulu DES ortamında, yüksek sıcaklıkta lipaz katlanmasına olumsuz etkileri olmuştur. Son olarak, anyonik deterjan sodyum dodesil sülfatın termoalkalofilik lipazların arayüzey aktivasyonu üzerindeki etkisi araştırıldı. MD simülasyonları, simülasyon sıcaklığından bağımsız olarak SDS'nin lipazı aktive ettiği gözlenmiştir. Yüksek SDS konsantrasyonlarında, SDS misel oluşturmayı tercih ederek lipaz ile etkileşim göstermemiştir. Ayrıca, yüksek sıcaklıklarda bile SDS'in lipazı denature etmediği görülmüştür. Son olarak, lipaz dimerik yapısının, özellikle yüksek sıcaklıkta yapısal stabiliteyi güçlendirdiği belirlenmiştir.

Anahtar Sözcükler: Lipazlar, Protein stabilitesi, Moleküler dinamik simülasyonlar, Susuz ortam, Biyokataliz.

ABSTRACT

Theoretical and Experimental Studies on The Structure and Dynamics of Thermostable Enzymes in Non-Aqueous Media

Thermoalkalophilic lipases are thermostable enzymes that carry a paramount industrial potential owing to the versatility of their catalyzed reaction. Understanding how these enzymes behave in non-aqueous environments can potentiate their implementation in chemical industry and contribute to the rational design of highly stable lipase variants for extreme industrial conditions. On the ground of this, here we report the results of three studies of thermoalkalophilic lipases in non-aqueous media. Firstly, the effect of organic solvents on lipase activity and stability was investigated. Briefly, molecular dynamics (MD) simulations showed that polar solvents improved lipase dynamics at low temperature, while non-polar solvents significantly stabilized lipase at elevated temperatures. These observations were reflected in high lipase activity in polar solvents at low temperature and improved thermostability in non-polar solvents at high temperature. Secondly, the effects of water content in deep eutectic solvents (DESs) on lipase structure was studied. MD simulations showed that pure DES highly stabilized lipase, while hydrating DES improved lipase dynamics. Notably, highly hydrated DES had negative impacts on the overall fold of lipase particularly at high temperature. Lastly, we investigated the effect of the anionic detergent sodium dodecyl sulfate on the interfacial activation of thermoalkalophilic lipases. MD simulations showed that regardless of the simulation temperature, SDS achieved lipase activations. At high SDS concentrations, SDS prefers to form micelles and ceases to interact with lipase. Furthermore, no lipase denaturation was noted in SDS even at high temperature. Finally, lipase dimeric structure was found to potentiate structural stability particularly at elevated temperature.

Keywords: Lipases, Protein stability, Molecular dynamic simulations, Non-aqueous media, Biocatalysis.

1 INTRODUCTION

Biocatalysis is recognized as a strong alternative for the conventional organic synthesis methods in chemical industry. A wide range of chemical products, ranging from fine chemicals such as pharmaceuticals intermediates to bulk chemicals such as biodiesel can be accessed by enzyme catalyzed reactions in an environmentally benign manner (1). The immense potential of biocatalysis in industry is a reflection of the advantageous properties of enzymes including high chemo-, regio- and enantioselectivity, biodegradability, operation under mild conditions, and catalytic promiscuity (2). However, the application of biocatalysis in chemical industry is limited by the fact that enzymes evolved to work in water (3). Although water is the solvent of cellular environments, it is a very poor solvent for synthetic chemistry (4). Only few synthetic substrates are soluble in water and most of the industrially attractive reactions occur exclusively in non-aqueous media. This made the search for an alternative reaction media for enzymatic reactions inevitable. The first attempts of introducing alternative media for enzymatic catalysis can be tracked back to the seminal work of Klivanov and co-workers in 1980's (5). In contrast to the common wisdom at that time, their findings showed that enzymes can function in neat organic solvent. Moreover, enzymes were found to acquire new desired properties in organic solvents such as enhanced thermal stability and improved selectivity (3). However, these improved properties in neat organic solvents came at the price of enzymatic activity. Moreover, high concentrations of organic solvents lead to denaturation of most of enzymes. Therefore, a complete understanding of enzymes stability mechanisms in organic solvents is required to avoid the drawbacks of utilizing them in these unnatural solvents.

Molecular dynamics (MD) simulations is an efficient approach that enable investigating the behavior of biomolecules at the atomistic level. Thus, using a combination of molecular dynamics simulations and experiments, the first chapter of this thesis aims to address the molecular impact of different organic solvents on the stability and dynamical equilibrium of lipase enzymes. Lipases are an optimal choice for such a study since their high stability enabled us to explore protein dynamics at

extreme conditions of organic solvents and temperatures, both computationally and experimentally. Moreover, lipases carry paramount industrial potential and have been already applied in manufacturing of many valuable products such as oleochemicals, biofuels, detergents, and pharmaceuticals (6).

Given the hazardous nature of organic solvents which is against the green concept of biocatalysis, a new generation of solvents known as deep eutectic solvents (DESs) have emerged recently as a green alternative for organic solvents (7). DESs are superior to organic solvents because of their promising characteristics such as non-toxicity, non-flammability, biodegradability, ease of preparation, and low cost (8, 9). DESs were applied in enzymatic reactions for the first time by Kazlauskas and coworkers in 2008 when they utilized them in lipase-catalyzed reactions (10). Since this pioneer work, several successful examples of utilizing DESs in biocatalysis have been reported (11, 12). Despite the promising potential of DESs in biocatalytic applications, preparation of these solvent is still a challenging task. For example, the high viscosity of pure DESs was found to have drastic effect on the enzymatic activity (13). Similarly, over-dilution of DESs lead to a complete inhibition of enzymatic activity in some cases (14). Hence, one would expect water to be a key factor in tailoring DESs for biocatalytic applications. Although many abiotic studies tried to account for DESs problems by investigating their physiochemical properties, many questions need to be answered at the atomistic level. For instance, what are the effects of water on DESs nanostructure? How pure DESs and their water binary mixtures affect protein activity and thermostability? Aiming to answer these questions, in the second chapter of this study we used molecular dynamics simulations to delineate the structure and dynamics of lipases in choline chloride/urea-based DES and its water binary mixtures. This chapter comprises one of the most comprehensive analyses of lipases in DESs owing to its longer MD time-scales than those used in literature and also because we allocated both equilibrium conformations of lipases in our simulations (15, 16).

Over the past decade, an increasing number of studies have investigated protein-surfactants interaction. The major focus of these studies was the anionic surfactant

sodium dodecyl sulfate (SDS) which is arguably the most used surfactant in biochemistry labs specifically in electrophoresis and crystallization experiments (17-20). Protein-SDS interactions are often detrimental to protein structure and usually unfold proteins, however, lipases can tolerate high concentrations of this very aggressive surfactant (19, 21, 22). Furthermore, low concentrations of SDS were shown to induce lipase activation (23). Given these encouraging implications, in the third chapter of this thesis, we studied lipase-SDS interactions at the molecular level. This chapter comprises the longest molecular dynamics (MD) simulations of lipases ever. Moreover, it is the first study that allocates both lipase equilibrium conformations for molecular dynamics simulations in SDS.

Altogether, the experimental and computational insights gained from this thesis work shed the light on the stability mechanisms of lipases; the most applied enzyme group in industry; in three distinct types of non-aqueous media. Understanding these mechanisms not only paves the way for improving the implementation of lipases in industrial applications, but also it represents a strong base for engineering new lipase variants for optimal operation in non-aqueous media.

2 BACKGROUND

2.1 Biocatalysis: A very Long History and A promising Future

Millions of years of evolution have resulted in an unimaginable number of enzymes to regulate the metabolic pathways and chemical reactions in living cells. Inspired by nature, for thousands of years, humans have utilized enzymes and whole cells in many industrial applications. This process is known as biocatalysis and currently defined by scientists as the process of using pure enzymes or whole cells in chemical transformation of a molecular substrate to a new product (24). The first application of biocatalysis in industry can be tracked back to 7,000 years ago when the Egyptians used it to make their cheese, the Sumerians to brew their beers, and the Chinese to prepare their alcoholic beverages (25). Over all these years, enzymes have been applied in biocatalysis in their raw form without any modification of their naturally evolved properties. However, a new era of biocatalysis started 45 years ago with the emergence of game changer technologies such as recombinant protein production, site-directed mutagenesis, structural genomics and the invention of polymerase chain reaction (PCR) (26). This revolution in biotechnology techniques made the process of enzymes production fast, simple, and economically viable. Thanks to these technologies, currently, a gene encoding an enzyme of interest can be mined from genomic databases, synthesized, transformed to a host microorganism, and produced at industrial scale in a few weeks (27). Therefore, biocatalysis has evolved to be a strong competitor to the conventional organic synthesis methods and it has been integrated in manufacturing of many chemical products (28-30). From the enantioselective synthesis of fine chemicals such as pharmaceuticals intermediates to the production of bulk chemicals such as oils, detergents, and biodiesel; a wide range of chemicals can be accessed by biocatalysis in an environmentally benign manner (1, 31-36). The widespread of biocatalysis implementation in industry can be attributed to numerous factors. First, unlike conventional metal catalysts which are hazardous and energy consuming, enzymes are non-hazardous, non-toxic, biocompatible, biodegradable, and can operate at mild conditions (37). Moreover, they can catalyze chemical reactions with very high chemo-, regio- and enantio- selectivity which is very

advantageous for organic synthesis (2). Additionally, some enzymes are catalytically promiscuous meaning that they can catalyze chemical transformations beyond their natural function (38). Second, the economic burden of biocatalysis has decreased with the ability to optimize the stability, activity, and specificity of enzymes for the target reaction by directed evolution (39-44). Furthermore, the progress in enzyme immobilization approaches also rendered biocatalysis more cost effective by enabling the reusability of enzymes in multiple reactions and enhancing their operation and storage stabilities (45). Third, multi-step chemical reactions can be achieved by biocatalysis in a single processing step since enzymes can simultaneously catalyze cascade of reactions in the same pot under the same conditions (46). Altogether, it is not surprising that the biocatalysis market value in 2020 is 10.6 billion USD, and it is anticipated to reach 14.9 billion USD by 2027 (47).

2.2 Lipases

This chapter is dedicated to gives an overview of the structure, function, and industrial applications of lipase enzymes.

2.2.1 Background

Lipids are a keystone in the chemistry of life. Many organisms store energy in the form of water-soluble lipids such as triglycerides. In order to metabolize these lipids and release chemical energy, they produce lipases, enzymes that are capable of hydrolyzing lipids to their principal components, glycerol and fatty acids (48). Lipases (EC 3.1.1.3), also known as triacylglycerol acyl hydrolases, are group of enzymes that belong to a subclass of serine hydrolases and act on carboxylic ester bonds. They were first discovered nearly 100 years ago by Christiaan Eijkman when he reported that several bacteria express and secrete lipases to their extracellular environments (49). Christiaan Eijkman also isolated the first lipases from *Bacillus fluorescens*, *Bacillus prodigiosus*, and *Bacillus pyocyaneus*, respectively (50). Since this pioneering work, innumerable lipases have been isolated from other sources including microorganisms, plants, and animals.

In addition to their natural substrates, triglycerides, lipases are versatile enzymes that can accommodate a broad range of substrates including bicyclic, alicyclic, aliphatic, and aromatic esters (48). Consequently, depending on the reaction medium used, they catalyze a broad range of chemical reactions such synthesis and hydrolysis of esters, esterification, transesterification, amidation, and thioesterification reactions (51-54). Moreover, they are known to be promiscuous enzymes, meaning that they can catalyze reactions beyond their natural function (55, 56). Lipase, in contrast to most of enzymes, are stable in non-aqueous media. As a result, they have been utilized in various industrial application including detergents, biodiesel production, (oleo)chemistry, and organic synthesis (49, 57, 58).

2.2.2 Structure

The first lipase structure was solved by X-ray crystallography in 1990 (59). Since then, hundreds of lipases crystal structures have been obtained from different sources such as bacteria, fungi, and animals. The analysis of all lipase structures that have hitherto been solved showed that all lipases share common structural properties. All lipases share a common α/β hydrolase fold in which the structure is formed by a central β sheets and connected together by α helices (60, 61). The catalytic machinery is highly conserved among lipases and is formed by a catalytic triad and Oxyanion hole. The catalytic triad consist of a serine acting as a nucleophile, a histidine, and an acidic residue which is either aspartate or glutamate (62, 63). The catalytic serine is found in a highly conserved γ -like pentapeptide turn (Gly-X-Ser-X-Gly) which is known as nucleophilic elbow (62). On other hand, the oxyanion hole is formed by the backbone amide groups of two residues, the first is located between β -strand and α -helix while the second is located at the nucleophilic elbow on the C-terminus of the catalytic serine (64).

Another common structural feature among most of lipases is an amphiphilic lid covering the catalytic site (59, 65). This lid is composed of α -helix sequence that vary in length among lipases and connected to the structure by a flexible domain. For example, it is composed of only 5 residues in guinea pig lipase while it consists of 70

residues in *Bacillus thermocatenuatus* lipase (66, 67). In spite of these common structural features, there are subtle variations in the geometry of the binding sites among lipase (68). The substrate binding sites of lipases were studied by Pleiss et al. and were classified based on their geometry into three groups; funnel-like, crevice-like, and tunnel-like binding sites (68). These differences in the geometry of binding site accounts for the diverse substrate specificity and selectivity among different lipases.

2.2.3 Reactions

Naturally, lipases catalyze the hydrolysis of triglycerides into their basic components, glycerol and fatty acids. However, they are also active against wide range of substrates such as aliphatic, aromatic and cyclic esters (48). Regardless of the substrate type, the hydrolysis reaction occurs at an interface where the substrate is dissolved in the hydrophobic phase. This process is an equilibrium reaction meaning that it can be controlled by changing the concentration of the reactants or products. Water as a reactant, plays a critical role in determining the direction of this reaction. For example, lowering the water content in the reaction medium shifts the reaction towards ester synthesis (69). As a result, lipases are capable of catalyzing esterification and transesterification reactions as well. It also worth mentioning that lipase substrates are not limited only to carboxylic esters, but also includes activated amines and thioesters which considerably expand their potential in synthetic chemistry (48). Lipases are also promiscuous enzyme that can catalyze the reactions of other evolutionary related enzymes such as cutinase, cholesterol esterase, amidase, and phospholipase (70). Moreover, they can catalyze other non-evolutionary related reactions such as Michael addition and epoxidation of phenolic compounds and fatty acids (71, 72).

2.2.4 Catalytic mechanism

As pointed earlier, the catalytic triad is highly conserved in all lipases and comprises a serine, a histidine, and an acidic residue (aspartate/glutamate) (62, 63). The catalytic mechanism in lipases is initiated by a hydrogen bond formation between the histidine and the acidic residue. This hydrogen bond increases the pKa of the imidazole nitrogen in histidine rendering it a strong general base that capable of deprotonating the catalytic serine. The deprotonated serine, with increased nucleophilicity, attacks the carbonyl carbon atom of the substrate forming the first tetrahedral intermediate which is stabilized later in the oxyanion hole. Then, the tetrahedral intermediate breaks down into an acyl enzyme intermediate and an alcohol. Similarly, another tetrahedral intermediate corresponding to the highest energy state in the reaction is formed. This tetrahedral intermediate breaks down to a free (deacylated) enzyme and an acid.

2.2.5 Interfacial activation

Lipases have been classified as esterases until 1958 when Sarda and Desnuelle reported that the activity of lipases is higher on aggregated substrates such as micellar solutions or emulsions than on monomeric substrates (73). This feature is not compatible with esterases which act on water soluble substrates. Thus, this unique behavior has been mysterious until the first two lipase structures were solved in 1990 (59, 65). These two structures were solved in active form and showed a conformational change of the lid domain covering the active site. The comparison between lipase structures and cocrystals of substrate analogues suggested that this conformational change is due to a contact of the lid domain with oil/water interface. This mechanism of catalysis was identified later as interfacial activation. Following this seminal work, this phenomenon was studied by a plethora of studies that provided ample amounts of information on the macroscopic characteristics of lipase catalysis (74-76).

Indeed, such a unique catalytic behavior accounts for the deviation of lipases from Michaelis-Menten kinetics which depend on the assumption that both substrate and

enzyme are dissolved in the same phase. This model cannot be applied to interfacial enzymes such as lipases. Two mathematical models were hitherto proposed to model the kinetics of lipase interfacial activation. The first model proposed by Verger et al. suggested a reversible adsorption of soluble lipase on the oil interface leads to a formation of more favorable energy state of lipase and after this, the kinetics fits into the classical Michaelis-Menten model (75). Then, lipase-substrate complex is formed and followed by the products formation. On the other hand, Martinelle and Hult proposed the second model which is based on the assumption that the lipase exists in dynamical equilibrium between open and closed conformations in solution (77). When lipase encounter the interface the lid domain is adsorbed to the oil phase and the equilibrium is shifted toward the open form. The main difference between these two models is that after product release, lipase return the bulk solution in case of the second model while it stays at the interface in case of the first model.

2.2.6 Selectivity

The preference of lipases to catalyze a given reaction is based on three distinct types of selectivity: substrate-selectivity, enantio-selectivity, and regio-selectivity. The basis of these selectivity types is explained in detail below.

2.2.6.1 Substrate-selectivity

Substrate-selectivity refers to the preference of an enzyme to a given substrate. Two factors were found to be associated with lipase substrate-selectivity. First, the type of the substrate. Lipases were found to have higher selectivity towards primary alcohols than tertiary alcohols (76). Additionally, lipases were reported to be more active toward the aggregated (insoluble) substrates than the monomeric (soluble) substrates (68). The second factor associated with lipase-substrate selectivity is the chain length of the substrate acyl group. Several studies have shown that, unlike esterases, lipases with very few exceptions have higher selectivity toward medium and long chain (C4-C16) than short chain fatty acids (63, 78-80). This distinction from esterases in substrate specificity is a reflection of the architecture of the substrate

binding pocket in lipases. In contrast to esterases which have small substrate binding sites, lipases have large hydrophobic substrate binding sites which enable them to accept long chain esters (68). Lipases were also reported to be active toward a wide range of substrates other than carboxylic esters such as activated amines and thioesters, which boosts their potential in synthetic chemistry considerably (81).

2.2.6.2 Regio-selectivity

In organic chemistry, regio-selectivity refers to the preference of a given catalyst to attack at one out of several possible bonds in the compound (82). Regio-selectivity in lipases refers to their ability to discriminate between the positions of ester linkages in triglycerides. Some lipases catalyze the reaction at the acyl position *sn*-1 or/and *sn*-3 and referred as 1,3-specific lipases. These lipases partially hydrolyze triglycerides free fatty acids, monoacylglycerols and/or diacylglycerols. Most of 1,3-specific lipases are isolated from microbial sources such as *Rhizomucor endophyticus*, *Rhizopusoryzae*, *C. antarctica*, *Aspergillus niger*, *Y. lipolytica*, *T. lanuginosus*, and *Bacillus thermocatenuatus* (63, 83-87).

On the other hand, there are non-specific lipases which are capable of catalyzing the reaction at all of the acyl positions, *sn*-1,2 and 3. They can catalyze complete hydrolysis of triglycerides to free fatty acids and glycerol. Examples of non-specific lipases includes those from *P. fluorescens*, *Staphylococcus aureus*, *B. cepacian*, *C. viscosum*, and *B. glumae*, and *C. rugosa* (63, 81, 88). It's also worth mentioning that there are very few lipases that are regio-specific only to *sn*-2 acyl position such as those isolated from *Geotrichum sp. FO401B* and *Staphylococcus* (89, 90).

Finally, some lipases were reported to be regio-specific only to fatty acids that have a long-chain and double bonds between the atoms C9 and C10. These lipases are known as fatty acid regio-specific lipases and produced from ungerminated oat seeds and *Geotrichum candidum* (91, 92).

2.2.6.3 Enantio-selectivity

In synthetic organic chemistry, enantio-selectivity refers to the preference of a given reagent or catalyst to form enantiomer (stereoisomer) of a chiral molecule over another. Lipases were reported to exhibit enantio-selectivity in their catalyzed reaction. Indeed, this is not surprising since their natural substrates, triacylglycerols, usually have a chiral center in their alcoholic part. Enantio-selectivity were found to vary among lipases. For instance, although most of the microbial lipases show moderate enantio-selectivity toward the substrate trioctanoin, two microbial lipases from *Pseudomonas aeruginosa* and *Pseudomonas sp.* exhibit high enantio-selectivity toward the same substrate (93).

Enantio-selectivity was also found to differ for the same lipase among different substrates. For example, *C. antartica* lipase B has a high preference toward *sn*-1 position of the substrate trioctanoin which changes to *sn*-3 when the substrate is triolein (94). Lipases enantio-selectivity was also reported to be dependent on other factors such as reaction medium and temperature (95). Lastly, the ability of lipases to distinguish between the enantiomers of various substrates is of great importance particularly in the production of chirally pure compounds which are the building blocks on pharmaceutical industry.

2.2.7 Lipases in industry

Lipases are considered as the most applied enzymes in industry. The global market of lipases has reached USD 600 million and is expected to increase by 7% during the coming five years (47). This paramount industrial potential of lipases is owing to their high stability in non-aqueous media, high thermostability, enantio- and regio-selectivity, catalytic promiscuity, wide range of substrates, and their ability to catalyze reactions without the need for the expensive cofactors (50). The next sections shed the light on the most important industrial applications of lipases.

2.2.7.1 Lipases in food industry

Lipases, particularly those isolated from microbial sources, have been utilized widely in manufacturing of several dairy products such as cheese, butter, oils, baby food formulations, and flavoring agents (96, 97). Lipases have been also used as emulsifiers to improve the quality of baked food and as additive to enhance animal feeding products (98). Finally, they have been utilized in the production of low-calorie fats and structured lipids (99).

2.2.7.2 Lipases in detergents industry

One of the most successful examples of lipases industrialization is their usage as additives in the formulations of detergents to facilitate the removal of fat and oil stains (99). In 1988, Novozymes was the first company to commercialize lipases in detergents industry when they introduced their product Lipolase which is a lipase isolated from *Humicola lanuginosa* (99). The same company later engineered three variants of this product with improved properties. Today, lipases are used in almost every detergent formulation. The reason behind this success is the ability of lipases to function at alkaline pH and high temperature and their high stability against the ingredients of detergents such as oxidants, surfactants, and complexing agents (100). Lastly, lipases have been utilized in the production of high quality soap at low cost through the hydrolysis of different fats and oils (48).

2.2.7.3 Lipases in pharmaceuticals and medical industry

Chirality is a key element in drug development. Therefore, obtaining enantio-pure molecules is of great importance for pharmaceutical industry. Lipases as they can resolve racemic mixtures and form enantio-pure compounds have been utilized in the manufacturing process of several drugs. For example, enantioselective esterification catalyzed by *C. antarctica* lipase has been used to produce the anti-inflammatory drug Ibuprofen (101). The same lipase has been also utilized in the preparation of chiral intermediates used in the production of anti-Alzheimer's drugs (102). *C. cylindracea*

lipase has been also used to resolve racemic mixture to produce Baclofen which is a muscle relaxant and a pain killer drug (103).

Another lipase from *G. candidum* was used in the stereoselective synthesis of the anticholesterol drug BMS-188494 (102). Similarly, other lipases have been used in the production of various drugs such as Taxol for cancer treatment, Diltiazem to prevent high blood pressure, and Deoxyspergualin as immunosuppressive agent (104-106). Finally, the high stereospecificity of lipases play a critical role in preventing toxicity in drug synthesis since in the synthesis of chiral molecules, only one enantiomeric form show bioactivity, whereas the other one is often toxic (107).

Apart from chiral synthesis of drugs, lipases specifically those isolated from plants have been used as digestive aids to treat digestive allergies and gastrointestinal disturbances (108). Lipases have been also commercially used in the production of vitamins and anti-obese drugs (102, 109). Another medical application of lipases is their usage diagnostic tools for different infections and diseases such as Acute pancreatitis (110).

2.2.7.4 Lipases in biodiesel production

Biodiesel has emerged as alternative type of fuel because of the limited resource of conventional fossil fuels and their economic and environmental burden. Biodiesel is basically produced by the transesterification of animal and vegetable oils with alcohols. Since lipases can catalyze transesterification reactions efficiently, they have been applied in biodiesel production. Most of the lipases used in biodiesel production are immobilized enzymes because they are cheaper than soluble lipases and maintain enhanced activity and stability. For example, the immobilized lipase from *P. cepacia* have been used in the transesterification of soybean oils with alcohol for biofuel production (111).

Similarly, the commercial lipases Lipozyme IM and Novozym 435 which are also immobilized enzymes have been utilized in the same reaction but in a solvent-free

medium. On the other hand, the immobilized *C. antartica* have been used in the production of biofuels from different sources such as vegetable and cooking waste oils (112). Lastly, lipases have been also used in the production of various additives to decrease the viscosity of biofuels (50).

2.2.7.5 Lipases in pulp and paper industry

Pitch control is a critical process in paper and pulp production. Pitch is the hydrophobic components of the wood which must be removed before processing the raw lumber to paper. Several lipases such as those produced from *C. rugosa* and *Pseudomonas* have been applied in paper industry to hydrolyze triglycerides and wax contained in raw lumber (113). In addition to their role in pitch control, lipases also improve whiteness and intensity of paper, decrease pollution of wastewater, limit chemicals usage, increase equipment life, and reduce the cost (102).

2.2.7.6 Lipases in textile industry

In textile industry, lipases have been used to help in removing the size lubricants. This process improves the fabric absorbency which results in enhanced dyeing levels. Lipases have been also used to minimize the cracks and streaks frequency in denim systems (102).

2.2.8 Thermoalkalophilic lipases

Extremophiles are the organisms that capable of tolerating extreme environmental conditions. They have been under intense scrutiny during the past two decades to understand the metabolic enzymes and structural proteins responsible for their unique properties. Most of these efforts have been focused on the isolation of extremozymes to employ them in industrial biocatalysis. Among these extremozymes are the lipases isolated from thermoalkalophilic species. These lipases are very attractive for industrial biocatalysis due to their high stability against proteases, chaotropic agents,

organic solvents, and surfactants. Moreover, they can operate at elevated temperatures and alkaline pH (114).

Thermoalkalophilic lipases have been isolated from several thermophilic bacterial strains such as *Bacillus thermocatenulatus*, *Bacillus stearothermophilus*, *Bacillus thermoleovorans*, and *Bacillus sp.* (16, 66, 115, 116). The size of thermoalkalophilic lipases is between 40–45 kDa which is significantly higher than the size of other microbial lipases which is usually less than 35 kDa (16). The reason behind the high molecular weight of thermoalkalophilic lipases is that they have an extra zinc binding domain which does not exist in other lipases families (16). This zinc domain was recognized later to be responsible for the high thermostability of thermoalkalophilic lipases.

All characterized thermoalkalophilic lipases were found to share about 95% sequence identity. They also show 30–35% sequence homology with the lipases isolated from *Staphylococcus* strains (16). Therefore, both staphylococcal and thermoalkalophilic lipases were combined together in group known as lipase family I.5 (117). In spite of this classification, thermoalkalophilic lipases show biochemical properties distinct from staphylococcal lipases. For instance, contrary to staphylococcal lipases which function optimally at low pH and temperature, thermoalkalophilic lipases operate optimally at elevated temperatures (60-75 °C) and alkaline pH (8-10) (118-120). Thus, *Staphylococcus* lipases were re-assigned to another lipase family known as family I.6 (49).

Thermoalkalophilic lipases are also characterized by a high hydrophobic amino acid content. For example, the two thermoalkalophilic lipases (BTL1 and BTL2) isolated from *Bacillus thermocatenulatus* were found to have 39.4% and 33.2%, respectively (115). The high hydrophobic content in these lipases accounts for their very high tendency to form highly molecular weight aggregates (750 kDa) formed by tens of lipase monomers (121). Furthermore, the ability of thermoalkalophilic lipases to be strongly activated by various surfactants such as Triton X-100, cholate, and CHAPS is attributed to their very hydrophobic nature (121). Altogether, the unique

properties of thermoalkalophilic lipases have made them a hot topic for structural biology investigations and industrial biocatalysis studies (122, 123).

2.3 Lipases in Non-aqueous Media

Non-aqueous media has been shown to be more efficient and advantageous for lipase catalyzed reactions compared to aqueous media. The following sections discuss the basic aspects of lipases catalysis and stability in three distinct types of non-aqueous media: organic solvents, deep eutectic solvents, and ionic surfactants.

2.3.1 Lipases in organic solvents

2.3.1.1 Background

For a long time, biochemists have believed that enzymes denature in organic solvents and operate only in aqueous media. Therefore, they have been skeptical of employing any solvents other than water in biocatalytic reactions. This concept was based on the theory that protein folding occurs in water and results in a hydrophobic core and hydrophilic surface of the protein. Thus, using organic solvents would disturb this arrangement and leads to a drastic decrease in stability and activity. Furthermore, they were misled by the fact that enzyme naturally works in aqueous environments. This common wisdom was dramatically changed after the groundbreaking publication of Zaks and Klibanov in 1984 on lipase stability in organic solvents (5). In this study they showed that porcine pancreatic lipase becomes highly active and extremely thermostable after several hours of heating at 100 °C in organic solvents. Following this seminal publication, the same group published two more studies in which they showed that different lipases such as mold and yeast lipases as well as other enzymes such as alpha-chymotrypsin and subtilisin also becomes more active and stable in organic solvents (124, 125). These landmark reports gained the attention of both industry and academia and were followed by a plethora of reports on improved stability and activity of different enzymes in organic solvents.

2.3.1.2 Advantages of lipase catalysis in organic solvents

Organic solvents are superior to water as a reaction media in lipase catalyzed reaction in many aspects. Most of lipase substrates are water-insoluble which often results in a diminished reaction rate. Therefore, using organic solvents enhance substrate solubility and extend lipases substrates to include new possible ones beyond those are insoluble in water. Moreover, due to their high volatility and low boiling point, organic solvents enable easier product recovery and higher reaction yields than water. They also inhibit side reactions, protect against proteolysis, and prevent microbial contamination (125). Another important advantage of using organic solvents in lipase-catalyzed reactions is that they render the esterification reaction thermodynamically favorable which is more desired reaction in organic synthesis than hydrolysis. Furthermore, most of the industrially attractive lipase reactions such as aminolysis, transesterification, and thioesterification occurs exclusively in organic solvents (126).

Regio- and enantio- selectivity of lipases are very valuable utilities for the enantioselective organic synthesis. The selectivity of lipases was found to vary dramatically upon switching from water to organic solvents and among organic solvents themselves (126). Indeed, this provides a tremendous opportunity to fine-tune the reaction medium for the target product. Such a strategy is termed as medium engineering and has been reported by several studies (127). For example, the enantiomeric ratio of the racemic esters hydrolysis catalyzed by *Bacillus subtilis* lipase was reported to be 16-fold higher in organic cosolvent than in water (128). In line with this example, the E-value of the enantioselective ester hydrolysis catalyzed by *Candida antarctica* lipase was reported to increase from 7 to 220 upon using polar organic cosolvents (129). Similar examples of significant enhancements in the enantioselectivity of different lipases upon shifting to organic solvents have been documented by several studies (130-136).

2.3.1.3 Lipases pH memory in organic solvents

The pH of reaction medium is one of the most influential factors that affects the enzymatic activity. This effect has no meaning in lipase reactions performed in organic media because enzymes maintain a “pH memory” of their last aqueous solution pH (124, 125). Consequently, lipase enzymatic activity in organic solvents can be not only protected from drastic pH changes, but also enhanced if lipases are lyophilized at their optimal pH (124, 125, 137).

2.3.1.4 Practical applications of lipase reactions in organic solvents

Given the advantages of lipase catalysis in organic solvents, it has been employed efficiently in the synthesis of industrially valuable products. For example, the enantioselective butanolysis in organic solvents catalyzed by yeast lipase was utilized in the synthesis of 2-halo-propionic acids which are used as intermediates in the production of several herbicides and pharmaceuticals (138). Such an important reaction is thermodynamically unfavorable in water because it decreases the resolution by increasing the racemization (138). Given the high yield of this reaction, it was scaled up for multikilogram level by the Austrian company Chemie Linz AG (126). Yeast lipase was also utilized in the asymmetrical acetylation of diols in organic solvents to for Azol synthesis which is used as antifungal agent. This process was also scaled up to kilogram level production by the American company Schering-Plough (139).

Asymmetric acylation for chiral amine synthesis is another industrially appealing example of lipase catalysis which takes place exclusively in organic solvents (124). Chiral amines are very important for pharmaceutical industry as they are used to inhibit monoamine oxidase. Therefore, they are used to treat several neurological diseases such as hyperactive syndrome, Alzheimer, Parkinson, depression, and memory loss (140). This reaction was commercialized and scaled up to multi-ton level by the German pharmaceuticals giant BASF (141).

Another interesting area for lipase catalyzed reactions in organic media is the modification and synthesis of industrially important polymers. For instance, optically active polyesters were produced through enantioselective polycondensations catalyzed by lipase in organic media (142). The physicochemical properties of the produced polymers were found to significantly depend on the reaction medium (142).

Currently, several companies including Pfizer, Sepracor, and Bristol-Myers Squibb are using lipase-catalyzed reactions in organic media for the production of a broad range of fine chemicals (143).

2.3.1.5 Challenges of lipase catalysis in organic solvents

Notwithstanding the advantages offered by organic solvents as a reaction media for lipase-catalyzed reactions, they suffer from several drawbacks that limit their industrial potential. Organic solvents are not environmentally friendly as they are toxic, volatile, non-biodegradable, hazardous, and flammable (27). Moreover, they produce large amount of chemical waste which is also considered as an environmental burden. Organic solvents are also laborious and expensive which increases the cost of lipase reactions.

Additionally, some organic solvents such as small alcohols may inhibit lipases by binding to their active sites (144). Despite the high stability of lipases in neat organic solvents, they usually exhibit lower activity due to the limited structural flexibility in such unnatural environment. In order to overcome this problem, water is usually used as a lubricant to increase the structural mobility of lipases. However, the amount of water in such case must be optimized carefully since adding extra amount of water may lead to extra mobility and eventually to protein denaturation. Furthermore, high water content may also shift lipase reactions from synthesis to hydrolysis which is not industrially desired. Therefore, a detailed understanding of lipases stability and activity in organic solvents is required not only for better implementation of lipases in such non-natural environment, but also to guide protein engineering studies in designing new lipase variants with enhanced stability and activity.

2.3.1.6 Molecular dynamics simulations of lipases in organic solvents

Molecular dynamics (MD) simulations is an efficient approach to investigate the structure and dynamics of biomolecular systems at the atomistic level. MD simulations have been utilized extensively to understand the determinantal effects of organic solvents on protein structure such as high conformational rigidity, loss of catalytic water from protein vicinity, binding of solvents to the catalytic site, and structural denaturation (4, 42, 141, 145).

A plethora of studies have investigated the stability of lipases in various organic solvents. For instance, Peters et al. studied the dynamics of *Rhizomucor miehei* lipase in water and in different organic solvents (146). Their findings indicated that lipase conformational mobility differs among solvents. They also provided insights on the substrate binding mechanism to the active site of lipase. Another investigation by Ramakrishnan et al. showed that the lid domain dynamics in *Candida rugosa* lipase depend on the solvent type and the pH of the reaction medium (147). Trodler et al. also simulated the flexibility of *Candida antarctica* lipase B in five distinct organic solvents and in water (148). Their results showed that lipase maintain more rigid structure in hydrophobic solvents than in water. They also indicated that the rigidity of lipase in hydrophobic organic solvents is not merely due to the lipase-solvent interaction, but also because of the formation of water network around the lipase structure. The same groups also reported another interesting investigation in which they studied the effect of different solvents on the interfacial activation of three different lipases isolated from *Rhizomucor miehei*, *Candida rugosa*, and *Thermomyces lanuginose*. Their MD simulations of the closed state of the three lipases showed a gradual lid opening in non-polar solvents such as toluene. On the other hand, no lid transition to open state was observed in the simulations of the three lipases in water (149). Another important study was reported by Kulschewski et al. in which they investigated the molecular mechanism of *Candida antarctica* lipase B inhibition by methanol (150). Using MD simulations and experiments they revealed that methanol inhibit lipase by binding to the substrate binding site. Apart from these examples, numerous studies have also utilized MD simulations to answer very critical questions about lipases stability in

organic solvents (151-159). Altogether, the insights gained from these studies have improved our understanding of lipase stability in organic solvents.

Such an improved understanding has led to the development of different medium engineering approaches such as utilizing stabilizing agents to optimize selectivity and activity of lipases in organic solvents (134, 160, 161). On the other hand, it also helped protein engineering studies to design lipase variants with enhanced stability and catalytic activity in organic solvents (162, 163). Lastly, despite the success of the previous MD simulations studies in improving our understanding of lipase stability in organic solvents, several questions need to be addressed in future studies such the role of water content in the medium, relationship between organic solvent stability and thermostability, and the reduced lipase activity in neat non-polar organic solvents.

2.3.2 Lipases in deep eutectic solvents

2.3.2.1 Background

Organic solvents are very efficient reaction media in lipase-catalyzed reactions and have been employed in several industrial applications of lipases. Nonetheless, their non-green characteristics such as high toxicity, high flammability, volatility, high cost, and poor biodegradability limit their potential in biocatalysis (27). Therefore, developing alternative solvents was inevitable to avoid these serious drawbacks of organic solvents usage. Deep eutectic solvents (DESs), a subclass of ionic liquids, have recently emerged as a green and safe alternative to organic solvents (7, 164). DESs are superior to the conventional reaction media because they are non-volatile, non-flammable, non-toxic, and biodegradable (165). Additionally, DESs are more cost-effective in large scale applications than organic solvents since they can be prepared from a broad range of cheap and environmentally friendly precursors which are produced at million-ton level every year (166).

DESs are basically prepared by mixing hydrogen bond acceptors such as quaternary phosphonium and ammonium salts or metal halides with hydrogen bond donors such as polyols, alcohols, amides, and carboxylic acids with continuous heating until a

homogeneous liquid is formed (167). Interestingly, DESs remain liquid even after cooling down the reaction to ambient temperatures which is due to a formation of extensive network of strong intermolecular hydrogen bonds between their components (168). DESs were developed for the first time by Abbot et al. in 2001 and since then, hundreds of DESs formulations have been reported (9). Reline which is one of the most widely utilized DESs formulation is a typical example of the sustainability of these unique solvents. Reline is simply produced by mixing urea and choline chloride at molar ratio 2:1 (169). Both of these components are environmentally friendly and naturally abundant in large quantities and produced in vast amount every year at low cost (170, 171). Overall, combining an environmentally friendly and cheap solvents with powerful and robust biocatalysts like lipases may accentuate the potential of lipases in chemical industry.

2.3.2.2 Lipase catalysis in deep eutectic solvents

After the development of DESs in 2001 by Abbot et al., they were mainly used in electrophoretic deposition (172, 173). The first introduction of DESs to biocatalysis was reported by Kazlauskas et al. 7 years later when they used DESs as a reaction medium in lipase-catalyzed ethyl valerate transesterification (10). Their findings showed high conversion rates in different DESs formulations than in organic solvents. Following this pioneering work, several successful examples of transesterifications and esterifications catalyzed by lipases in DESs have been reported (11-13, 165, 174).

The success of using DESs in lipase reactions is not limited to enhanced reaction rates but it also includes better medium engineering approaches. For instance, several studies have shown that glycerol-based DESs are optimal reaction media for lipase-catalyzed biodiesel production because they allow an easy product purification procedure since the reaction side-product glycerol can be easily separated to the DES phase (175-179). Furthermore, DESs were shown to act as water sink in esterification reactions and thus, it achieves high conversion rates by preventing the reaction equilibrium from shifting to the hydrolysis direction (180). For example, the esterification activity of *Candida antarctica* lipase B was found to be 200-fold higher in DESs than in organic solvents (12).

Another interesting application of DESs in lipase reactions is their ability to serve as both solvent and substrate at the same time. For instance, sugar-based DESs have been applied in glycolipids synthesis as 2-in-1 medium in which sugar acted as a substrate and a component of DES (181). Moreover, by using this system the poor solubility of sugars in organic solvent can be avoided. Such a reaction media also allows tailoring glycolipids by changing the sugar part of the DES.

Apart from the natural reactions catalyzed by lipases, DESs have been also used as a reaction medium in the promiscuous reactions of lipase. For example, a glycerol-based DESs was recently used as a solvent in the porcine pancreas lipase-catalyzed C–C bond formation between acetone and 4-nitrobenzaldehyde. Interestingly, 82% substrate conversion was achieved in DES compared to only 8% in toluene (182). Similarly, using DESs as solvent in the synthesis of the antimicrobial agent dihydropyrimidin-2(1H)-ones catalyzed *Rhizopus Oryzae* lipase was found to decrease the reaction time by more than 50% compared to organic solvents and achieve 95% reaction yield (183).

2.3.2.3 Challenges of lipase catalysis in deep eutectic solvents

The water content in DESs formulations is one of the major challenges in applying them in lipase-catalyzed reactions. DESs formulations are highly viscous in their pure form and such high viscosity limits the structural mobility of lipases and dramatically reduce their catalytic activity. Water is usually added to DESs formulation to serve as a lubricant to improve lipases structural flexibility. Therefore, the yield of lipase-catalyzed reactions is highly dependent on the water content in DESs formulations (13). For instance, Durand et al. evaluated the effect of the water content in reline on the substrate conversion in the lipase-catalyzed transesterification of methyl p-coumarate (13). They reported 0% substrate conversion in pure reline which increased to 20% upon adding 2% (w/w) water to reline. Moreover, 100% substrate conversion was achieved by increasing the water content in reline to 10–20% (w/w). Such an example may mislead the reader by implying that increasing the water content in DESs always enhances the reaction yield of lipases which is not true. Several abiotic studies have shown that increasing the water content in DESs to a certain level disturb their

nanostructures and alter their physicochemical properties which may result in a drastic decrease in lipase activity. For instance, Guajard et al. reported 60% increase in the Novozyme 435 lipase-catalyzed monobenzoate glycerol synthesis by adding 8-20% (v/v) water to DES (14). Surprisingly, adding more water decreased the reaction yield dramatically. Therefore, preparing aqueous solutions of DESs formulation for lipase reaction should be tailored carefully to avoid any negative effects of water (184-188).

Another important challenge in applying DESs in lipase reactions is the possible competition between the components of DESs and the substrate for the desired reaction which may result in serious effects on the reaction yield. For instance, alcohols- and acids-based DESs components were found to compete with the substrate in the *Candida antarctica* lipase-catalyzed alcoholysis reactions leading to the formation of side products and destruction of the DES nanostructure (10, 11). Moreover, the formed side products were found to increase the DESs viscosity which significantly decreases the lipase activity and makes the reaction medium recycling and stirring process more complicated. Another important factor that should be taken into consideration while choosing DESs for lipase reactions is the chemical nature of the target substrate. Interaction of some substrates with the components of DESs may disturb the DESs hydrogen bonding network and lead to diminished reaction yields. For example, the interactions between the substrate 1-butanol and the DES components in the esterification of acetic anhydride catalyzed by Novo 435 lipase resulted in a significantly diminished reaction yield (174). Another problem in utilizing new DESs formulations in lipase reactions is that the stability and activity of lipases cannot be anticipated in DESs. Therefore, trial and error process is inevitable to choose the proper DES formulation (166).

Altogether, the challenges discussed here are originated from the fact that DESs are a new generation of solvents and the knowledge of their characteristics is still limited. Thus, several efforts are needed to decipher the properties of these promising solvents at the molecular level.

2.3.2.4 Molecular dynamics simulations of lipases in deep eutectic solvents

Notwithstanding the considerable number of studies of lipase catalysis in DESs, all of them are experimental proof-of-concept studies, which just report that a specific lipase reaction can be performed in DESs formulations. Unfortunately, none of these studies could account for the molecular basis of lipases stability and activity in DESs formulations. On the other hand, theoretical approaches such as MD simulations can draw a detailed picture of lipases stability and activity in DESs at the molecular level. Hitherto, MD simulation have been used extensively to investigate the molecular properties of DESs formations, however, the number of studies that investigated the structural stability of different enzymes in DESs is very limited (184-188). To our knowledge, the structural stability of lipases in DESs have been investigated by only two studies (15, 189). Both of the studies simulated *Candida antarctica* lipase (PDB ID: 1TCA) but in two different DESs. The first study was reported by Monhemi et al. in 2014 in which they evaluated the lipase stability in reline. Using MD simulation, they tried to explain why lipase remain stable in reline despite it is composed of 66% urea which is a very common protein denaturing agent. Their simulations showed that in reline, urea cannot diffuse to denature the hydrophobic core of the lipase because it is involved in strong hydrogen bonding network with choline chloride. On the other hand, the second study was reported by Nian and coworkers in 2020 in which they simulated the lipase in betaine:xylitol and chloride:glycerol which are both naturally occurring DESs formulations. Their results suggested that the enhanced stability of the lipase in these two DESs formulations is due to hydrogen bonding between lipase surface residues and DESs components.

Candida antarctica lipase was a good choice for these two studies since it is widely used in industrial biocatalysis (190). Yet, because this lipase has no lid domain, the insights gained from the simulations were limited to the overall stability of lipase without addressing how DESs affect lipase activation. Therefore, future investigation should focus on the lipases that possess lid domain to investigate how different DESs formulations affect the interfacial activation of lipases. Furthermore, future simulations should not be carried out only in neat DESs formulations, but also in

aqueous solutions of DESs to evaluate how water in DESs formulations affect lipase stability in and activity. Additionally, future studies should also investigate the effect of different DESs formulations on lipase thermostability.

Overall, investigating the molecular basis of lipase activity and stability in DESs is a very fertile area of research that can provide many solutions to the challenges of applying DESs in lipase reactions.

2.3.3 Lipases in surfactants

2.3.3.1 Background

Lipases are soluble enzymes that act on aggregated or emulsified insoluble substrates. Therefore, unlike hydrolases and other enzymes, they are not dissolved in the same phase with their lipid substrates. Because of this difference, lipase structures hold an extra mobile structural element, the lid domain, varying in composition and size among lipase (59). In the absence of lipid substrates, the lid domain blocks the access to the active site leading to the closed conformation. When lipase comes in contact with lipid substrates, the closed conformation undergoes a conformational change particularly at the lid domain adapting an open conformation with an accessible active site. This process is known as interfacial activation (191). Surfactants are tensioactive amphiphilic compounds that act at interfaces due to their energy requirements. At very low concentrations they are water-soluble while at high concentrations they self-assemble in micellar form. They can either be synthetic or naturally occurring such as bile salts, proteins, and peptides (192). Surfactants as they are similar to lipase natural substrates, they can induce interfacial activation of lipases. Therefore, they are usually used in lipase crystallization studies to capture the open conformation of lipases (193). Surfactant are also widely used as emulsifiers in lipase-catalyzed reaction to improve the reaction yield by increasing the substrate accessible surface area to lipase (194). Herein, this chapter discusses the effects different surfactant groups on lipase activity. It also sheds the light on the nature of lipase-surfactants interactions.

2.3.3.2 The Effects of surfactants on lipase catalytic activity

The effects of different surfactants groups on the catalytic activity of various lipases have been investigated by a plethora of studies (194-204). Generally, the effect of surfactants on lipase catalytic activity was found to be highly variable and strongly dependent on the concentration of the surfactants used (192). For instance, Mogensen et al. evaluated the effects of the cationic, anionic, nonionic, and Zwitterionic surfactants on the activity and thermostability of *Thermomyces lanuginosus* lipase (194). Their results showed that low concentrations of all of these surfactants improved lipase activity. On the other hand, at high surfactant concentrations, the activity of lipase either significantly decreased in ionic and cationic surfactants or completely lost in zwitterionic and nonionic surfactants.

The effects of surfactants on lipases catalytic activity were also found to be highly dependent on the chemical nature of the surfactants. For example, premicellar concentrations of the anionic surfactants sodium dodecyl sulfate (SDS) were reported to enhance the activity of *Thermomyces lanuginosus* Lipase, while high SDS concentrations lead to a diminished lipase activity (23). On the other hand, the nonionic surfactant octylpentaglycol was reported to have an opposite effect on the same lipase, as submicellar concentrations decreased the lipase activity, while high concentrations dramatically improve the lipase catalytic activity (205).

Additionally, the effects of surfactants on the enzymatic activity of lipases were reported to be strongly dependent on the source of lipases. Same surfactants were found to have diverse effects on different lipases (206). For example, the nonionic surfactant Tween 80 was reported to improve the catalytic activity and enantioselectivity of several lipases isolated from *Pseudomonas aeruginosa* BN-1, *Rhizopus homothallicus*, and *Candida rugosa*, while it significantly reduced activity of lipases isolated from different sources including *Bacillus cereus* C7, *Fusarium oxysporum*, and *Pachira aquatica* (201, 202, 207-210). Similarly, the nonionic surfactant Triton X was found to have diverse effects on lipases isolated from several sources (209, 211-213).

Overall, the diverse effects of different surfactants on the catalytic activity of lipases arise from the fact that changing different factors such as surfactant type and concentration and the source of lipases alters the nature of lipase-surfactant interactions. Therefore, understanding lipase-surfactant interaction is of a great importance to understand their catalytic mechanisms.

2.3.3.3 Factors affecting lipase-surfactant interactions

Generally, lipases interact with surfactants by two main types of interactions. First, through electrostatic interaction between lipase charged residues and the charged groups of the surfactant (214). Second, through hydrophobic interactions between the nonpolar residues of lipases and the hydrophobic chain of the surfactant (214). Therefore, the charge of the surfactant plays a critical role in determining the nature of lipase-surfactant interactions (215). For example, nonionic surfactants interact with lipases through weak hydrophobic interactions. On the other hand, charged surfactants construct strong interactions with the charged amino acids of lipase.

Proteins are amphoteric molecules, and it can become positive, negative, or neutral depending on the pH of the solution (216). Thus, the pH of the aqueous phase significantly affects lipase-surfactant interactions. For example, *Rhizomucor miehei* lipase has a very low isoelectric point (3.5) which makes it negatively charged in most of aqueous solutions and more attractive to cationic surfactants (217). The ionic strengths of the solution were also reported to strongly affect lipase-surfactant interactions.

Additionally, lipase-surfactant interactions were found to be highly dependent on the concentration of the surfactant used. At low concentrations, most of surfactants construct favorable interactions with lipases that induce lid opening, while at higher concentrations they often inhibit lipases by accumulating at the lid domain and hinder substrate binding (194). On the other hand, the geometry of surfactants was reported to play a key role in shaping lipase interactions. For instance, linear chain ethoxylates surfactants were found to be a competitive inhibitor in the hydrolysis of palm oil

catalyzed by *Rhizomucor miehei* lipase, while branched-tail ethoxylates surfactants had no inhibitory effects on the lipase (197). Furthermore, the chain length of surfactants was also reported to affect lipase-surfactants interactions. For instance, long chain cationic surfactants were found to construct more favorable interactions with *Pachira aquatica* lipase than other shorter chain cationic and anionic surfactants (201).

Overall, classification of lipase–surfactant interactions is not a simple task since all the information in literature about these interactions are obtained from experimental studies that lack the physical aspects and the atomistic details. Therefore, deeper investigations at the atomistic level are required to reveal the nature of these unique interactions.

2.3.3.4 Molecular dynamics simulations of lipase-surfactants interactions

Despite several decades of extensive investigations of Lipase-surfactants interactions, the molecular basis of these interactions is not understood yet. MD simulations can be utilized to decipher the nature of this interactions. However, the number of MD studies that investigated lipase-surfactants interactions is extremely limited. This is anticipated because lipase-surfactants systems are highly complex and require extensive computational power. Moreover, finding the correct parameters for surfactant MD simulations is not a straightforward task since most of them are not included by default in the available MD simulations forcefields.

The first MD simulations study of lipase-surfactants interactions was reported by Peters in 2002 (218). They investigated the effect of charged surfactants on the activation of *Rhizomucor miehei* lipase. Their simulations showed that the charged surfactants enhance lipase activity by increasing the fluctuations at the substrate gating domain which increase the accessibility of substrate to the active site. Yet, the insights gained from this study was very limited due to the short simulation period (2ns) which is mainly because of the limited computational power at that time. Another investigation was reported by Das et al. in which they studied the effect of two different

pHs (8.5 and 10) on the orientation of *Bacillus subtilis* lipase at the water–surfactant interface (219). Shifting the pH from 10 to 8.5 was found to induce a rotation of the substrate binding residues toward the hydrophobic phase. This observation is in agreement with the previous studies that showed an enhanced activity of this lipase at pH 8.8 compared with pH 10 (220).

Luo et al. also investigated the effect of the charge of surfactants on the stability of *Burkholderia cepacia* lipase at the lipid monolayer surfaces of sea spray aerosol (221). Their MD simulations showed that the lipase-lipid complex is stabilized by electrostatic interactions between the charged amino acid at the surface of the lipase and the charged of surfactant molecules.

Overall, there is still long way to go with MD simulations to explain the physical basis of lipase-surfactants interactions. Several questions still need to be answered at the atomic level. For instance, how surfactants achieve interfacial activation of lipases? How change in temperature affect lipase-surfactants interactions? What is the mechanism of lipase unfolding in surfactants?

3 MATERIALS AND METHODS

3.1 Computational Methods

3.1.1 Structures

Crystal structures of the active (open) (PDB ID: 2W22, resolution= 2.2 Å) and the inactive (closed) (PDB ID:1KU0, resolution=2.0 Å) conformations of thermoalkalophilic lipases were obtained from Protein Data Bank. Before the simulations, the ligands and water molecules were removed from the structures, while the metal ions, Ca⁺² and Zn⁺² were kept. No atoms with multiple occupancies were reported in both of the structures.

3.1.2 Systems generation

3.1.2.1 Lipase in organic solvents

Both of the lipase conformations were solvated in five different solvents: methanol, ethanol, water, cyclohexane, and toluene by using PACKMOL (222). The solvation was carried out by placing the lipase at the center of a cubic box which was filled later with solvent molecules. To ensure the stability of the systems and to avoid any unfavorable clashes between atoms during the equilibration process, the solvent molecules were initially located at least 2 Å far from each other.

The simulation box dimensions were set to 45 Å in each direction, and the protein was placed at least 10 Å from the edges of the box. Prior to simulations, all of the generated systems were neutralized by Na⁺ and Cl⁻ counter ions using VMD (223). The details of the generated systems are given in **Table 1**.

Table 1. Details of lipase simulated systems in organic solvents.

Number of residues (number of atoms)				
System	Protein	Solvent	Ca ⁺²	Zn ⁺²
Ethanol	388(5986)	8000(72000)	1 (1)	1 (1)
Methanol	388(5986)	20000(120000)	1 (1)	1 (1)
Water	388(5986)	20000(60000)	1 (1)	1 (1)
Toluene	388(5986)	5000(75000)	1 (1)	1 (1)
Cyclohexane	388(5986)	4000(72000)	1 (1)	1 (1)

3.1.2.2 Lipase in deep eutectic solvents

Both of the lipase structures were solvated in three different concentrations of reline, 8M urea, and water by using PACKMOL (222). Reline systems were prepared by mixing urea and choline chloride at molar ratio 2:1. All of the produced systems were neutralized by counter ions using VMD (223). A summary of the generated systems is given in **Table 2**.

Table 2. Details of lipase simulated systems in deep eutectic solvents.

Number of residues (number of atoms)						
System	Protein	Choline Chloride	Urea	Water	Ca ⁺²	Zn ⁺²
Reline (100%)	388(5986)	3000(66000)	6000(48000)	0(0)	1(1)	1(1)
Reline (70%)	388(5986)	4200(92400)	8400(43200)	3600(10800)	1(1)	1(1)
Reline (30%)	388(5986)	2700(59400)	5400(67200)	12600(37800)	1(1)	1(1)
8M Urea	388(5986)	0(0)	2210(17280)	15000(45000)	1(1)	1(1)
Water	388(5986)	0(0)	0(0)	19888(59664)	1(1)	1(1)

3.1.2.3 Lipase in sodium dodecyl sulfate

Open and closed lipase structures were solvated in two different systems containing 20 or 180 SDS molecules by using PACKMOL (222). Structures were also solvated in systems containing only water molecules to be used as control simulations. To ensure the stability of the systems during the equilibration, SDS molecules were placed at least 6 Å apart from each other in low-density cubic simulation boxes with dimensions of 200 Å. concentrations of reline, 8M urea, and water by using PACKMOL (222). Before the simulations, counter ions were added to neutralize the systems by using VMD (223). A detailed summary of the resulting systems is given in **Table 3.**

Table 3. Details of lipase simulated systems in sodium dodecyl sulfate.

Number of residues (number of atoms)					
System	Protein	SDS	Water	Ca ⁺²	Zn ⁺²
180SDS	388(5986)	180 (7740)	10000(30000)	1(1)	1(1)
20SDS (monomer)	388(5986)	20 (860)	10000(30000)	1(1)	1(1)
20SDS (dimer)	773 (11923)	20 (860)	25000 (75000)	2(2)	2(2)
Water	388(5986)	0(0)	10000(30000)	2(2)	2(2)

3.1.2.4 Molecular dynamics (MD) simulations

A multi-step minimization and equilibration procedure was followed to relax the generated systems. Initially, solvents molecules were energy minimized for 40,000 steps and equilibrated for 0.25 ns in NVT ensemble wherein the protein atoms were fixed. Then, the same relaxation steps were carried out on the whole system without fixing the protein. Next, the systems were equilibrated for 10ns in NPT ensemble at 1 bar and 298 K using Langevin dynamics temperature and Langevin piston pressure methods (224). All production simulations were carried out with CHARMM36 all atom force field with map correction by using NAMD v2.9 or v2.13 (225-228). All production simulations were performed as NPT ensembles with the periodic boundary

conditions applied in all directions. A 2fs integration time was applied in all the simulation and water was simulated by TIP3P model (229). The particle-mesh Ewald (PME) algorithm was used to compute the long-range Coulomb interactions with a grid spacing set to 1.2 Å and cutoff radius set to 12 Å (230).

3.1.3 Data analysis and visualization

The visualization and analysis of the trajectories were carried out by different plugins of VMD (223). The analysis of trajectories includes the root mean square deviation (RMSD) of the protein backbone, fluctuations of protein backbone C α atoms, solvent accessible surface area (SASA), radius of gyration (Rg), radial distribution functions (RDF), hydrogen bonding, salt bridges, dihedral angles and atomic distances. Additionally, all-to-all RMSD analysis and fraction of native contacts were calculated via MDAnalysis (231). Essential dynamics were analysed by Bio3D and MDTRAJ (232, 233). Tunnel analysis was implemented by the Caver 1.0 webserver (234). Contact maps were conducted by MDTRAJ (233).

3.2 Experimental Methods

3.2.1 BTL2 lipase expression and purification

For experimental analysis, the thermoalkalophilic lipase from *Bacillus thermocatenuatus* (BTL2) was expressed in Escherichia coli BL21 (DE3) cells and purified by metal affinity chromatography as described previously (235). The purified enzyme solutions were concentrated to 2.50 mg/ml by ultracentrifuge tubes. The concentration of the purified lipase was calculated by Bradford assay (236). A 12% SDS-PAGE gel was used to confirm the expression and purification of BTL2 lipase.

3.2.2 Lipase activity assays

Lipase activity was measured by fluorescence assay utilizing 4-methylumbelliferyl butyrate (4-MU) as substrate. The hydrolytic activity of 6 nM of BTL2 lipase was measured in 25 mM sodium phosphate buffer containing 250 μ M of 4-MU at pH 7.00. The 4-MU-fluorescence was measured by a 355 nm excitation wavelength and a 460 nm emission wavelength in a kinetic manner at every 30 seconds of 60 minutes. The measurements were performed in triplicates and the initial velocities are calculated by using the software SoftMaxPro of the fluorimeter.

3.2.3 Lipase stability assays

600 nM of BTL2 lipase were incubated at different concentrations (0–90% v/v) of six distinct organic solvents (cyclohexane, acetone, ethanol, toluene, methanol, and 2-propanol) for 30 min at 25 °C. For thermostability assays, same amount of lipase was incubated at different concentrations (0–70% v/v) of three different solvents (ethanol, water, and cyclohexane) for 30 min at 60 °C. The residual activity of 6 nM of the incubated lipase solution was measured by the same activity assay mentioned earlier.

4 RESULTS

4.1 Lipase in Organic Solvents

To understand the molecular impact of organic solvents on the structure and dynamics of thermoalkalophilic lipases, molecular dynamics (MD) simulations of the open (2W22) and the closed (1KU0) conformations of thermoalkalophilic lipases were carried out in five different solvents (ethanol, water, toluene, methanol, cyclohexane) for 100ns at 310 K (**Figure 1**).

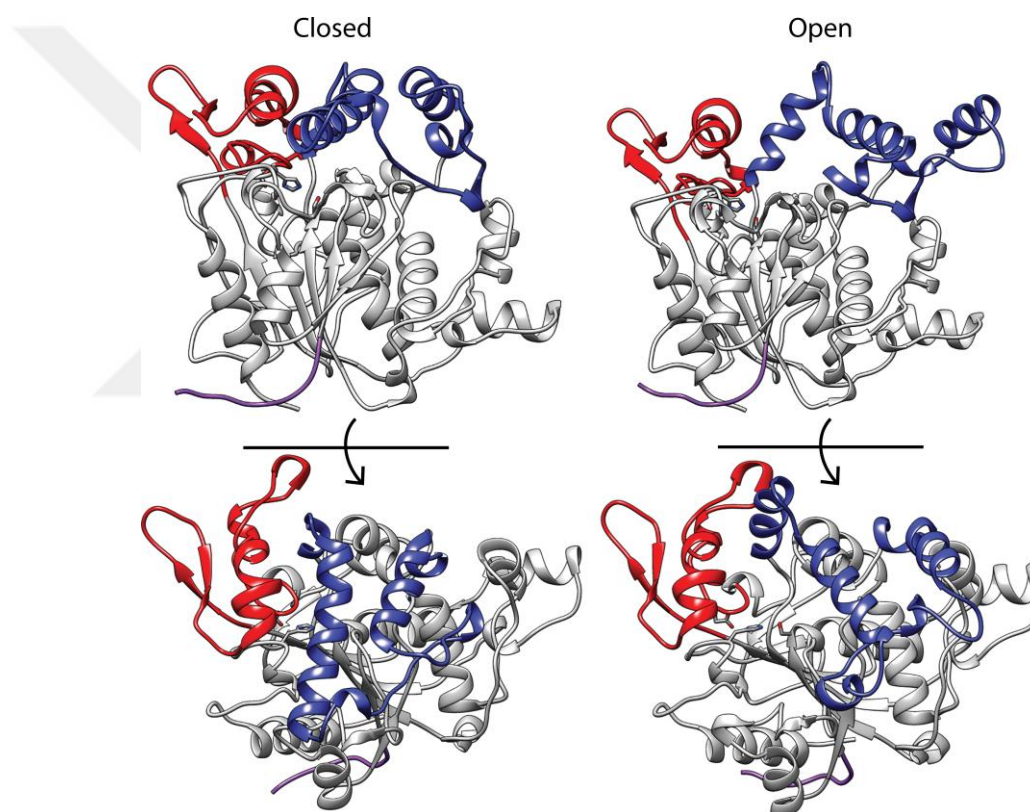


Figure 1. Two different views of the aligned crystal structures of the closed (1KU0) and the open (2W22) conformations of thermoalkalophilic lipases. The lid domain is coloured in blue. The β -flap region is coloured in red. Top panel shows the top side of the catalytic cleft and bottom panel shows the top view of the cleft.

Given the high sequence similarity between these two structures (97%), they can be treated as valid representations of the closed and open conformations of thermoalkalophilic lipases (**Figure 2**). To unravel the relationship between organic

solvent stability and thermostability in lipases, these systems were also simulated at 450 K. Although 450 K is an unrealistic experimental temperature, such elevated temperature simulations are utilized to sample structural changes in shorter time scales. Several examples of such “out of range“ elevated temperature simulations have been documented as they provide a tradeoff between limited computational resources and extreme conditions (237-239). Overall, a total of 20 MD simulations were performed to account for the molecular behavior of thermoalkalophilic lipases in organic solvents at low and elevated temperatures.

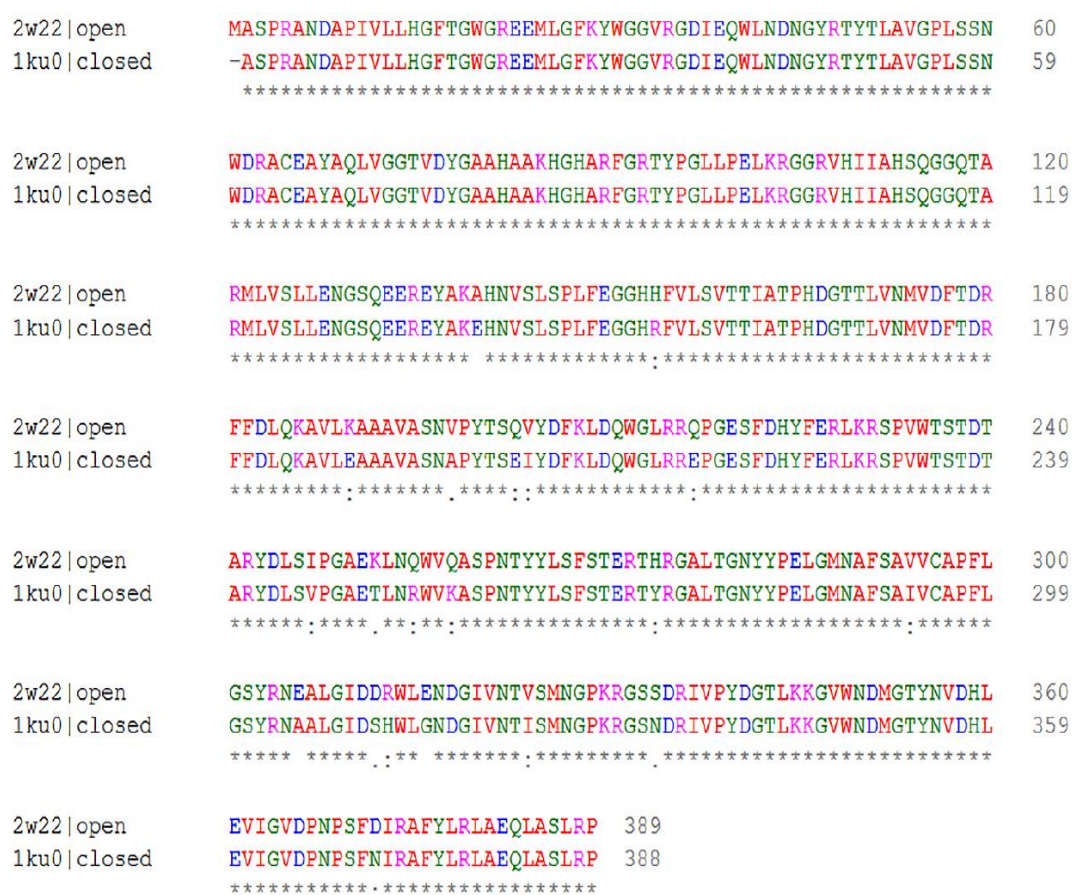


Figure 2. Pairwise sequence alignment of the closed and open states of lipase.

4.1.1 Stability of lipase backbone in organic solvents

To assess the stability of the simulated systems, the root mean square deviation (RMSD) of lipase backbone atoms was computed. MD simulations indicated stabilized RMSD profiles of both the open and the closed conformations at 310 K in all of the simulated systems (**Figure 3A**). On the other hand, as expected, MD simulations performed at 450 K indicated an increased RMSD profiles of both of the lipase conformations fluctuating around 3 Å during the last 20 ns of the simulations (**Figure 3B**). Overall, the RMSD patterns shows equilibrated structures of both of lipase conformations in all the simulations. Therefore, we underscore the applicability of the MD simulations performed here for investigating the molecular behavior of lipase in response to changes in the solvent environment.

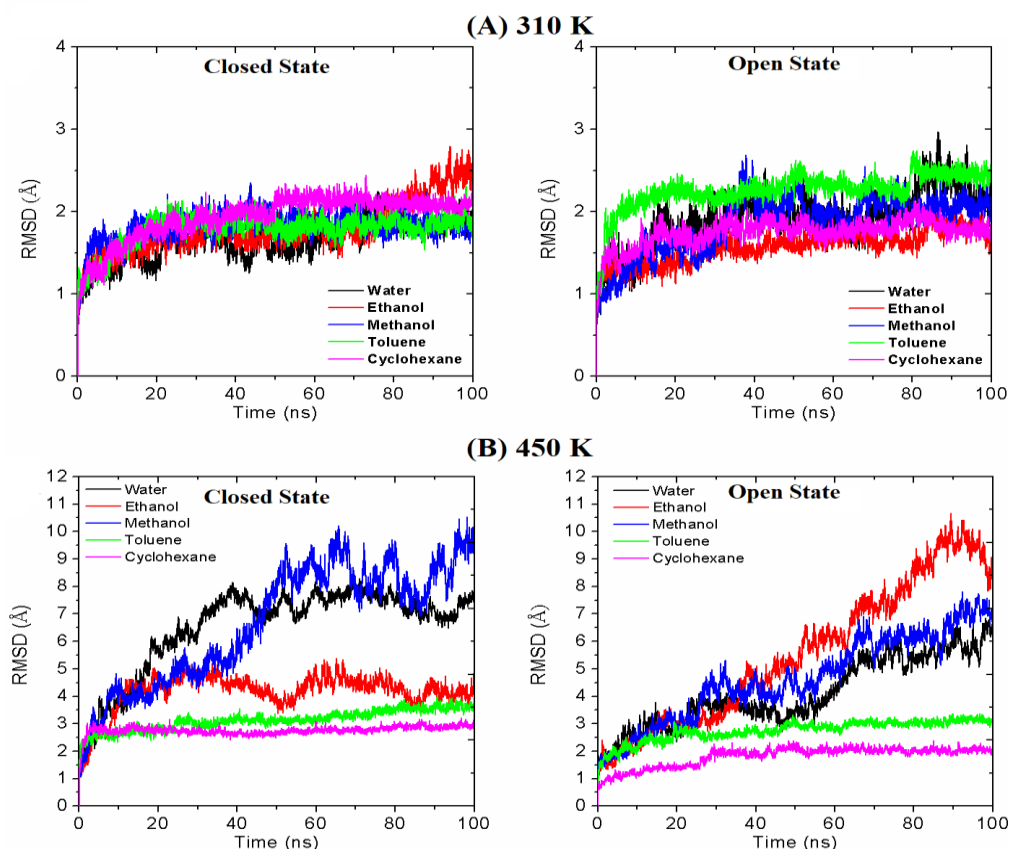


Figure 3. RMSD analysis of the open and closed conformations of lipase in different solvents.

4.1.2 Fluctuations of lipase backbone in organic solvents

To evaluate the flexibility of lipase structures in different solvents environments, the root-mean-square fluctuations (RMSF) analysis of lipase backbone was calculated. At 310 K, regardless of the lipase conformations, enhanced fluctuations of the lid domain spanning the residues 169 to 239 were observed in the presence of polar solvents (**Figure 4A**). The highest fluctuations of the lid domain were observed in water followed by ethanol and methanol, respectively. These enhanced fluctuations of the lid domain were absent in the presence of non-polar solvents including cyclohexane and toluene. On the other hand, RMSF analysis of 450 K simulations showed a striking difference between lipase flexibility in polar and non-polar solvents (**Figure 4B**). Regardless of the lid conformation, thermal unfolding of lipase structure was observed in polar organic solvents, while in non-polar solvents lipase structure remained stable throughout the whole simulation period (**Figure 5**).

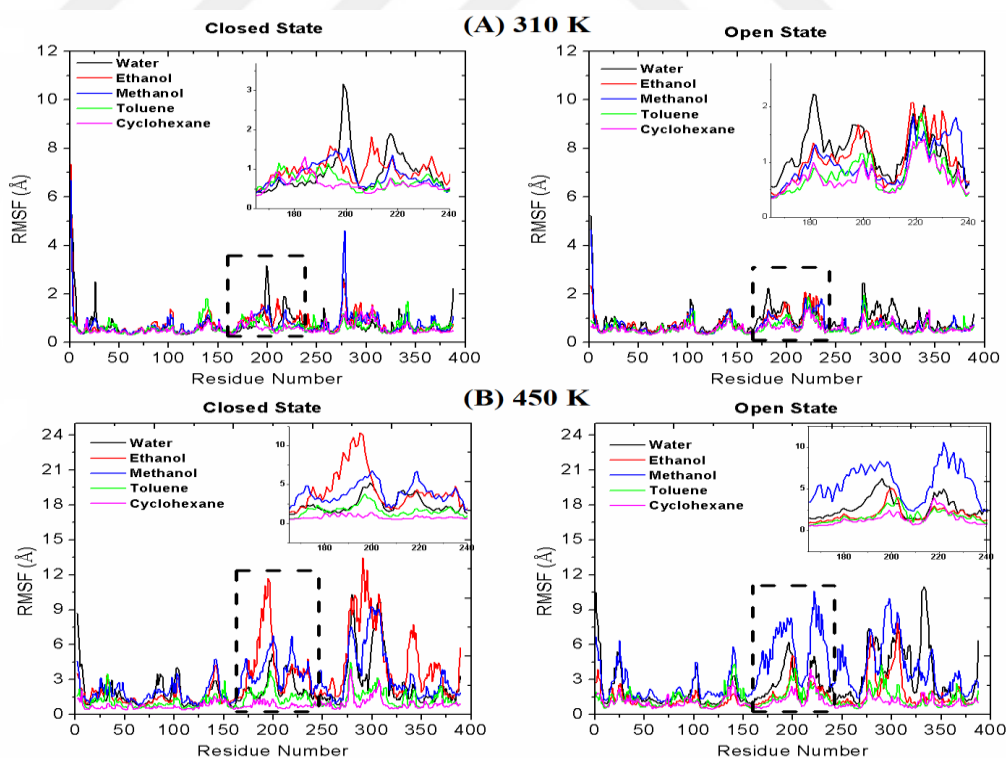


Figure 4. RMSF analysis of the open and closed conformations of lipase in different solvents.

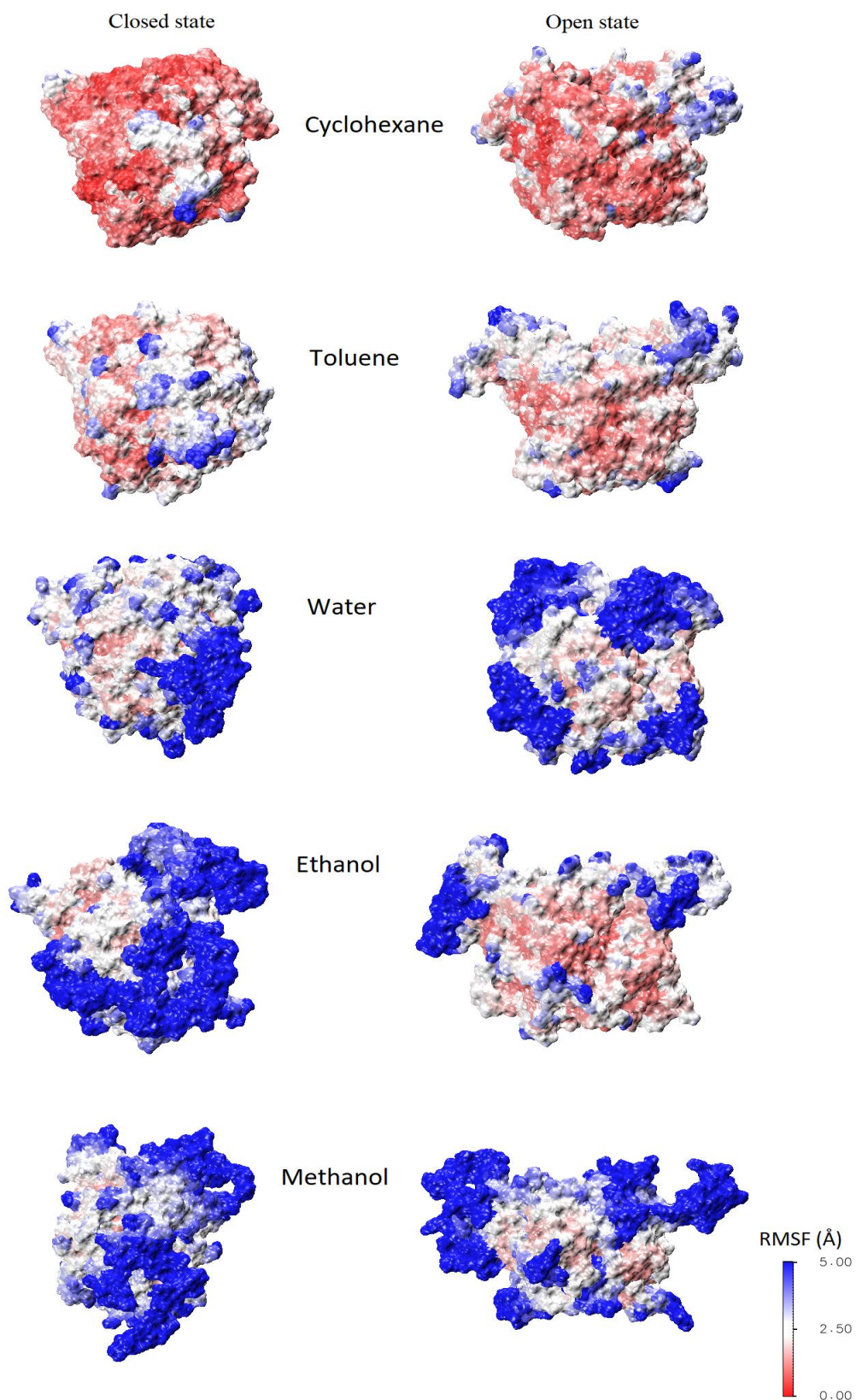


Figure 5. Flexibility of the open and closed states of lipase at 450 K.

4.1.3 Compactness of lipase structure in organic solvents

To investigate the compactness of lipase secondary structure in different solvents, the radius of gyration (R_g) of lipase was analyzed. At 310 K, regardless of the lid conformation, R_g analysis indicated that lipase maintains a more compact structure in non-polar solvents compared to polar ones (**Figure 6A**). On the other hand, at 450 K, high R_g profiles were observed for both of the lipase structures in polar solvents suggesting a thermal unfolding of lipase in these solvents (**Figure 6B**). Interestingly, regardless of the lid conformation, lipase maintained a tightly packed structure despite this very elevated temperature.

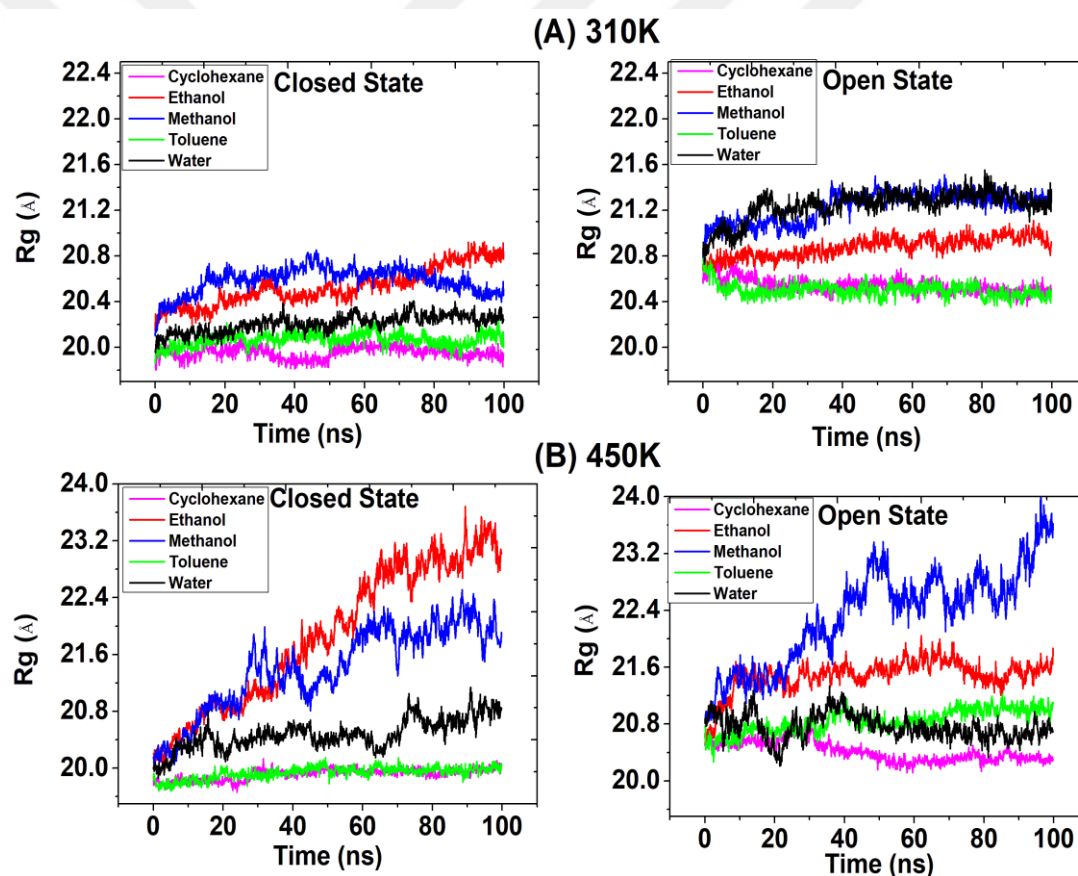


Figure 6. R_g analysis of the open and closed conformations of lipase in different solvents.

4.1.4 Solvent accessible surface area of lipase structure in organic solvents

To evaluate the response of lipase structure to different solvent environments, the solvent accessible surface area (SASA) of lipase structures was computed. At 310 K, both of the lipase conformations showed significantly lower SASA in the non-polar solvents than in the polar ones (**Figure 7A**). At 450 K, regardless of the lid conformation, no change of the SASA of lipase was observed in non-polar solvents (**Figure 7B**). On the other hand, the SASA of both of lipase structures significantly increased at 450 K in polar solvents suggesting a strong structural destabilization of lipase in these solvents at elevated temperatures.

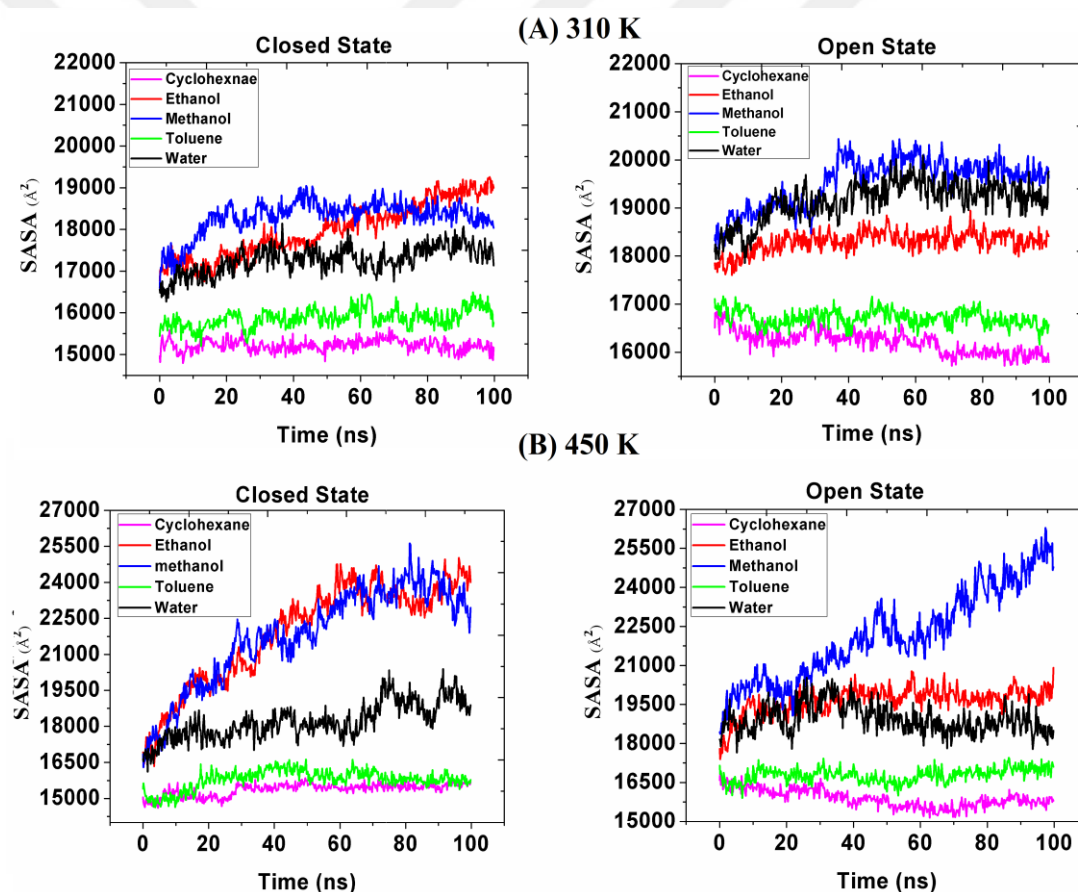


Figure 7. SASA analysis of the open and closed conformations of lipase.

4.1.5 Essential dynamics analysis of lipase in organic solvents

To evaluate the essential dynamics (ED) of lipase in different solvents, the principal component analysis (PCA) was performed for all of the production trajectories. PCA analysis of the simulations performed at 310 K indicated that both of the lipase structures spanned larger conformational space when solvated in polar solvents than in non-polar solvents (**Figure 8A**). On the other hand, PCA analysis of the simulations performed at 450 K showed that regardless of its lid conformation, lipase sampled very limited conformational space in non-polar solvents (**Figure 8B**). In contrast, both of lipase structures sampled very wide conformational space when solvated in polar solvents at 450 K suggesting a highly disturbed lipase structure.

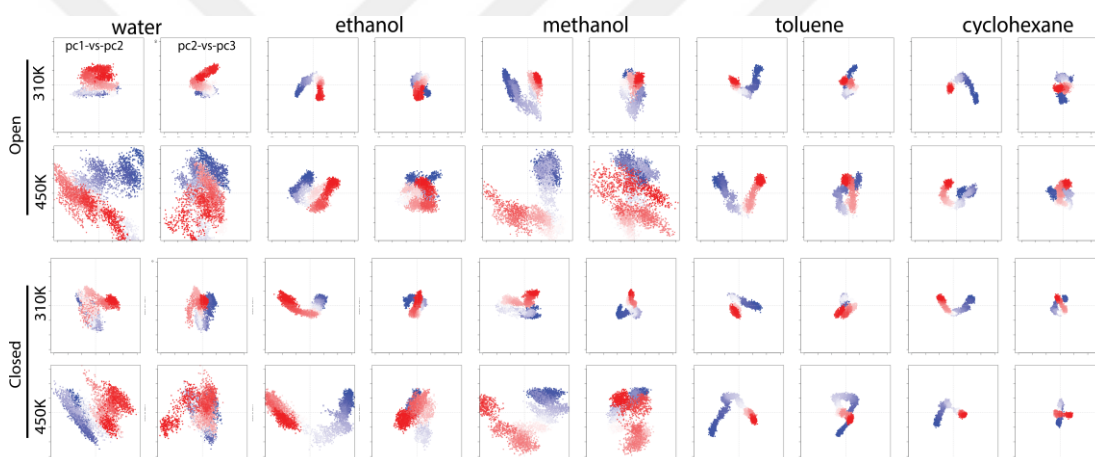


Figure 8. Essential dynamics of lipase conformations in different solvents.

4.1.6 Correlation of lipase motions in organic solvents

To assess the correlation of lipase motions in different organic solvents, the dynamic cross correlation maps (DCCM) of lipase were constructed. DCCM analysis showed that regardless of the simulation temperature or the lid conformation, lipase showed a strongly correlated motion in non-polar solvents, underscoring high stability of lipase in these solvents (**Figure 9**). On the other hand, both of lipase conformations showed correlated motion at 310 K which decreased dramatically at 450 K, suggesting a significantly low stability of lipase in polar solvents at this elevated temperature.

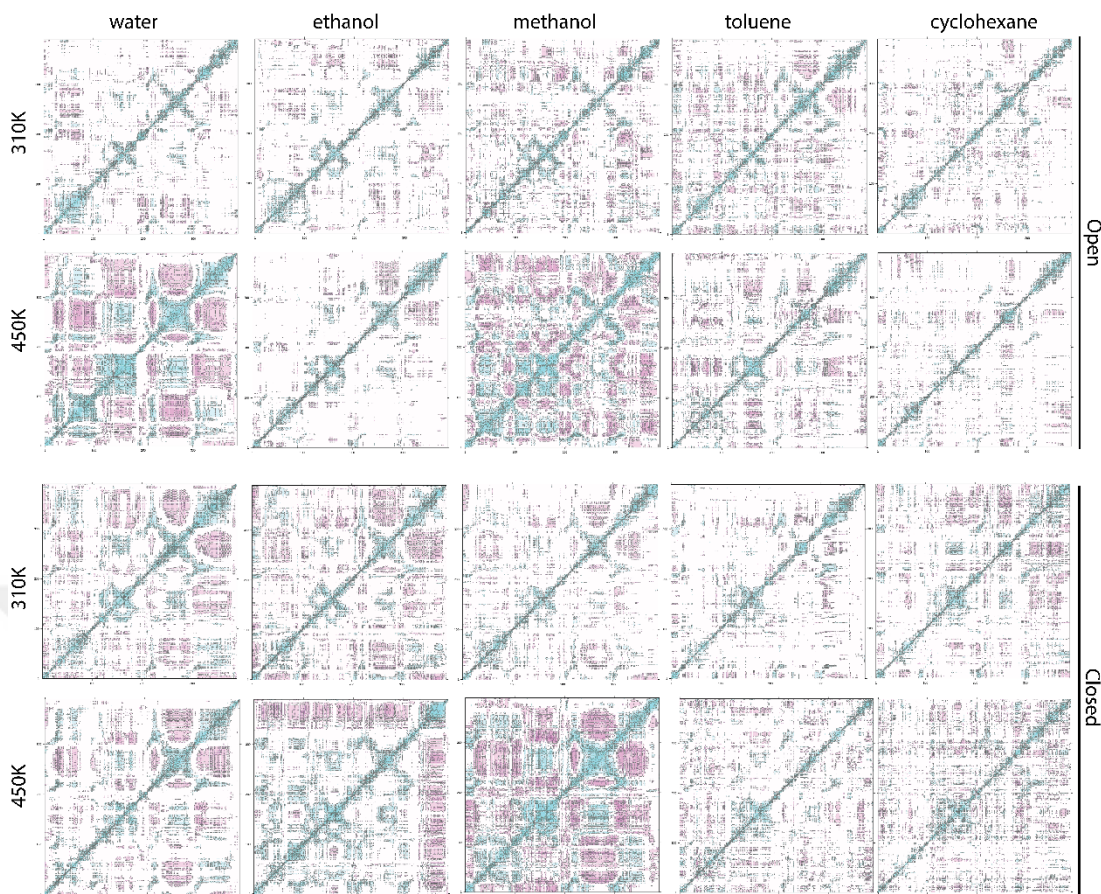


Figure 9. DCCMs of lipase conformations in different solvents.

4.1.7 Stability of lipase catalytic machinery in organic solvents

The catalytic machinery in lipases is formed by the catalytic triad and the oxyanion hole. The catalytic triad is formed by Asp318, His359, and Ser114 in the open conformation and by Asp317, His358, and Ser113 in the closed conformation. The oxyanion hole, on the other hand, is formed by the backbone amide groups of Gln115 and Phe17 in the open form and by the amide groups of Gln114 and Phe16 in the closed form. To evaluate the structural stability of the catalytic machinery in different organic solvents, the catalytic triad distances and the compactness of the catalytic machinery were analyzed. At 310 K, all the solvents were found to have no effect on the catalytic triad distances and the radius of gyration of the catalytic machinery (**Figure 10**) and (**Figure 11A**). It is also worth mentioning that the difference in catalytic triad distances and the compactness of the catalytic machinery

between the closed and the open conformations is because of the difference of the oxyanion hole fold between the two states. Similarly, the active site of the open conformation was found to be less compact than that of the closed conformation, probably because of the enhanced flexibility of the catalytic site in the open state.

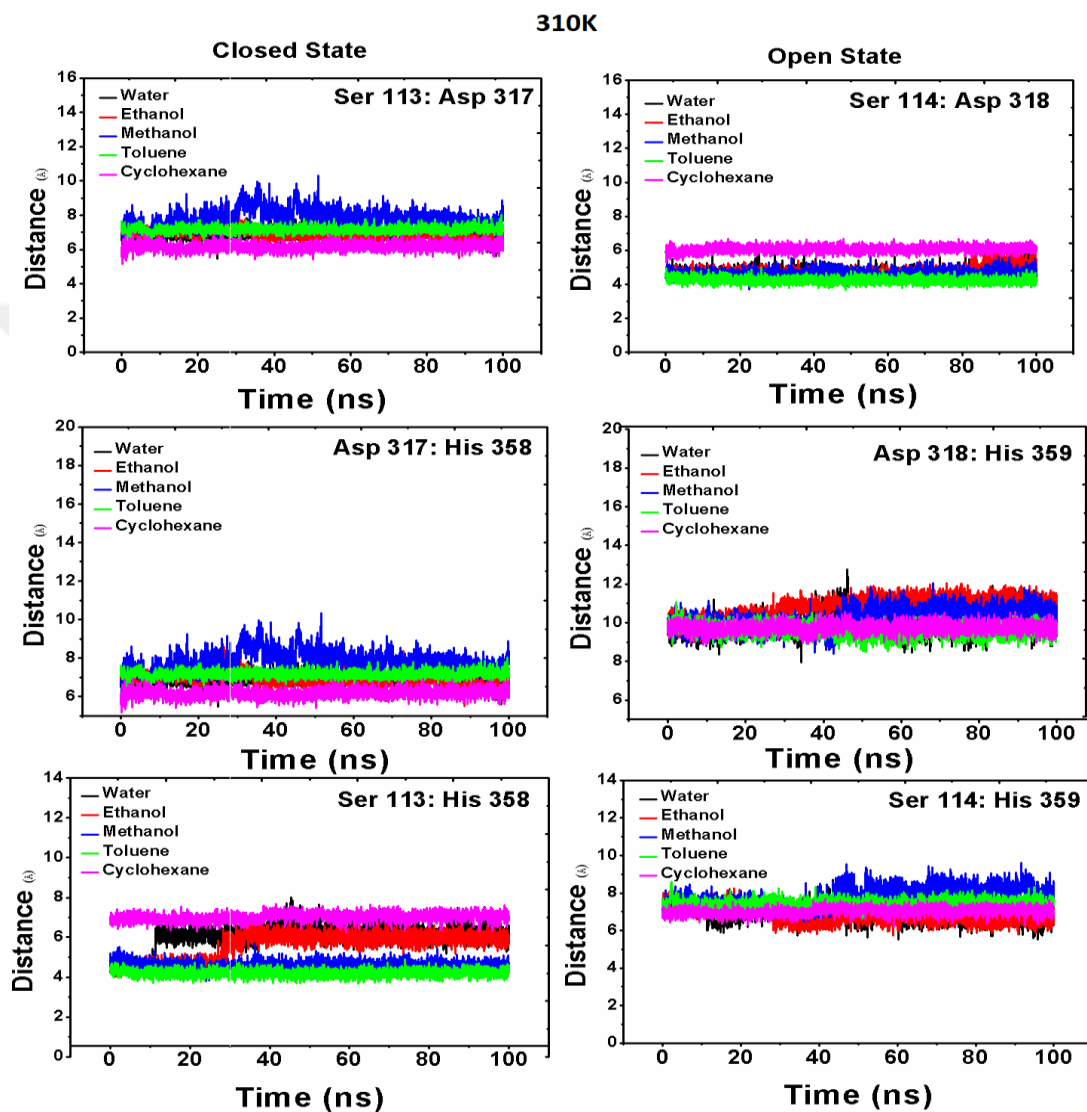


Figure 10. Distances between the catalytic triad of lipase at 310 K.

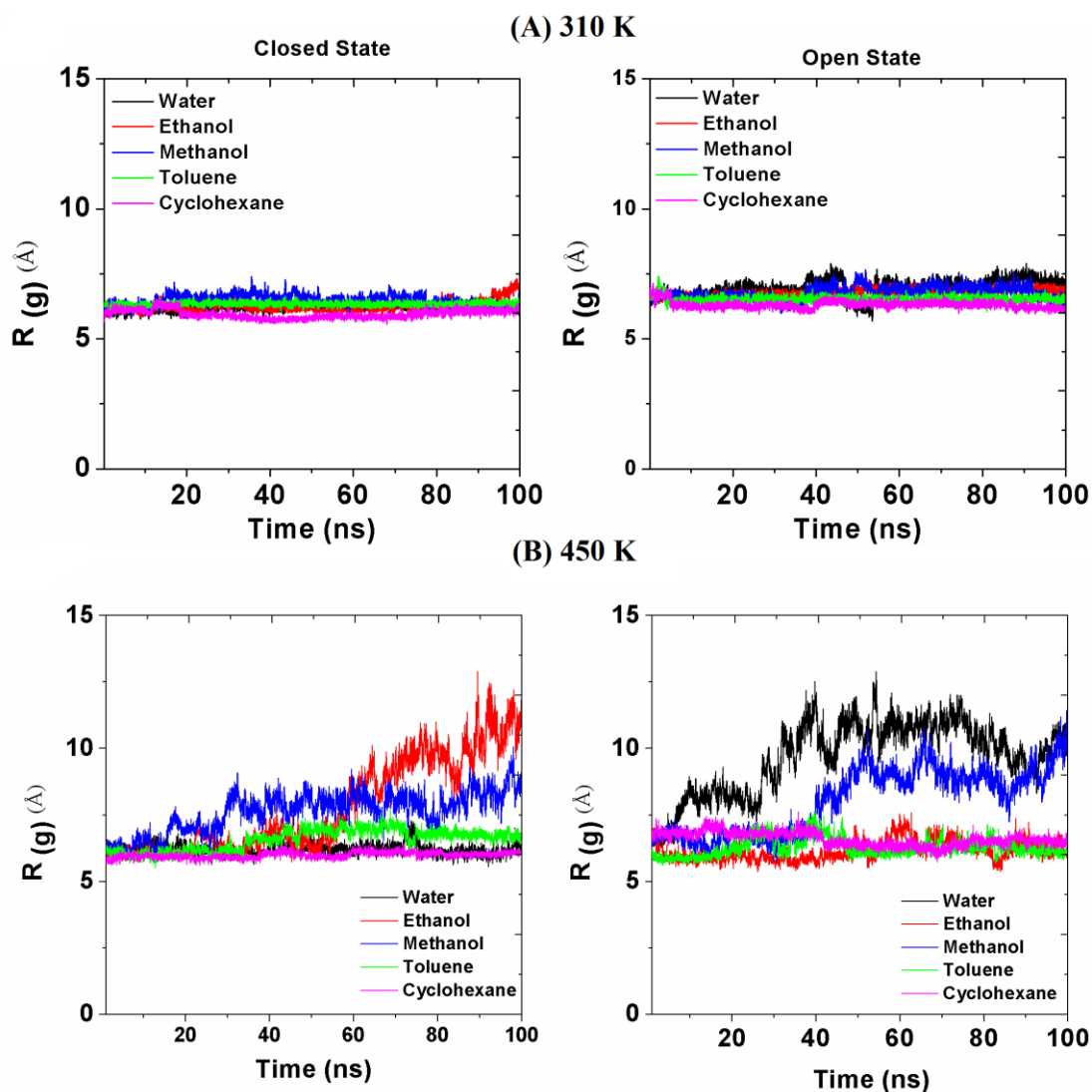


Figure 11. Rg of the catalytic machinery of lipase conformations in different solvents.

On the other hand, the nature of the solvent was found to have a strong effect on the stability of the catalytic machinery at 450 K (**Figure 11B**) and (**Figure 12**). As such, no changes were observed in the compactness of the catalytic machinery and the distances between the catalytic residues were found in non-polar solvents, while the catalytic machinery was found to be significantly destabilized in polar solvents, suggesting a thermal unfolding of lipase in polar solvents.

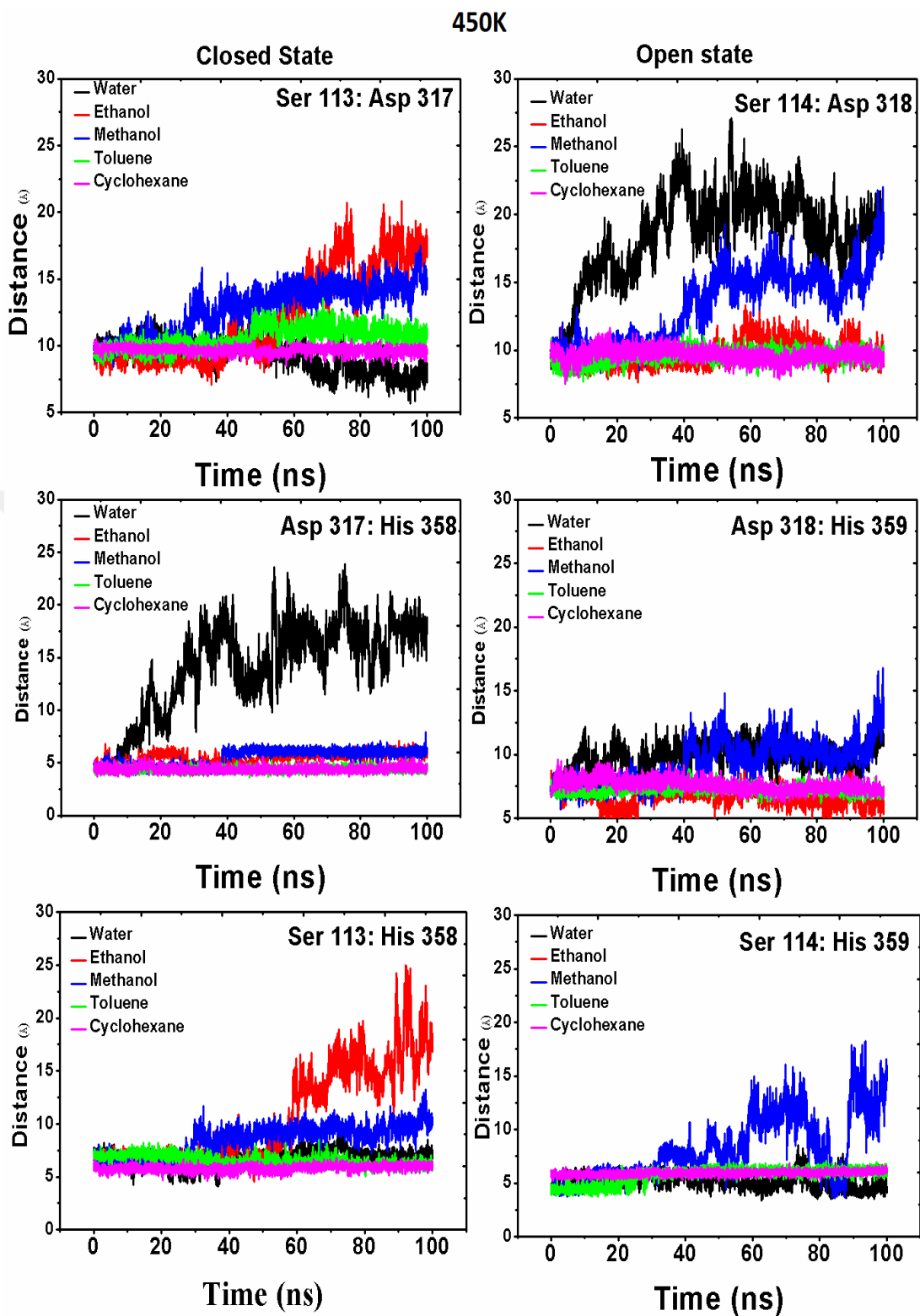


Figure 12. Distances between the catalytic triad of lipase at 450 K.

4.1.8 Stability of the lipase critical salt bridges in organic solvents

The salt bridge formed between Arg 142 and Asp179 plays a crucial role in the interfacial activation of thermoalkalophilic lipases (66). This salt bridge stabilizes the open conformation of lipase by connecting a critical hinge region in the lid domain to the lipase hydrophobic core (66). Therefore, any disruption of this salt bridge would lead to closing of the lid domain. Another two important salt bridges are those formed between Asp210:Arg93 and Lys208:Glu24. Although they don't play a role in the interfacial activation, they play a critical role in the stabilization of lipase overall fold.

To investigate the effect of different solvents on the lipase dynamical equilibrium, the stability of these critical interactions was monitored. The simulations carried out at 310 K showed that all the salt bridges were stable in all of the organic solvents all over the simulation period (**Figure 13A**). On the other hand, all salt bridges were less stable in water, suggesting that lipases prefer to adopt the closed state in water. The simulation performed at 450 K, showed that all the salt bridges except that formed between Lys208 and Glu24 were stable in non-polar solvents while all of them were either partially or completely lost in polar solvents. Particularly, the salt bridge formed between Asp210 and Arg93 was only partially disturbed in the presence of polar solvents while that formed between Lys208 and Glu24 was completely lost in water (**Figure 13B**).

Lastly, the salt bridge interaction between Arg142 and Asp179 was stable in ethanol while it was totally lost in methanol and water. The separation in the salt bridge interaction between Lys208 and Glu24 was found to reach values between 20–30 Å in polar solvents (**Figure 13B**). Such a large separation is an indication of thermal unfolding of lipase in polar solvents.

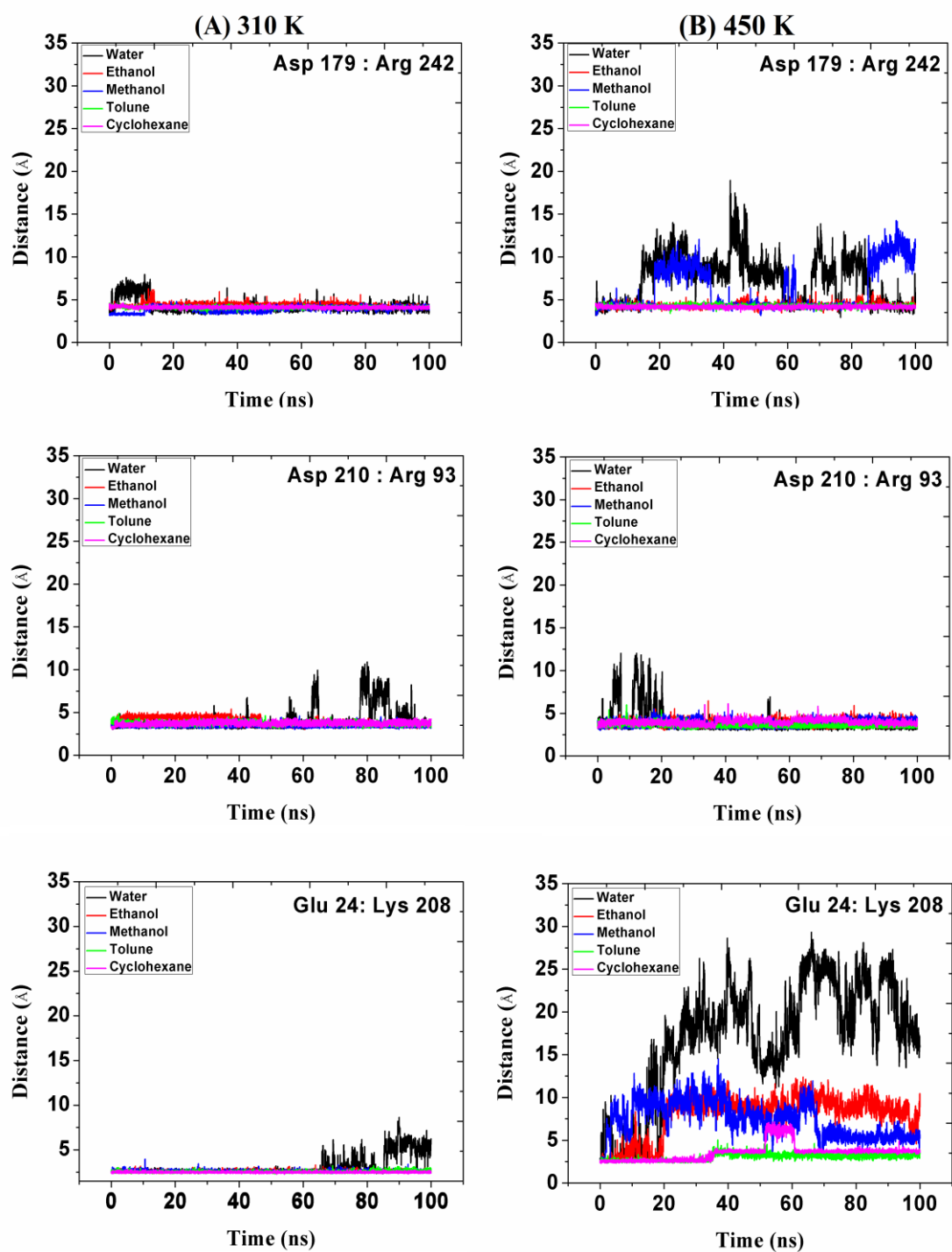


Figure 13. Stability of the open conformation critical salt bridges.

4.1.9 Interactions between lipase and organic solvents

To evaluate the interactions between lipase and organic solvents, the radial distribution functions (RDF) between the center of mass of lipase structure and solvent molecules were analyzed. At 310 K, RDF analysis showed that the probability of finding non-polar solvent molecules in the vicinity of the lipase core is lower than that of the polar solvents molecules (**Figure 14A**). This observation was true for both of the lipase conformations. Indeed, this is expected since unlike the bulky non-polar solvents, polar solvents such methanol and water are small enough to diffuse to the lipase hydrophobic core. Indeed, this is a destabilizing interaction since the diffusion of polar solvent molecules would disturb the hydrophobic residues buried in the lipase hydrophobic core. At 450 K, on the other hand, no changes were observed in the interactions between lipase and non-polar solvents while the rate of diffusion of polar solvents molecules was found to increase (**Figure 14B**). This could be a result of a more exposed hydrophobic core due to lipase thermal unfolding.

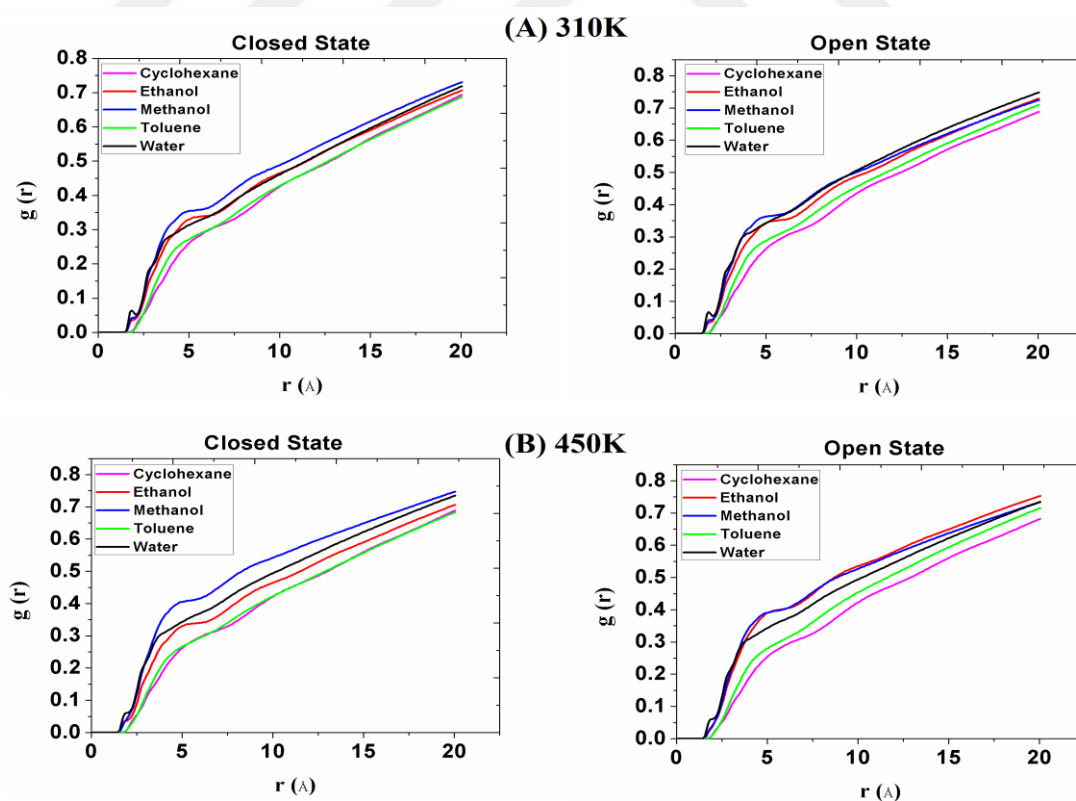


Figure 14. RDF analysis between the center of mass of lipase and solvent molecules.

4.1.10 Conformational change of Phe17 in organic solvents

One of the main differences between the open and the closed state of lipase is the conformation of the side chain of the residue Phe17. In the closed conformation this residue is tightly packed with the catalytic serine blocking the substrate access to the active site. Upon lipase activation, Phe17 changes the torsion angle of its side chain by 100° to adapt an open conformation that allow the substrate to reach the catalytic site (66). Therefore, it is of a great importance to check the effect of the solvent environment on the conformation of this critical residue.

Our analysis of Phe17 dihedral angles at 310 K showed that it maintains an open conformer in all of the solvents except methanol (**Figure 15**). It is worth mentioning that this analysis was not performed at 450K since it becomes meaningless with the lipase thermal unfolding in the polar solvents.

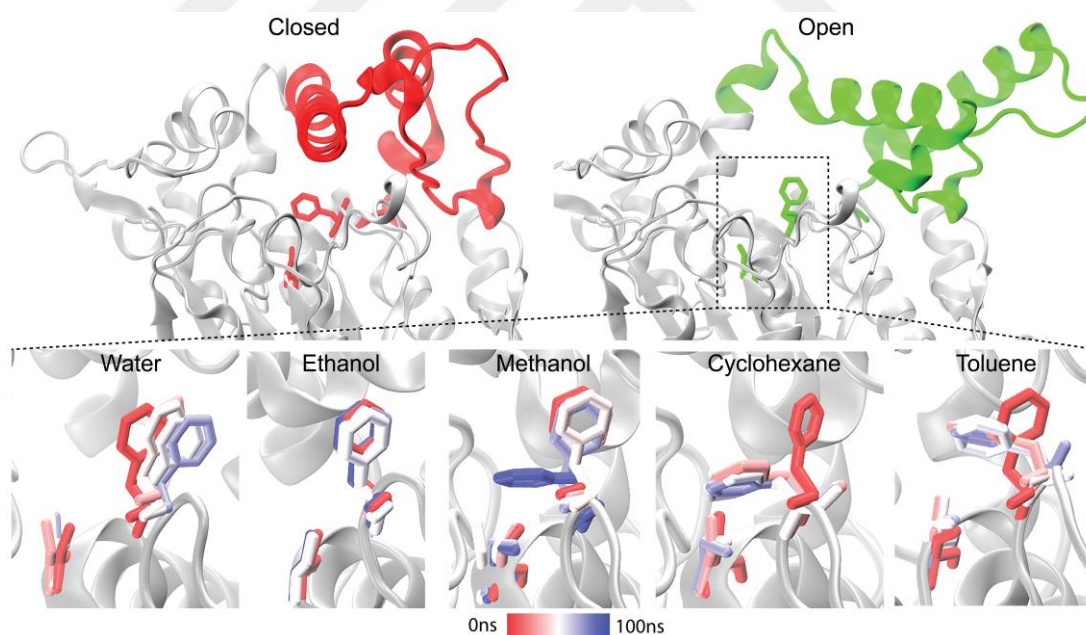


Figure 15. Change in residue Phe17 side chain conformation in different solvents.

4.1.11 Experimental validation of lipase stability in organic solvents

To validate the theoretical insights obtained from our MD simulations, the residual activity of lipase was experimentally measured upon incubation in different concentrations of organic solvents at room temperature. Generally, lipase activity was found to increase upon incubation in all organic solvents up to a specific concentration after which it either decreases or completely diminishes (**Figure 16A**). The improvements in lipase activity were found to be generally higher in polar solvents than in non-polar ones. The activity of lipase increased by 3.46 and 4.75-fold in 70% of ethanol and 80% of 2-propanol, respectively (**Figure 16A**). Beyond these two concentrations, lipase activity started to decrease which is natural because at this point the hydrolysis reaction is not favorable anymore and the reaction equilibrium is shifted towards the esterification.

The improvements in lipase activity were found to be less in methanol and acetone than in the rest of polar solvents. Lipase activity was found to increase by 1.72 and 1.66 in 60% acetone and 40% methanol, respectively (**Figure 16A**). Higher concentrations of these two solvents completely inhibited the lipase activity. Such inhibitory effect is very likely to happen because high concentrations of acetone is known to decrease protein solubility and usually used in protein precipitation experiments (240). On the other hand, the inhibiting effect of methanol can be due to the closed Phe17 conformation that blocks the access to the active site (**Figure 15**).

On the other hand, in non-polar solvents, lipase activity improved by 1.73 and 2.78 folds in 50% toluene and 70% cyclohexane, respectively. Contrary to polar solvents, a severe decrease or a complete inhibition of lipase activity was not observed at high concentrations of non-polar solvents (**Figure 16A**).

Overall, these observations are consistent with our ambient temperature simulations which showed that in contrast to non-polar solvents, polar solvents improve lipase fluctuations which are critical for lipase activity at low temperature.

Aiming to understand the effect of organic solvents on lipase thermostability, the residual activity was measured after incubation of the lipase in varying concentrations of organic solvents at high temperature. Generally, lipase activity was higher in cyclohexane and ethanol than in water (**Figure 16B**). Lipase activity increased by 4.89 folds in 25% ethanol while higher concentrations of ethanol completely inhibited the activity of lipase. On the other hand, the activity of lipase improved by 2.5 and 2.8 folds in 50% and 70% cyclohexane, respectively. Interestingly, no inhibition or denaturation of lipase was observed at high concentrations of cyclohexane (**Figure 16B**).

Altogether, these observations are in agreement with our elevated temperature simulations which indicated that lipase regardless of its lid structure, maintains intact and rigid structure in non-polar solvents while it was thermally unfolded in polar solvents.

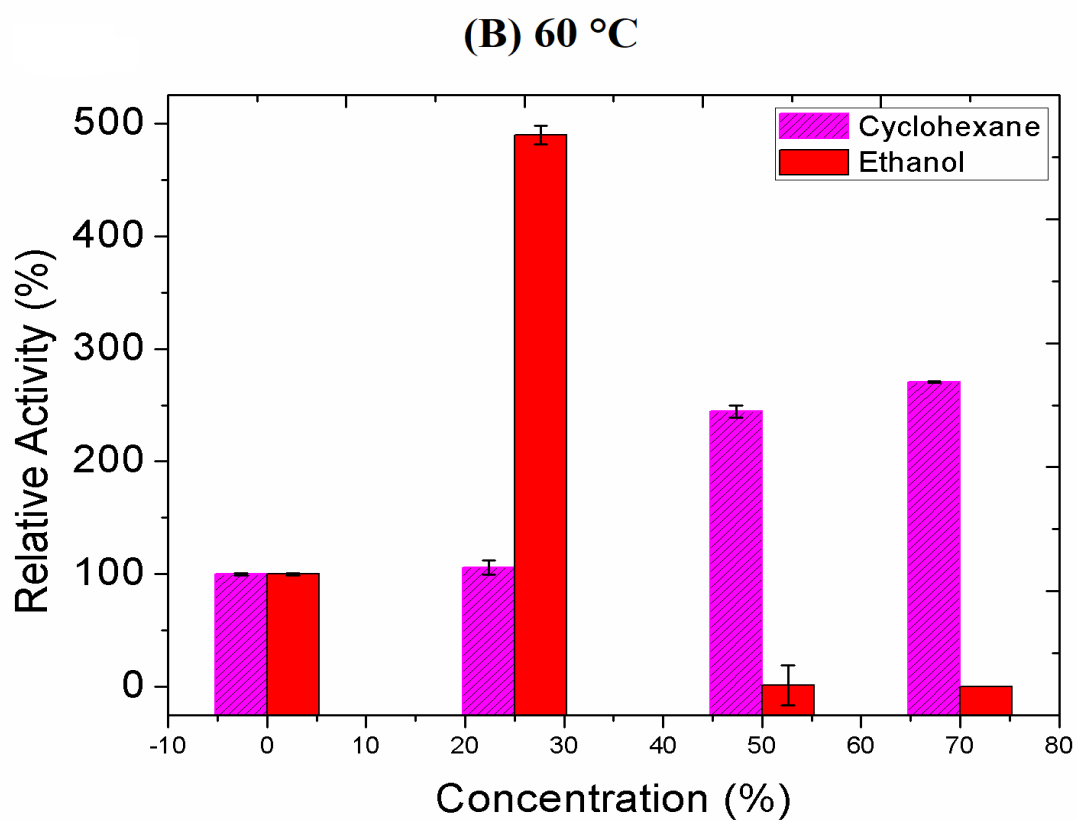
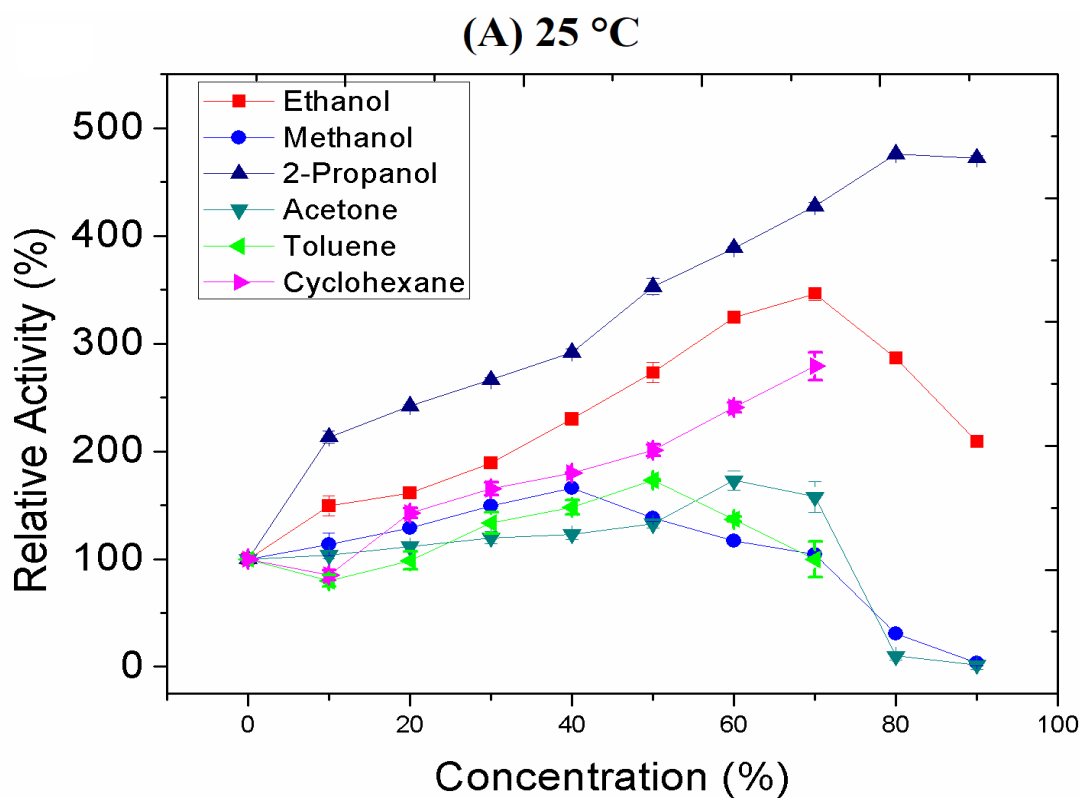


Figure 16. Effect of different organic solvents on BTL2 lipase activity.

4.2 Lipase in deep eutectic solvents

To investigate the effect of the water content in DESs formulations on the dynamics and structure of thermoalkalophilic lipases, MD simulations were carried out for the open and the closed conformation of lipase in 3 different formulations of reline with different hydration levels (**Figure 17**). MD simulations were also carried out for both of the structures in water and 8M urea as control simulations. The simulations lasted for 300ns and were performed at two different temperature, 310 and 373 K. Because of the complex nature of DESs structures and to ensure the reproducibility of the data, all the simulations were carried out in duplicates starting from different initial structures and using different velocity seeds.

Before the production simulations, all the systems were equilibrated for 10ns. Pure reline density measured after the equilibration was 1.203 g.cm^{-3} which is very close to the value measured experimentally (1.197 g.cm^{-3}) (241). The agreement between these two values indicates a well equilibration of reline systems. Reline density remained stable throughout the 300 ns of the production simulations.

Overall, a total of 40 MD simulations were carried out which incorporate one of the most comprehensive theoretical investigations of lipase in DESs because of its longer time scale than the previous investigation in literature and because of allocating both of lipase conformations (242).

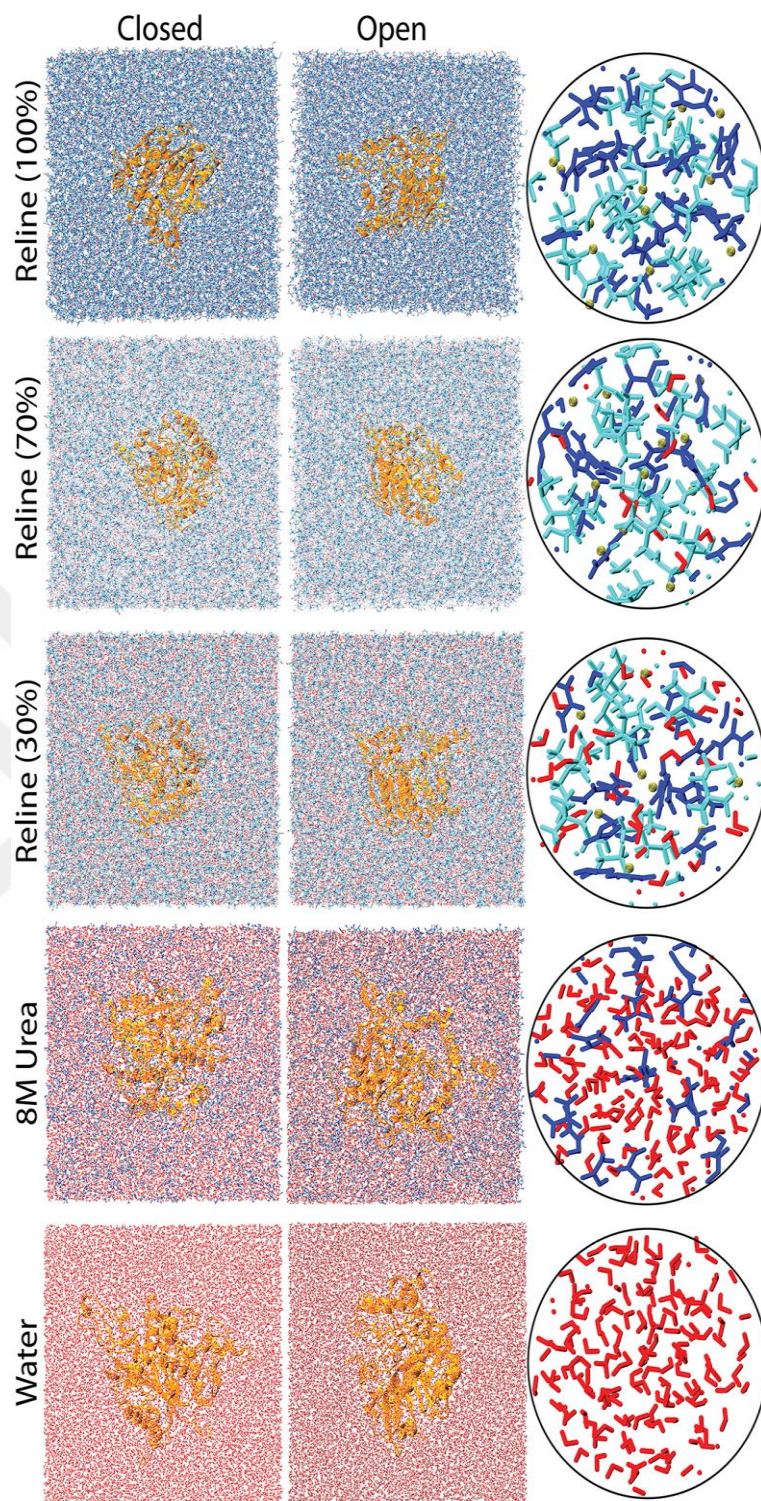


Figure 17. Snapshots of the equilibrated systems before MD simulations. The circled illustrations represent a closed-up view of a licorice representation of the solvent molecules (choline: cyan, urea: blue, chloride: yellow, and water: red).

4.2.1 Stability of lipase backbone in different reline formulations

To evaluate the convergence of the simulated systems, RMSD of lipase backbone atoms was calculated. Regardless of the lid structure or the simulation temperature, no significant movement of lipase backbone atoms was observed in any of the reline formulations. On the other hand, no significant deviation of lipase backbone was observed in water and 8M urea at 310 K, while a strong destabilization of the backbone was observed at 373 K (**Figure 18**).

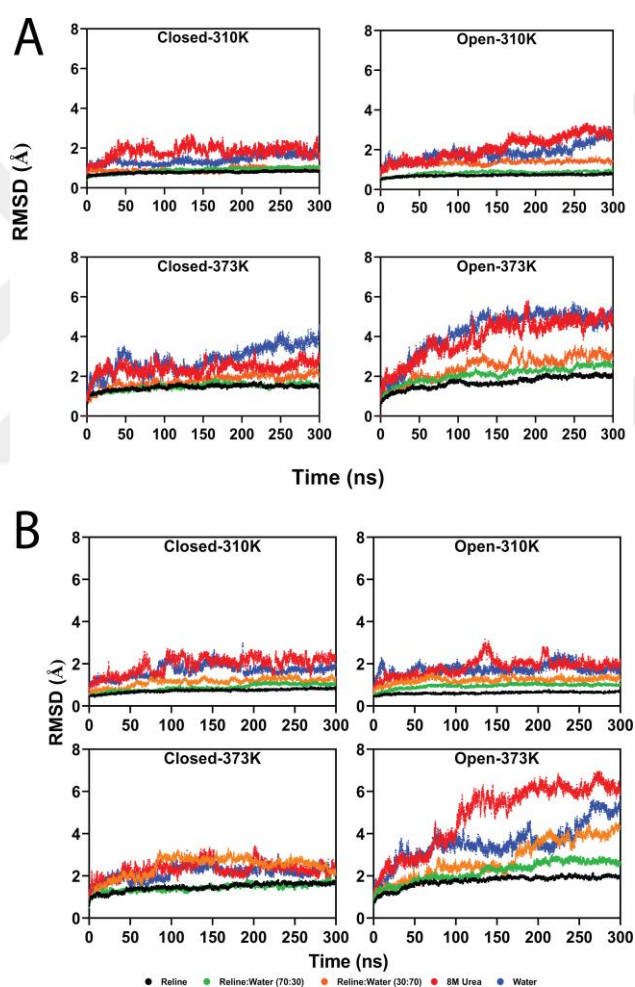


Figure 18. RMSD of lipase backbone atoms. (A) and (B) shows simulations replicates. For all figures, the reference structure was set as the last frame of the equilibrium simulation. (water: blue, 8M Urea: red, pure reline: black, water:reline (30:70): green, water:reline (70:30): orange).

To confirm the convergence of the systems, pairwise RMSD analysis was computed over 10000 frames of the simulations. In line with RMSD profiles, pairwise RMSD plots showed a highly stable lipase backbone in all of the simulations except those performed in water and 8M urea at 373 K (**Figure 19**).

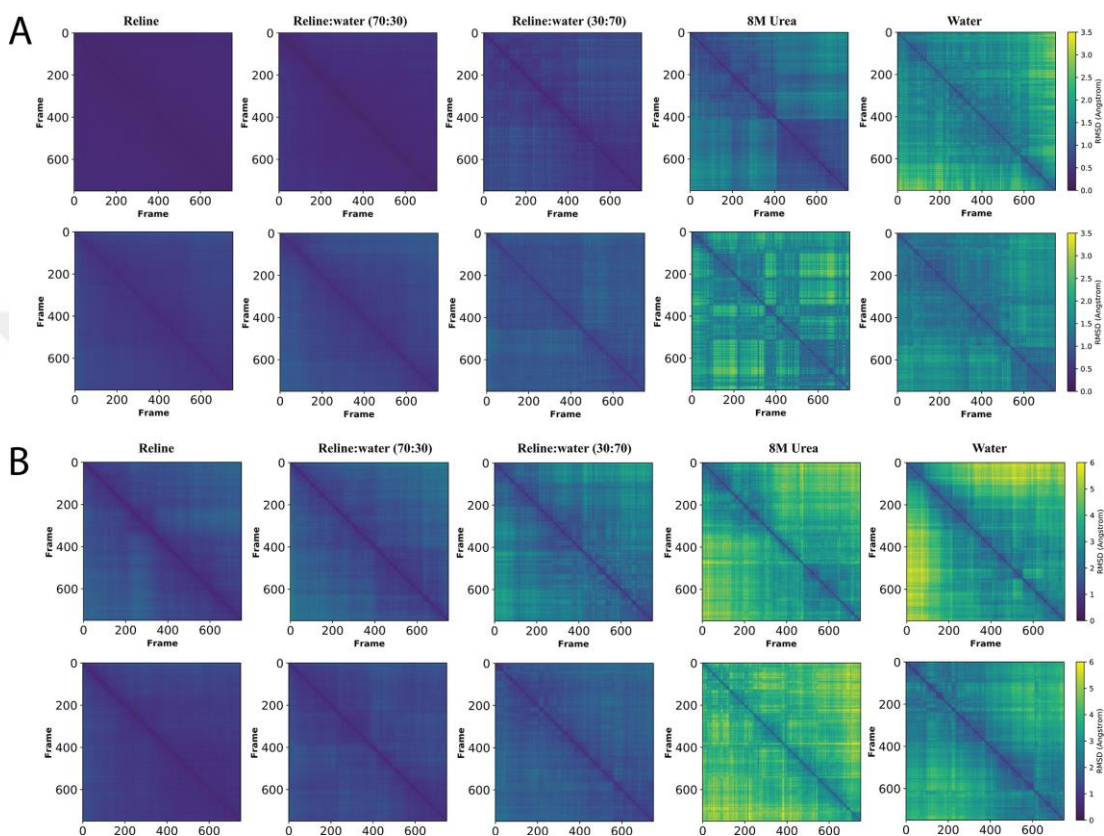


Figure 19. Pairwise RMSD plots of lipase backbone C-alpha atoms. (A) and (B) shows 310 and 373 K simulations respectively. For both subfigures, top and bottom panels show open and closed conformations, respectively

4.2.2 Flexibility of lipase backbone in different reline formulations

To assess the flexibility of lipase backbone in response to the change in reline formulations, the fluctuations of the backbone C-alpha atoms were analyzed. At 310 K, pure reline was found to freeze the backbone of the lipase as very limited fluctuations ($<1\text{\AA}$) were observed (**Figure 20**). Although higher fluctuations are naturally anticipated at high temperature, interestingly, only very slight increase in lipase backbone mobility ($\sim 1\text{\AA}$) was observed in reline at high temperature. This

freezing effect was found to decrease with increasing the hydration level of reline (Figure 20). On the other hand, at 310 K, higher fluctuations of lipase backbone were observed in 8M urea and water simulations which were found to significantly increase at high temperature (Figure 20). No significant differences in the flexibility profiles of the open and the closed structure of lipase were observed.

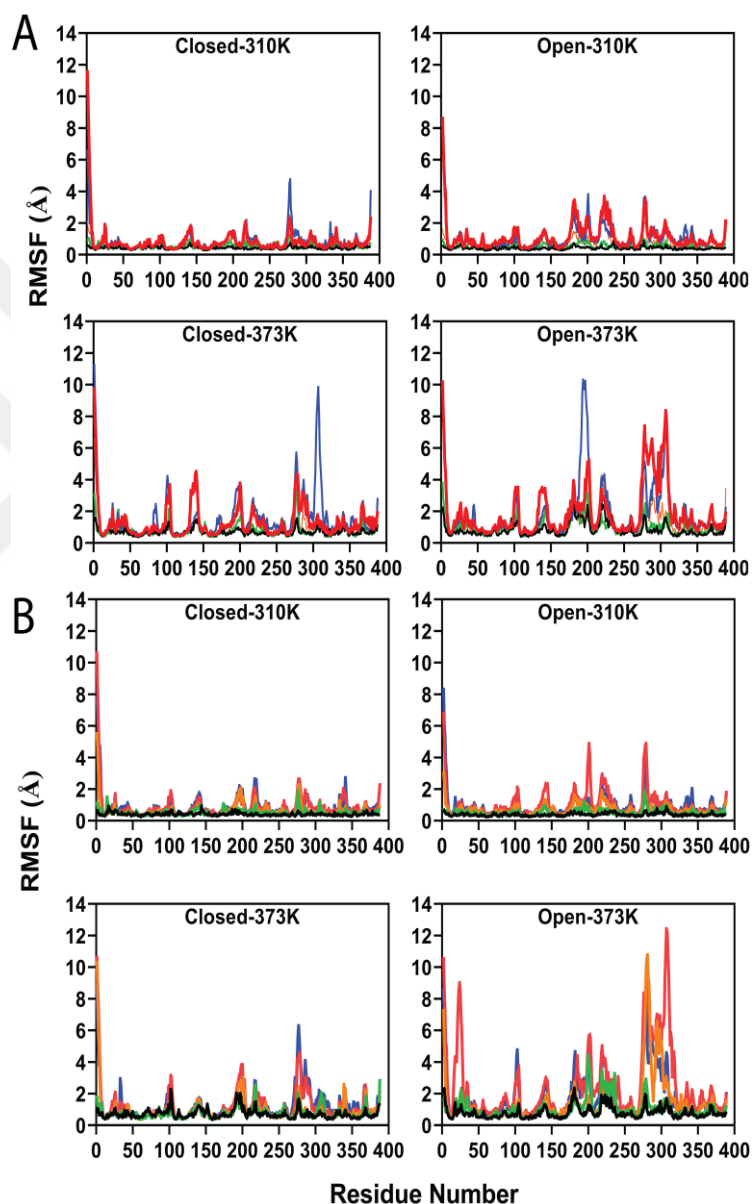


Figure 20. RMSF analysis of lipase backbone in different reline formulations. (A) and (B) show replicate simulations.

4.2.3 Compactness of lipase structure in different reline formulations

To evaluate the effect of different reline formulations on the compactness of lipase structure, the radius of gyration (R_g) of lipase was measured. R_g plots showed a highly compact structure of lipase in reline at both low and elevated temperatures (**Figure 21**). Adding more water to the reline formulation was found to reduce the compactness of lipase structure especially at high temperature. On the other hand, higher R_g values of lipase structure were observed in water and 8M urea indicating low stability of lipase in these two solvents. The destabilizing effects of 8M urea and water was found to increase at high temperature. These observations are valid for both of the lipase structures, albeit less pronounced for the open conformation. An exception from these observations is the highly compact structure of the open conformation in water at high temperature which could be due to a collapsed and unfolded lipase structure (**Figure 21**).

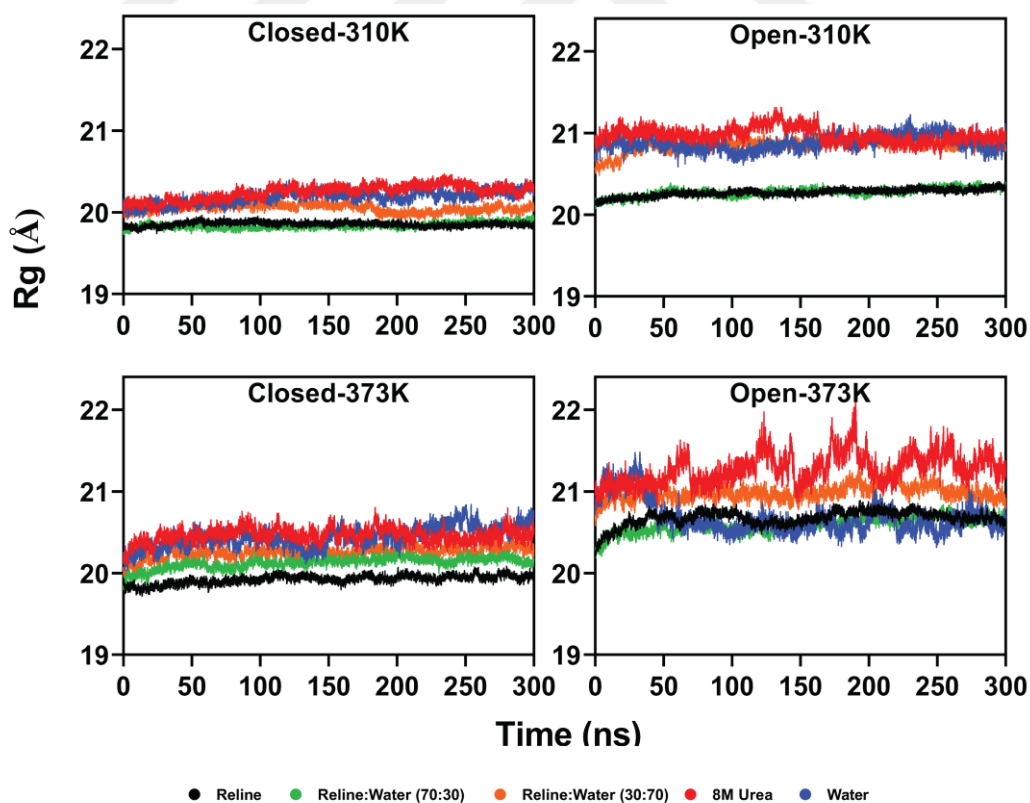


Figure 21. R_g analysis of lipase backbone in different reline formulations.

4.2.4 Solvent accessible surface area of lipase in reline formulations

To gain more insights on the effect of reline formulations on lipase structure, the change in lipase solvent accessible surface areas (SASA) in different solvents was measured. No significant changes in the SASA of both of the lipase structures were observed in pure reline regardless of the simulation temperature (**Figure 22**). The addition of water to reline resulted in a marked increase in the SASA which was more pronounced at high temperature. On the other hand, a significantly increased SASA of both of lipase structures was observed in water and 8M urea at both low and high temperatures, suggesting a disturbed structure of lipase in these two solvents. It is also noteworthy that the SASA of lipase in highly hydrated reline was strikingly similar to those of lipase in water and 8M urea (**Figure 22**).

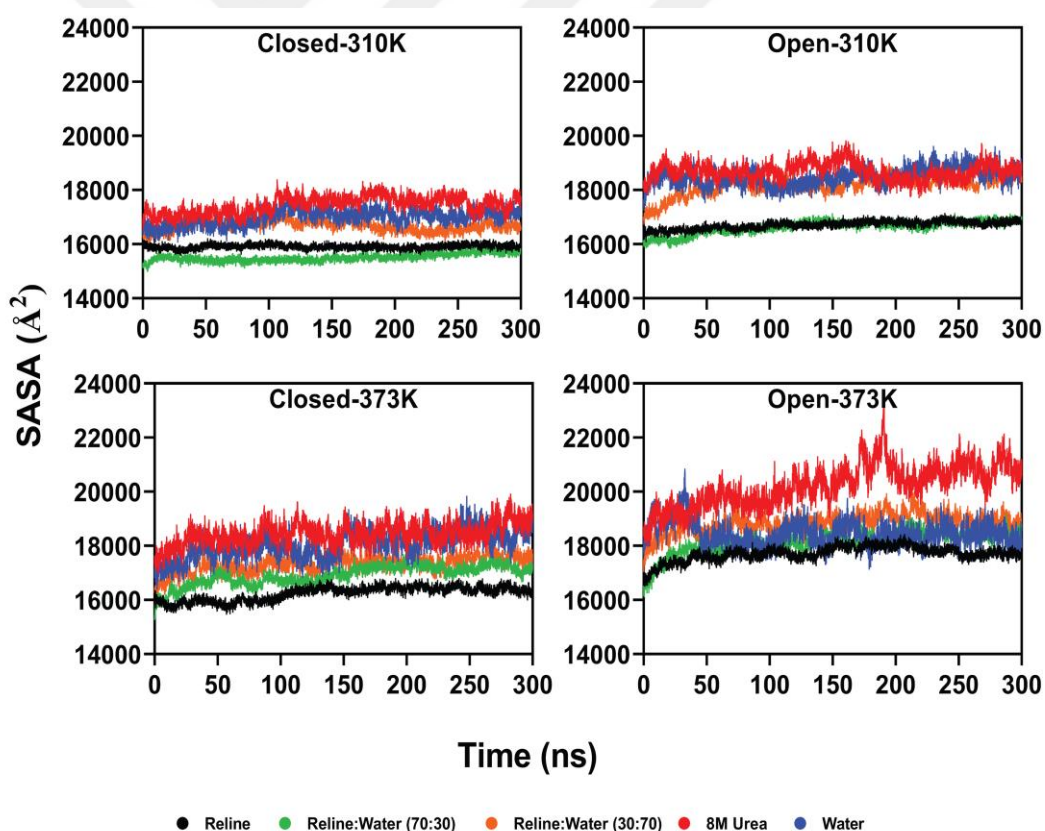


Figure 22. Change of lipase SASA analysis of in different reline formulations.

4.2.5 Essential dynamics of lipase in different reline formulations

To assess the dynamics of lipase structure in different reline formulations, principal component analysis (PCA) was carried out for all of the production simulations. As indicated by scree plots of the PCA, the first two components had the highest variance (**Figure 23**). Therefore, they were used to delineate the dominant motion of lipase throughout the simulations time.

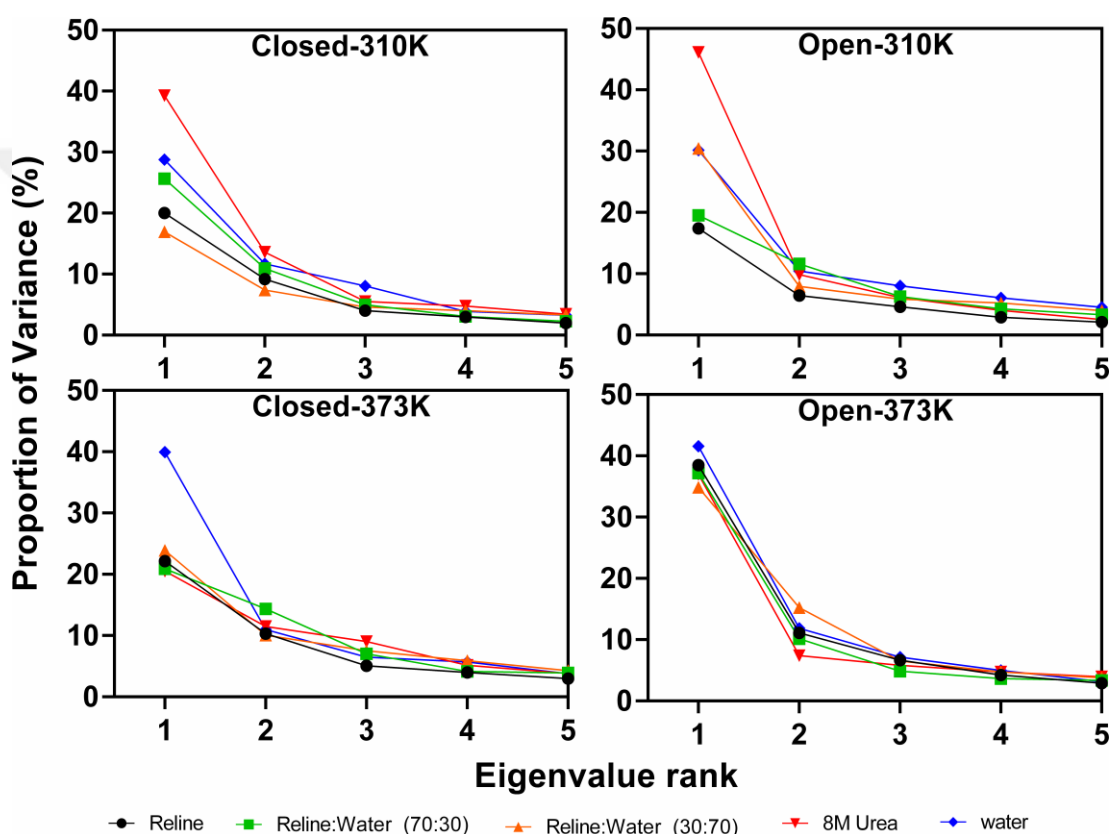


Figure 23. Scree plots of the PCA of production trajectories showing the first five principal components.

PCA plots showed that both of the lipase structures sampled a very limited conformational space in reline at both low and high temperature (**Figure 24**). The number of conformations sampled by lipase was found to gradually increase by the addition of water to reline. On the other hand, both of lipase structures spanned very large conformational space in water and 8M urea indicating a significant destabilization of lipase structure in these two solvents (**Figure 24**)

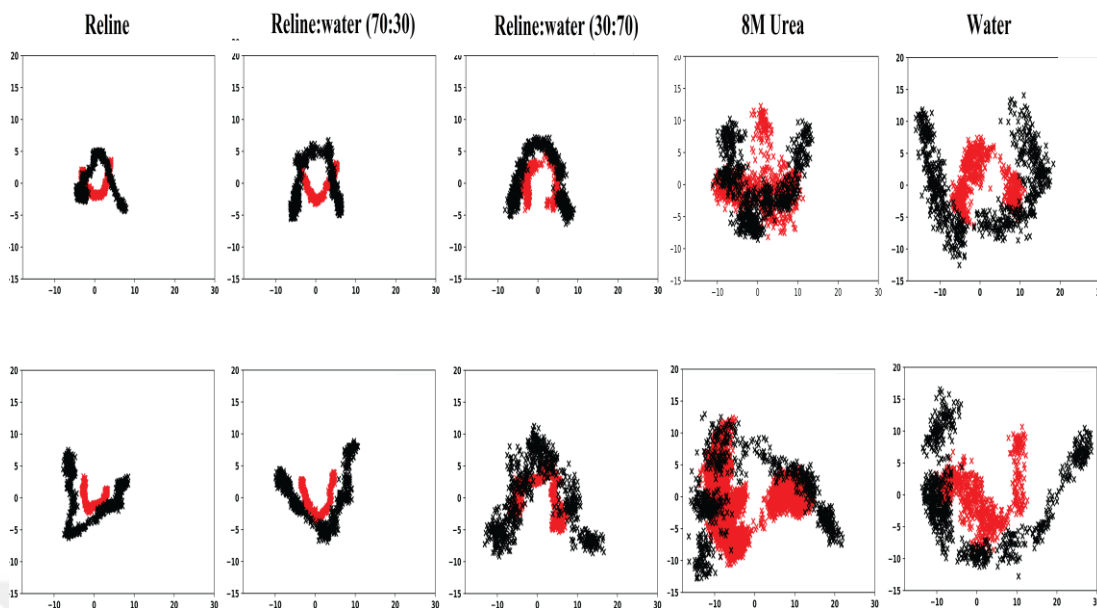


Figure 24. Plots of the top two principal components. Top panel indicates the closed structure and bottom panel indicates the open structure. the red color represents 310 K simulations and black color represents high 373 K simulations.

4.2.6 Contact maps analysis of lipase in different reline formulations

To evaluate the changes in lipase overall structure during the simulations, contact maps of the first and last frame of the simulations were constructed and compared. At 310 K, none of the solvents led to any significant changes the native contacts of any of lipase structures (**Figure 25**). On the other hand, at 373 K, noticeable changes in the native contacts of both of the structures were observed only for the β -flap domain in 8M urea and water (**Figure 26**). These observations are consistent with the structural visualization of lipase flexibility at low and high temperatures.

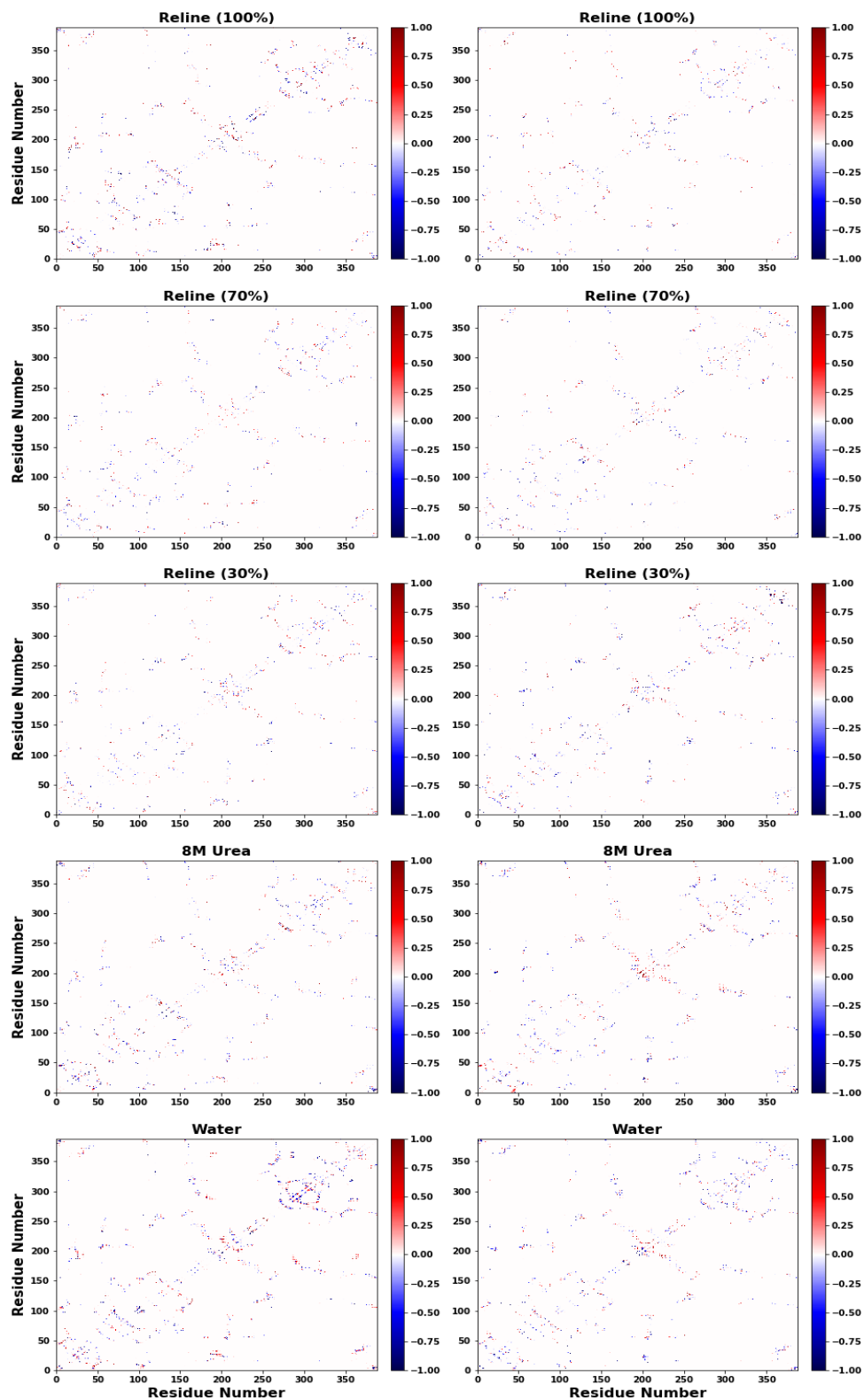


Figure 25. Contact map analysis of lipase at 310 K. Blue points indicates the initial contacts that were lost after the simulations while red points indicate those that formed after simulations.

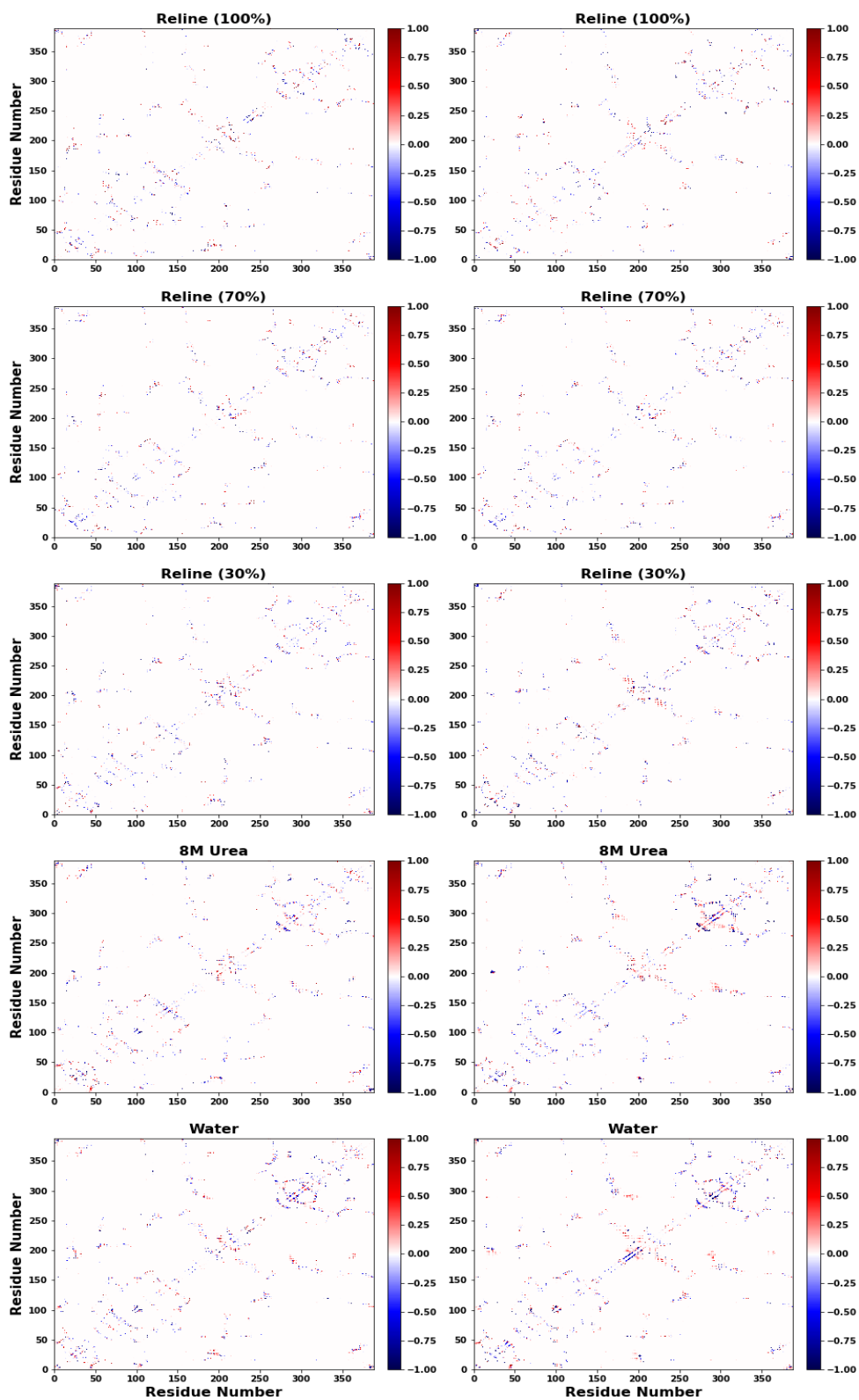


Figure 26. Contact map analysis of lipase at 373 K.

4.2.7 Identification of lipase regions stabilized in reline

To unravel the regions of lipase stabilized in reline, the residue contributions to lipase dynamics were analyzed and the change in overall structure of lipase were visually analyzed throughout the simulation (**Figure 27-29**). For both of lipase structures, three different domains were identified to be highly stabilized in pure reline. These are (i) the N-terminal region, (ii) the β -flap domain (270-320) and (iii) the lid domain (170-245) (**Figure 27**). For both structures, increasing the simulation temperature and/or the hydration level in reline led to a significant increase in the fluctuations of these three regions (**Figure 27 and 29**).

On the other hand, the maximum fluctuations of these three domains were observed in 8M urea and water at 373K (**Figure 27 and 29**). Differences in the degree of flexibility of these regions were observed between the two lipase structures. For instance, regardless of the temperature or the solvent, the lid-domain was found to be the most fluctuating region in the open structure, while the β -flap region was found to be the most flexible domain in the closed conformation (**Figure 27**). However, combining high water content in reline with high temperature of the simulation rendered both the lid-domain and the β -flap region highly flexible in both of the conformations (**Figure 29**).

Despite the high flexibility of the β -flap domain of the closed form in hydrated reline, the flanking α -helix harboring the catalytic Asp318 did not show any significant motion (**Figure 27**). Interestingly, this flanking α -helix was found to be strongly destabilized in water at high temperature suggesting a negative effect of water on the catalytic activity of lipase at high temperature.

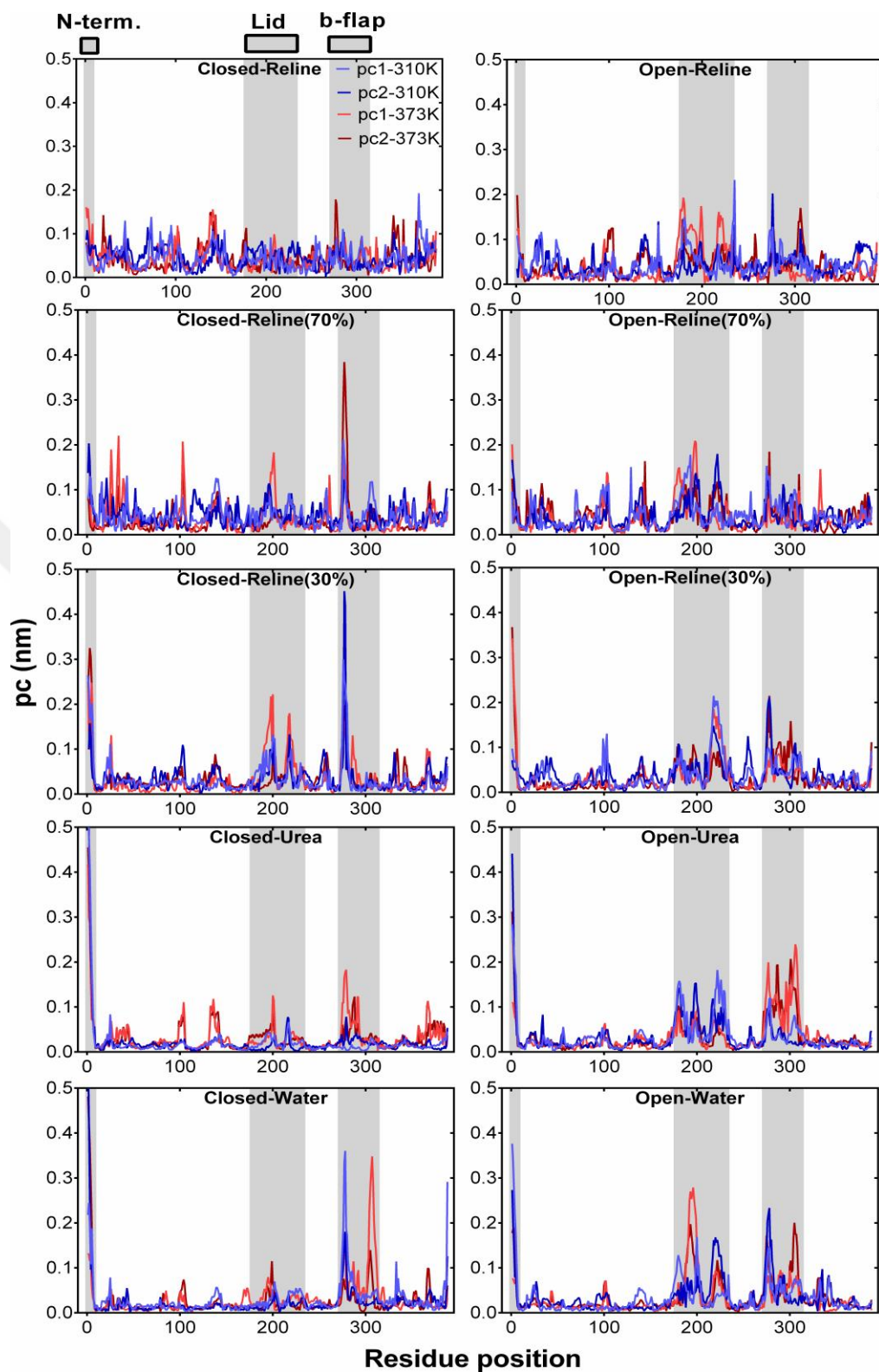


Figure 27. Residue contribution to the first two principal components. The shaded regions corresponding to the β -flap domain, N terminal, and the lid region mark the highest contributions.

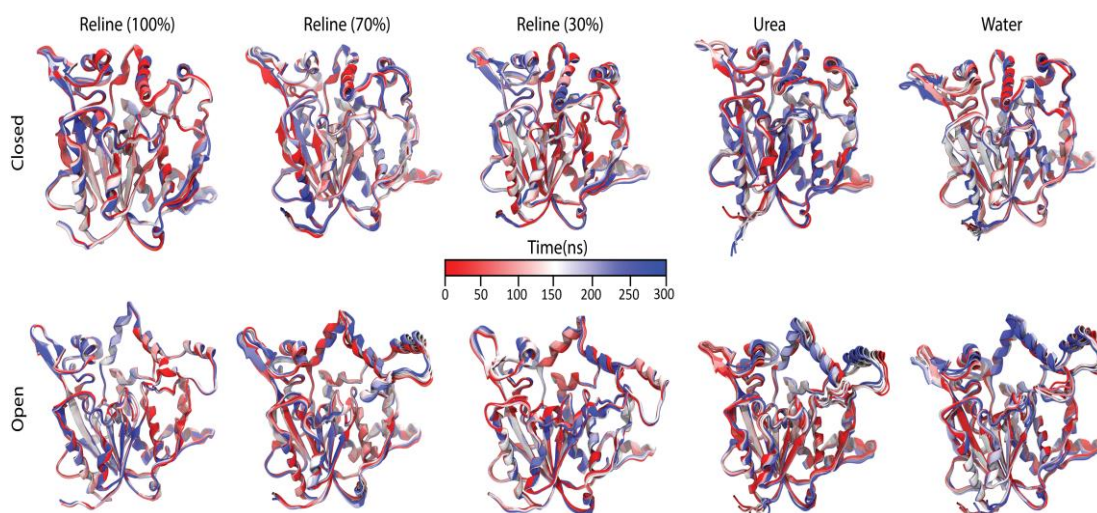


Figure 28. Reduced trajectory of the 310 K simulations. N-terminal region (purple), B-flap domain (red) and the lid region (blue).

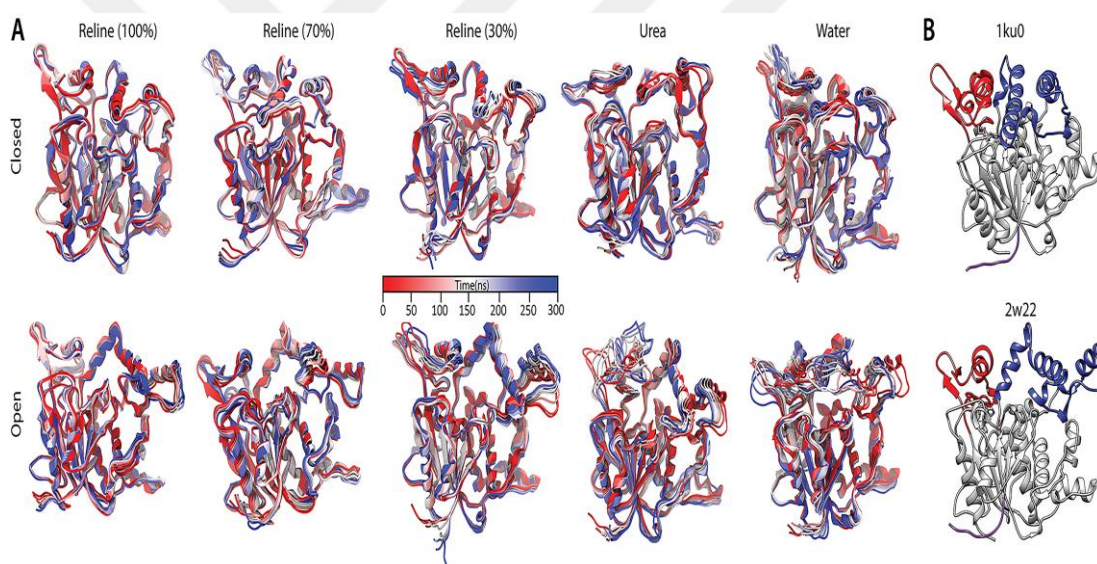


Figure 29. Reduced trajectory of the 373 K simulations. N-terminal region (purple), B-flap domain (red) and the lid region (blue).

4.2.8 Stability of lipase catalytic machinery in reline formulations

To assess the stability of the lipase catalytic machinery in different reline formulations, the interatomic distances between the catalytic triad and the radius of gyration of the catalytic site were measured (**Figure 30-32**). The catalytic machineries of both of the structures were highly compact in all of the solvents at 310 K, while

they became less compact in hydrated reline, 8M urea, and water at high 373 K (**Figure 30**). On the other hands, no significant changes in the catalytic triad distances were observed in any of the reline formulations regardless of the simulation temperature or the lid structure (**Figure 31 and 32**). In contrast, 8M urea and water was found to significantly disturb the interactions between the catalytic Asp and His of both of the structures at low and high temperature (**Figure 31 and 32**). Additionally, urea was found to destabilize the interaction between the catalytic Ser114 and Asp318 of the open form at 310 K and the interaction between the catalytic Ser113 and His 358 of the closed form at 373 K (**Figure 31 and 32**).

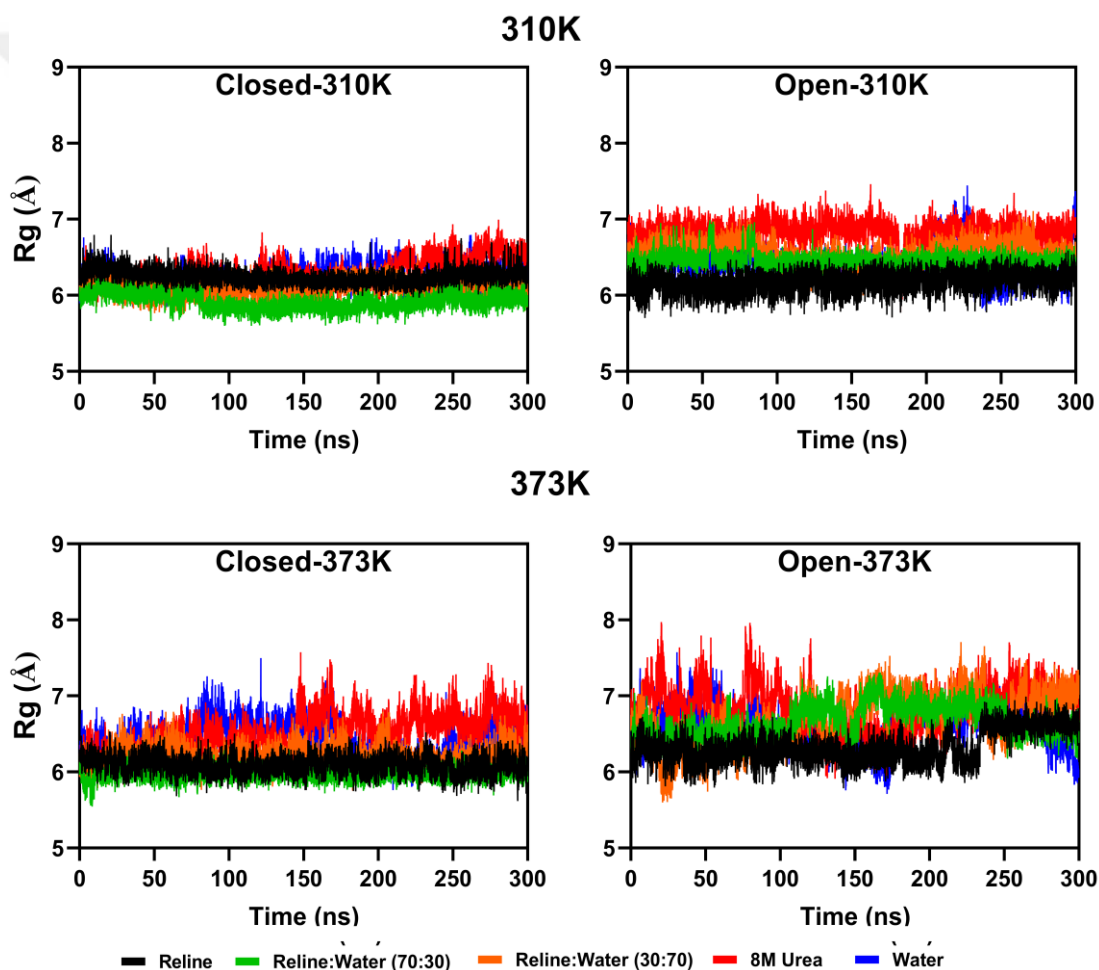


Figure 30. Rg of the catalytic machinery of lipase.

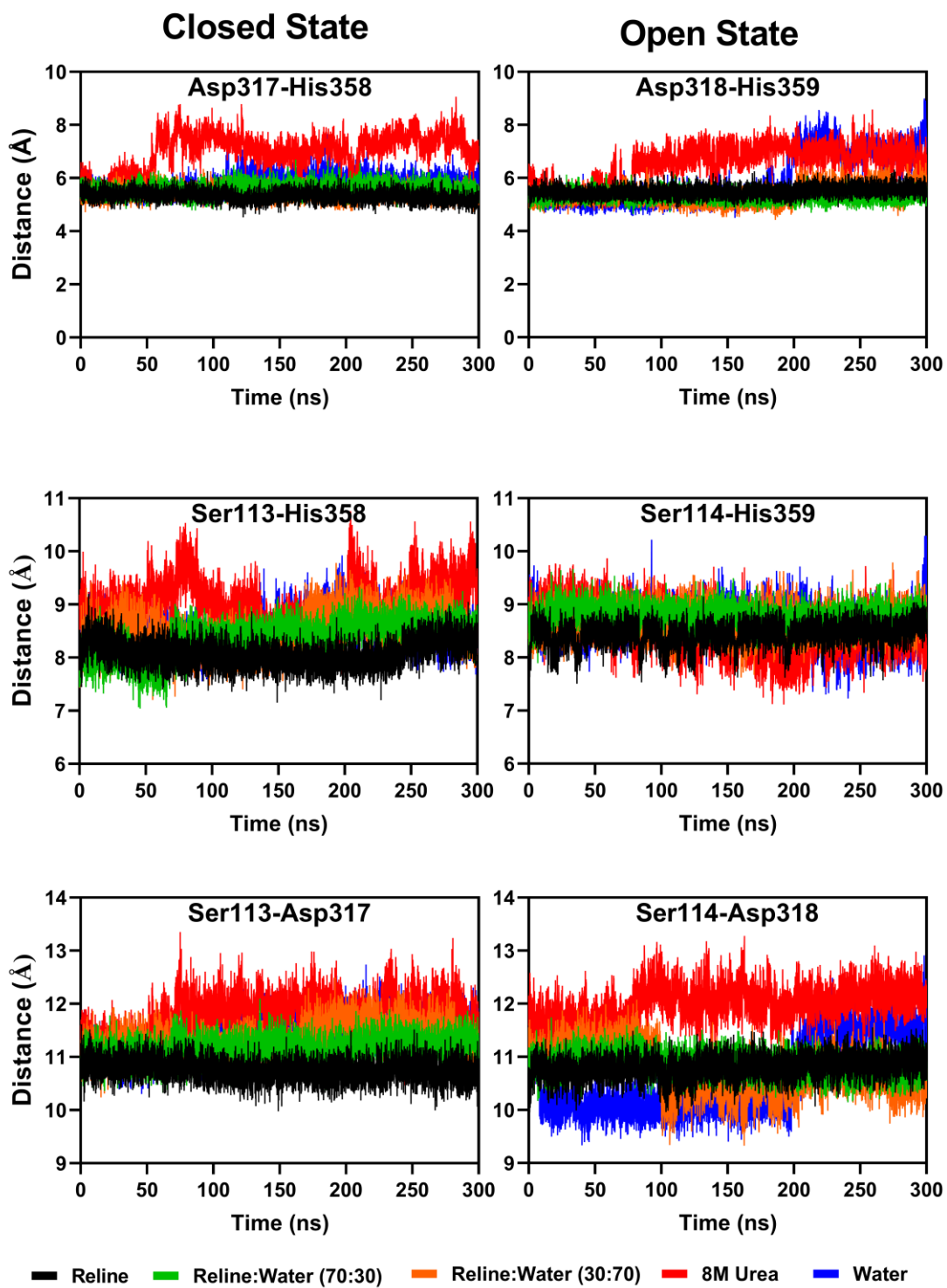


Figure 31. Distances between the catalytic triad C-alpha atoms at 310 K.

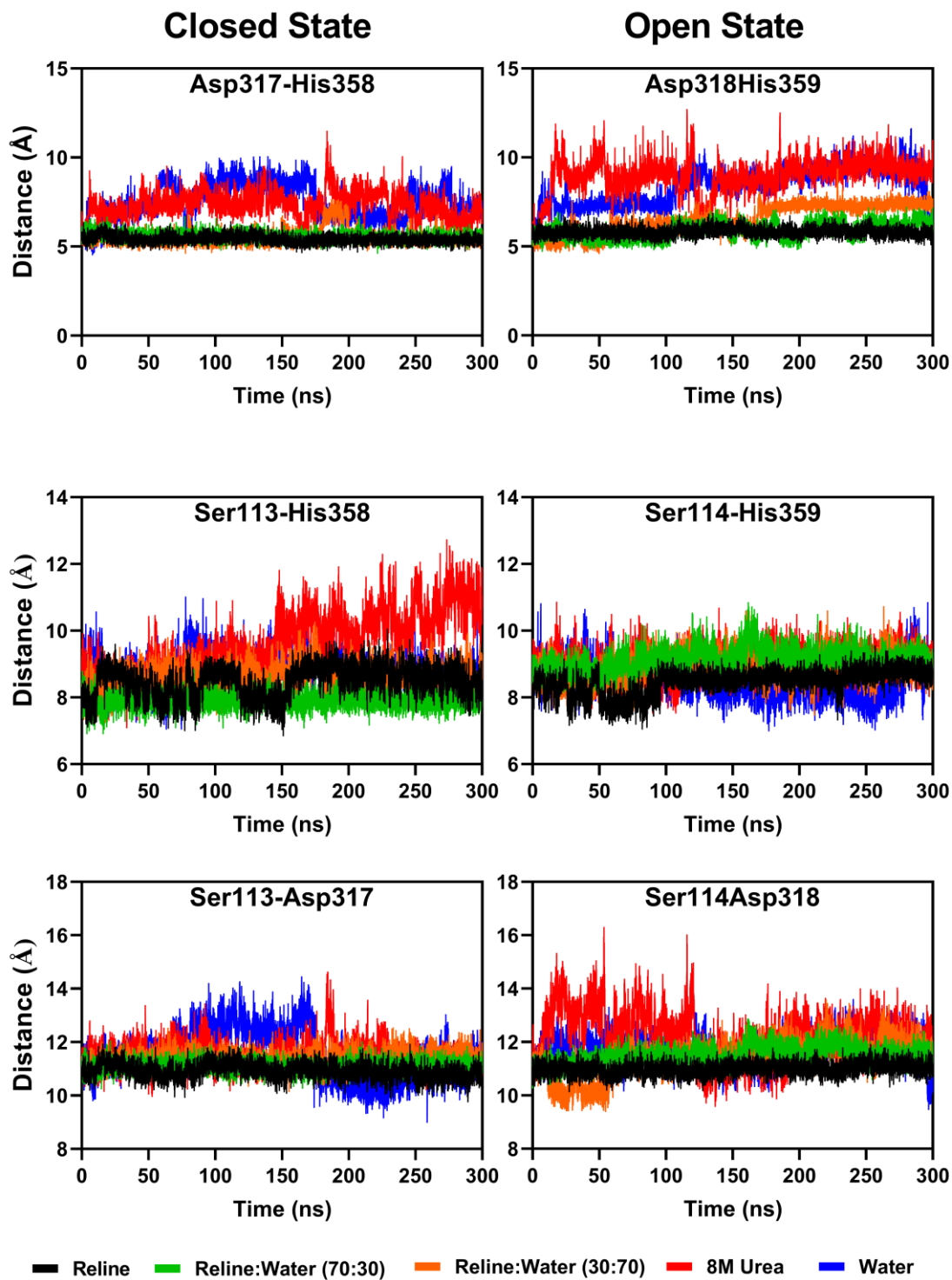


Figure 32. Distances between the catalytic triad C-alpha atoms at 373 K.

4.2.9 The effect of water and temperature on lipase-reline interactions

To investigate how water and temperature affect the interactions between lipase and reline, the arrangement of reline around lipase was analyzed by calculating the center of mass radial distribution functions (COM-RDF) between the reline moieties and lipase (**Figure 33**). A small peak at ~ 2 Å was observed in the COM-RDF plots of lipase in hydrated reline, water, and urea, while it was not observed in pure reline. Moreover, the following peaks observed in hydrated reline, water and urea were larger in size than those observed for pure reline. These observations basically suggest a diffusion of the solvent molecules into the lipase core in case of hydrated reline, urea, and water. Despite the differences in the measured SASA and R_g between the closed and the open conformations, no discernible difference in their solvation shells was observed. This identical COM-RDF plots indicates that the diffusion of solvents into the lipase core is not because of the opened lid; instead, due to the change in the solvent formulation. These results are valid for both low and high temperature simulations.

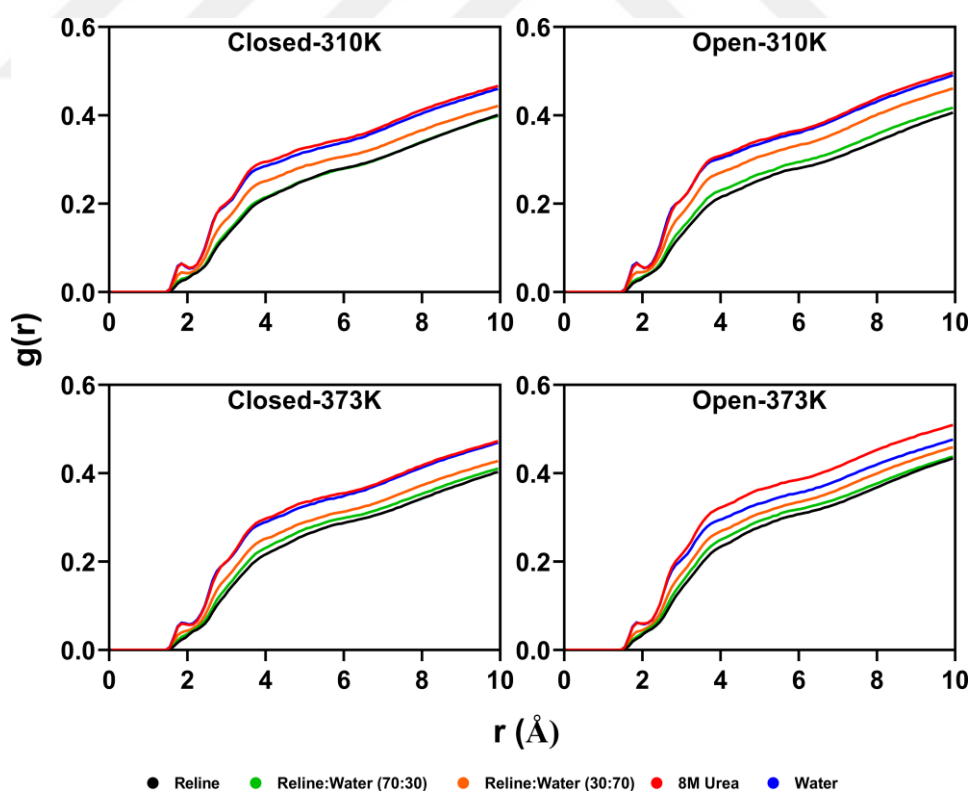


Figure 33. COM-RDF analysis of lipase and solvents.

To further investigate the diffusion of the solvent moieties into the lipase core, the number of solvent molecules in close vicinity to the catalytic site ($<5 \text{ \AA}$) was calculated (**Figure 34-35**). Smaller solvent moieties such as urea and water were found to diffuse into the lipase catalytic cleft in case of the hydrated system. Generally, the diffusion rate of water was higher than urea, and as the hydration level of reline or temperature increased, higher diffusion rates of both water and urea were spotted. Additionally, the diffusion rate of solvent moieties into the closed conformation core was lower than the diffusion into the open conformation core, an observation that can account for the lower flexibility of the closed conformation than the open one. On the other hand, for both of the structures, no diffusion of the solvent moieties into the core was observed in pure reline regardless of the simulation temperature, an observation that indicates a more arranged nanostructure of pure reline than the hydrated ones.

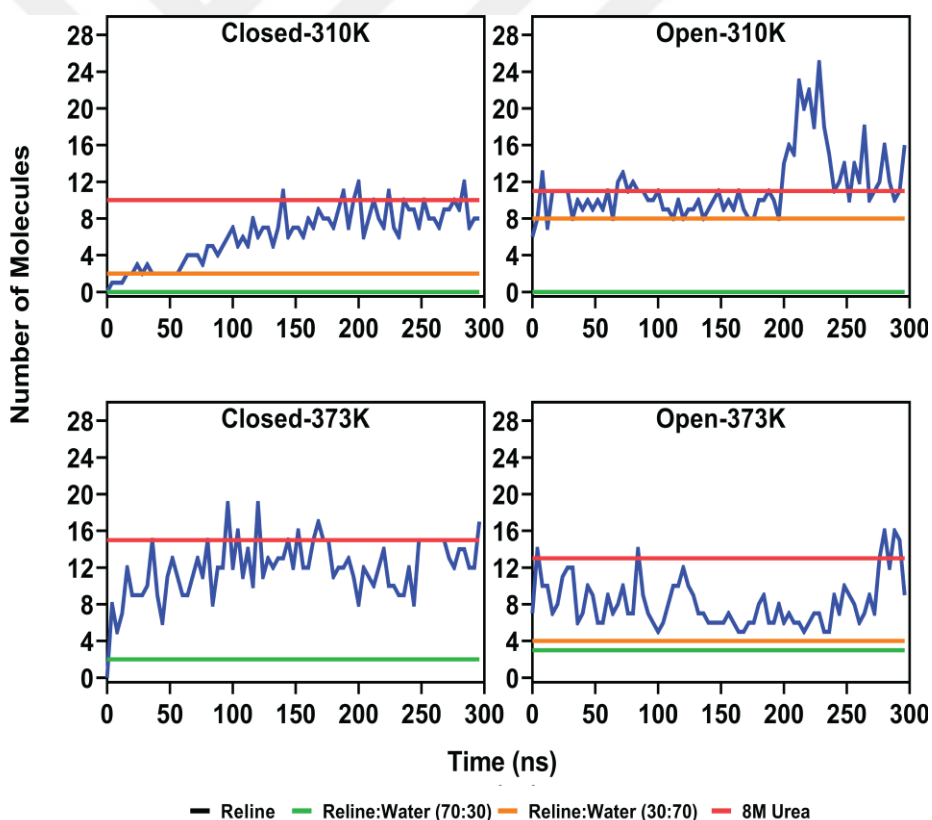


Figure 34. Number water molecules in close contact with any of the catalytic site.

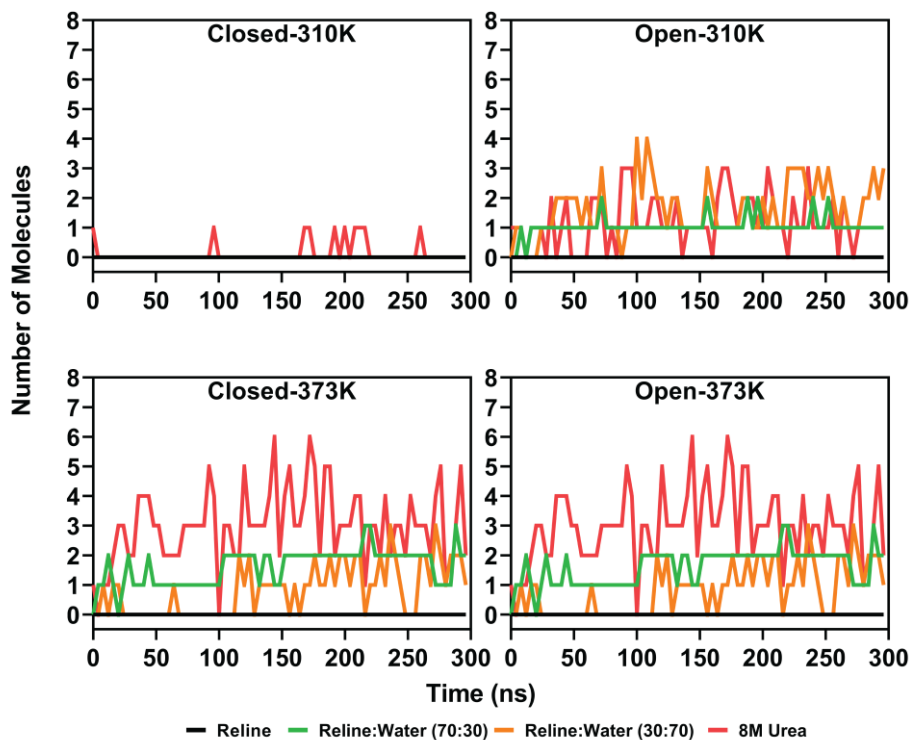


Figure 35. Number urea molecules in close contact with any of the catalytic site.

4.2.10 The effect of hydration level on reline nanostructure

To investigate how the water content and temperature affect reline nanostructure, the COM-RDFs between the solvent molecules were computed (Figure 36-37). COM-RDFs plots showed that reline hydrations disturb the interactions between the solvent components which result in an increase in the self-interactions between the solvent molecules. For instance, the addition of water to reline decreased chloride-choline and chloride-urea interactions while it increased choline and urea molecules self-interactions. These observations which are true for both lipase structures and simulation temperatures suggest that increasing the water level disturbs the eutectic nanostructure of reline.

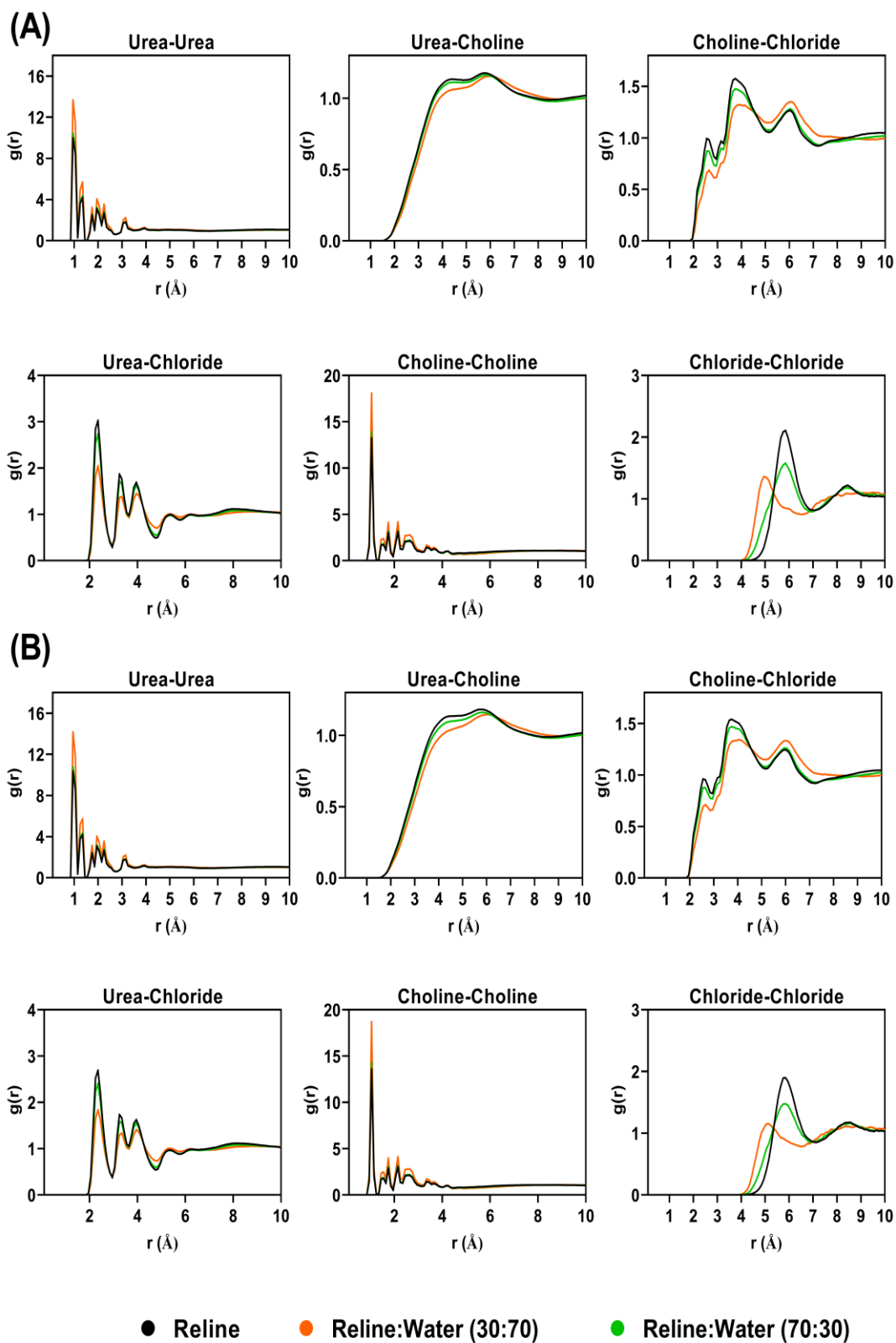


Figure 36. COM-RDF analysis of reline molecules around the open conformation at (A) 310K and (B) 373 K.

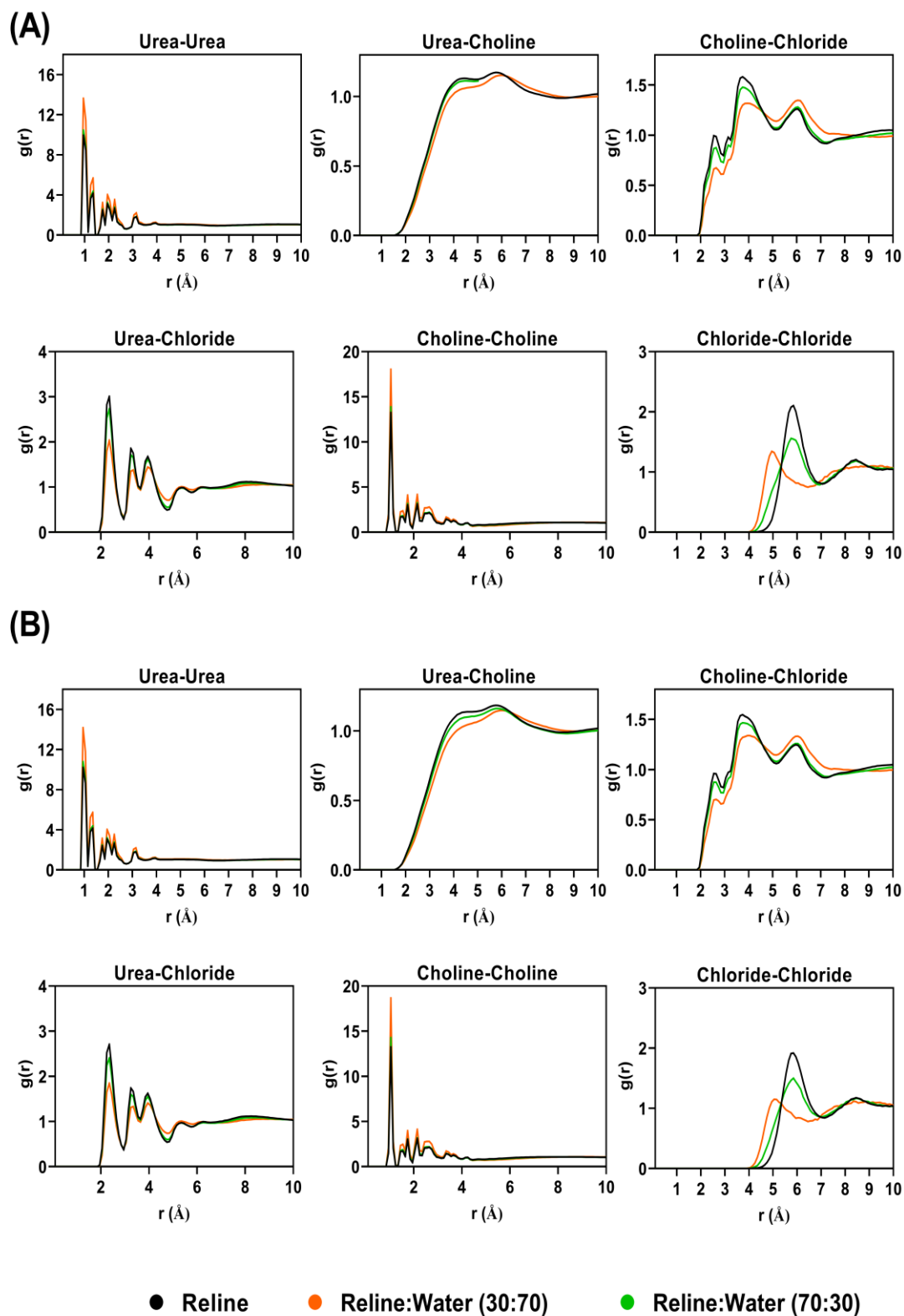


Figure 37. COM-RDF analysis of reline molecules around the closed conformation at (A) 310K and (B) 373 K

To investigate the dominant interactions in reline nanostructure, atomic RDFs between reline molecules were also computed (**Figure 38**). Atomic RDFs indicated that the hydrogen bonding between the chloride ion and the hydrogens of urea and the oxygen of choline is the dominant interaction in reline nanostructure. This critical interaction was found to be significantly destabilized upon hydration of reline at both low and high temperatures.

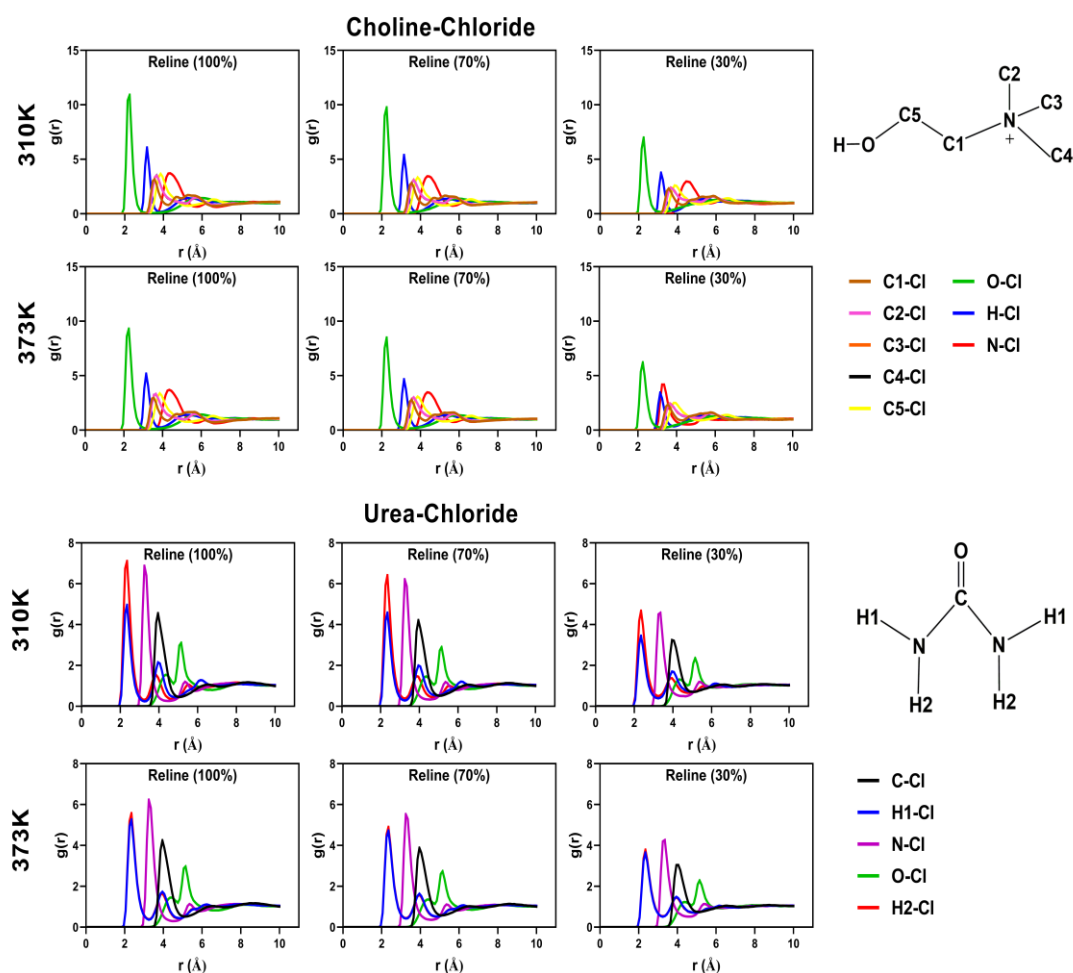


Figure 38. Atomic RDF analysis of reline components.

Given the fact that hydrogen bonding plays a critical role in the stability of reline nanostructures, the hydrogen bonds formed between reline components were analyzed (Figure 39-43) (243). Increasing the water level in reline was found to weaken the intermolecular hydrogen bonding interactions between the solvent components. For instance, increasing the water amount in reline was found to gradually reduce the number of hydrogen bonds formed between choline-urea, chloride-urea, and urea-urea, while it increased those formed between water and urea. Moreover, a parallel decrease in the hydrogen bonds number formed between reline and lipase in response to raising the hydration level in reline. Overall, these observations collectively indicated that water significantly disturbs the nanostructure of reline by competing to interact with its components, while neither high temperature nor the conformations of lipase had an effect on the nanostructure of reline.

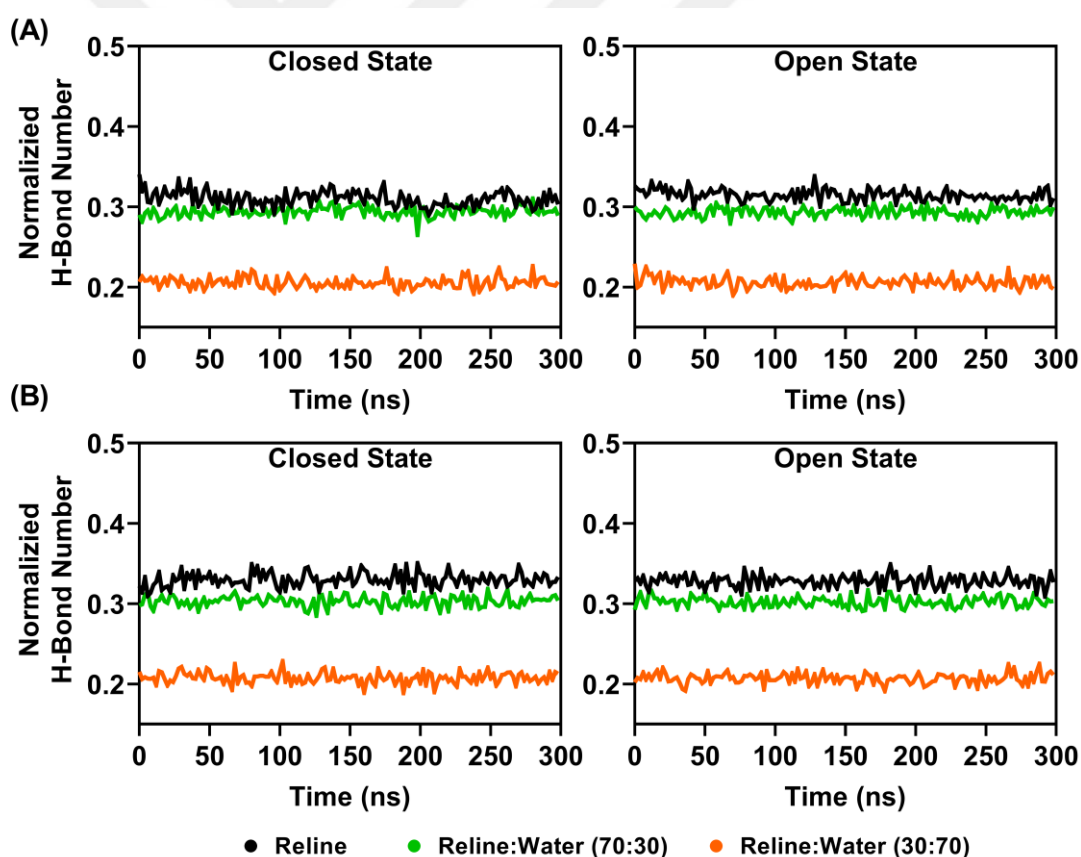


Figure 39. Normalized hydrogen bonds count between urea and choline.

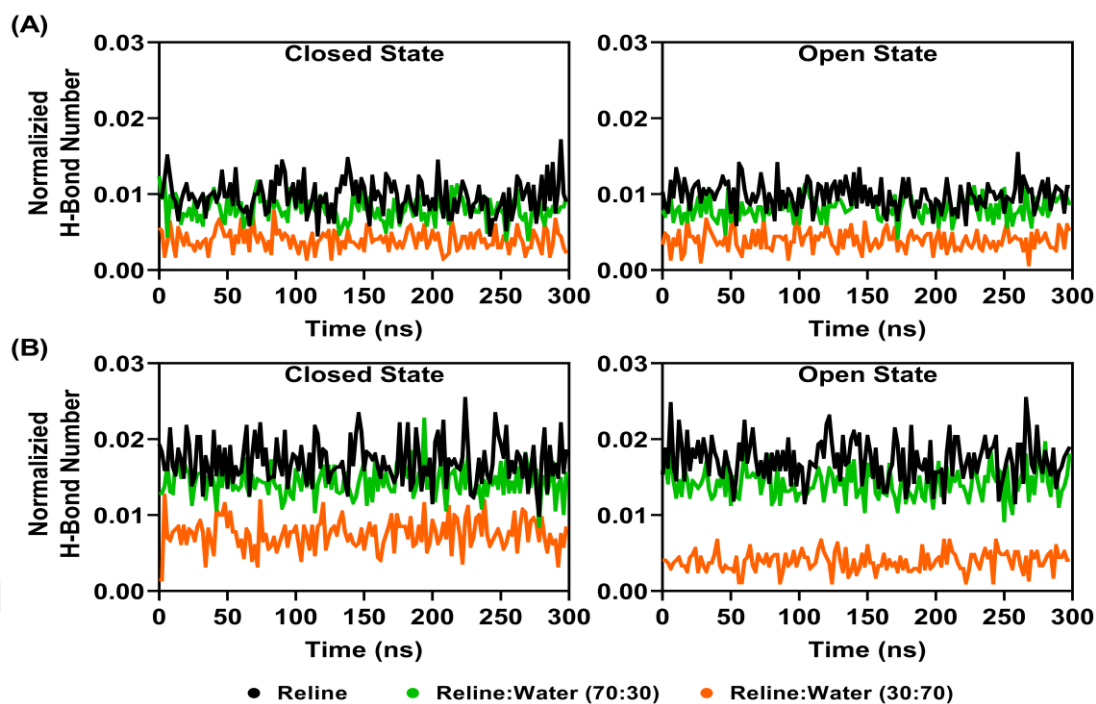


Figure 40. Normalized hydrogen bonds count between urea and chloride.

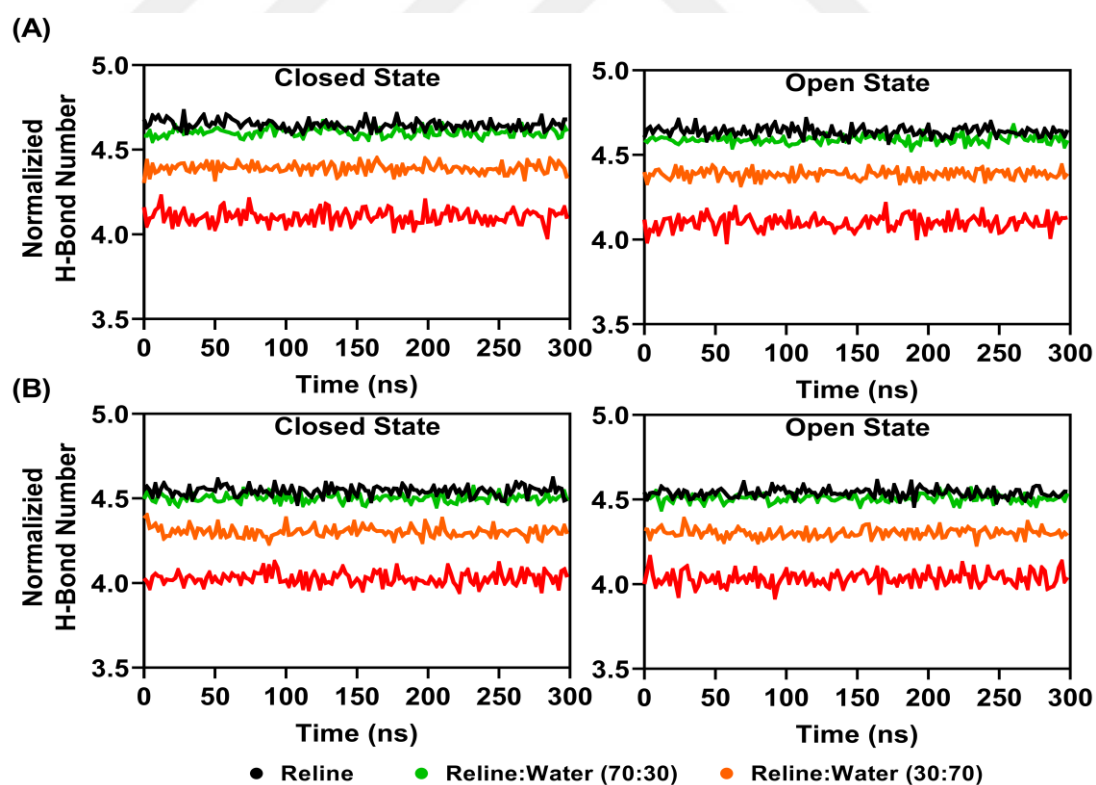


Figure 41. Normalized hydrogen bonds count between urea and urea.

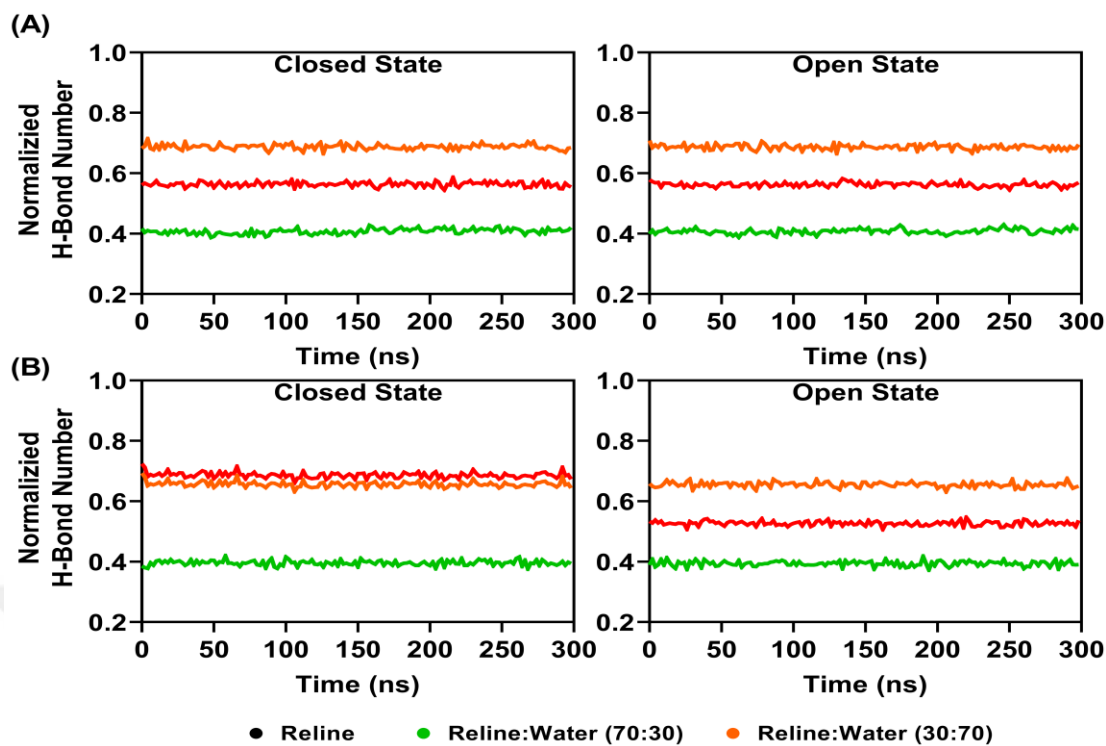


Figure 42. Normalized hydrogen bonds count between urea and water.

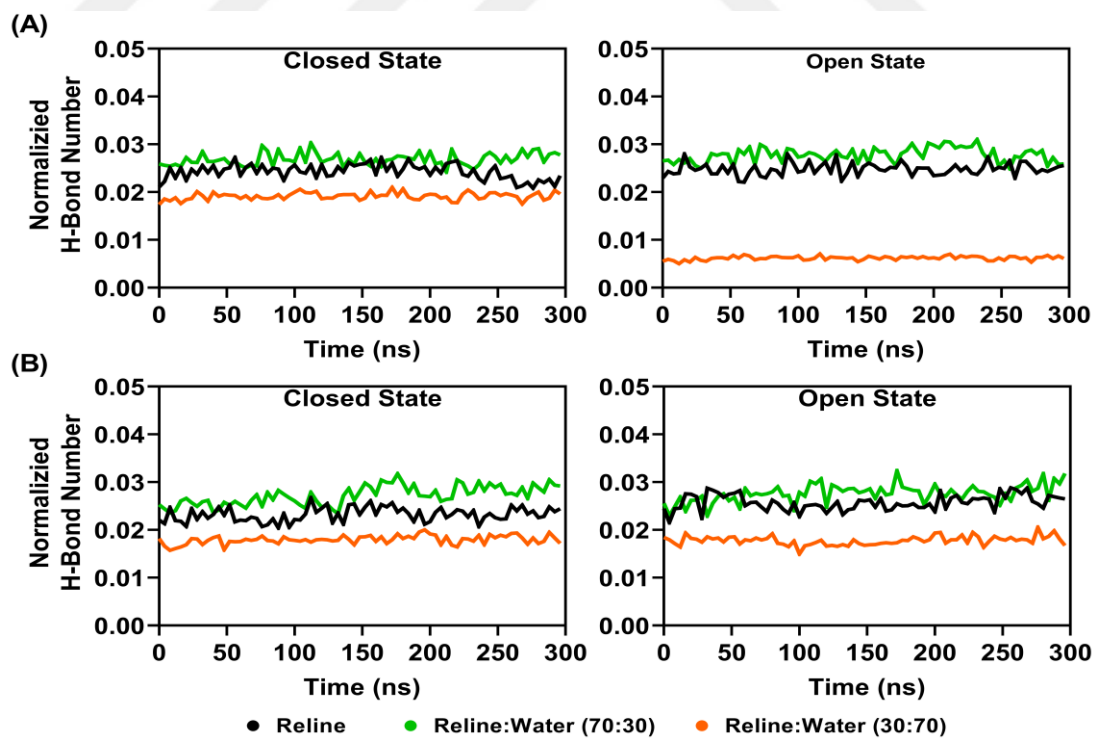


Figure 43. Normalized hydrogen bonds count between lipase and reline.

4.3 Lipase in sodium dodecyl sulfate

To investigate the impact of the anionic surfactant, SDS, on lipase structure and dynamics, all-atom MD systems including either the open (PDB ID: 2W22) or closed (PDB ID: 1KU0) conformations were generated. Because these conformations differ in shape and accessible surface area, recruiting them to our study unequivocally provided us with a deeper understanding of the effects of SDS on the active and inactive forms of thermoalkalophilic lipases.

Four SDS-containing systems were built for sampling both of the lipase conformations at different SDS concentrations. Two control systems in which lipases were dissolved in water without any SDS were also built. After a short equilibration for 5 ns at 298 K and 1 atm, stable densities for all of these 6 systems whose snapshots are illustrated were confirmed, particularly a close agreement of the water systems with the experiments ($d \sim 0.99$ g/L) (**Figure 44**).

Equilibrated systems promptly showed that lipases were embedded in larger boxes of water than those of SDS containing boxes, matching with the relatively higher number of waters in the aqueous systems. However, no additional efforts were put to make the box sizes equal for all systems prior to production simulations. Mainly because of the observation that the lipase structures were sufficiently covered by solvent molecules in every system. Furthermore, given the fact that differences in box sizes are expected to exert negligible effects on protein dynamics, we have progressed with our production simulations using these systems (244).

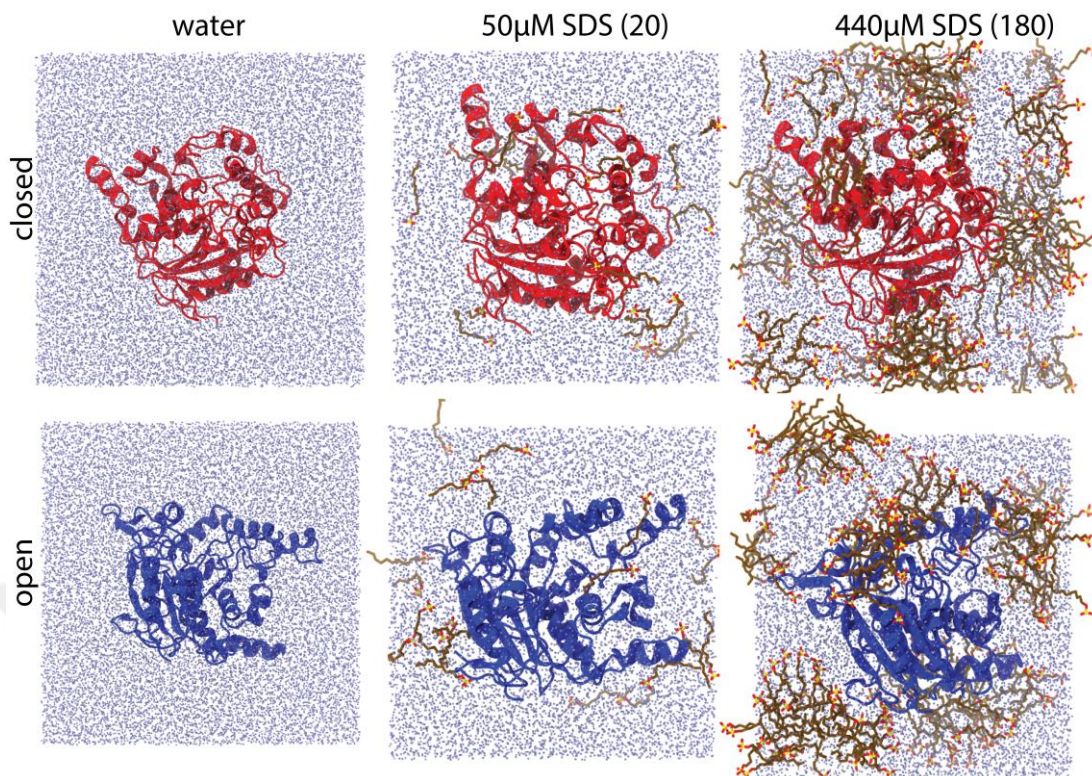


Figure 44. Snapshots of the MD systems were shown after 10 ns of equilibration. Water oxygen: blue CPK, SDS: licorice (C: tan, S: yellow, O: red), open lipase backbone: blue cartoon, closed lipase backbone: red cartoon.

SDS is typically supplied at a concentration of 1-2% (w/v) in the sample preparation buffer of the SDS-PAGE experiments (245). After 10 ns, the systems with 20-SDS reached a concentration around 1.4% (w/v) at 298 K exemplifying the typical denaturing concentration of SDS. Proportional with the increase in the number of SDS molecules, the systems with 180 SDS resulted in a much higher SDS concentration, 12.8% (w/v). However, the concentration reached by 180 SDS-containing systems is still in the range of previous MD studies analyzing protein-SDS interactions, providing us with the opportunity to assess the impact of high SDS concentration on the lipase-SDS interactions (246, 247).

Notably, for the short relaxation period, initially randomly positioned SDS started to self-assemble for the 180-molecule containing system but not for the 20-SDS systems. Following the initial equilibration, all the systems were simulated for an additional 2 μ s, at two distinct temperatures; 298 and 373 K. The reason behind high

temperature simulations is not only to replicate the experimental condition to which protein samples are often exposed during SDS-PAGE experiments, but also to provide the increased kinetic energy required to activate thermoalkalophilic lipases (16). Otherwise, at ambient temperatures, thermoalkalophilic lipases are not activated even if they were introduced to a water-lipid-like interface (155).

To our current knowledge, our simulations have comprised the longest trajectories obtained hitherto for any lipases, including thermoalkalophilic lipases. Overall, 6 different MD systems and their MD simulations at low and high temperatures allowed us to unravel the microscopic effects of SDS accompanied with high temperature on thermostable lipase structures and dynamics.

4.3.1 Stability of lipase backbone in SDS

To assess the convergence of the simulations, all-to-all RMSD of the C-alpha atoms was quantified (**Figure 45**). SDS induced a larger displacement in the C-alpha atoms at 373 K than it did at 298 K for all the systems. Particularly, a dose-dependent effect was noted for both conformations at 373 K while it was not the case at 298 K. The closed lipase at 373 K and in the presence of 180 SDS adapted a different backbone configuration with an RMSD change of 10 Å after 1 μ s. Similar transitions, albeit not as sharp, were observed for the open conformation as well. The backbone of thermoalkalophilic lipases tended to significantly mobilize in SDS containing buffers and at high temperatures. Otherwise, high temperature or SDS presence alone did not alter backbone configurations more than 6 Å. Furthermore, the open conformation showed consistently higher RMSD change than did the closed conformation as a response to temperature and SDS presence, which was in close agreement with one of the previous MD reports (242).

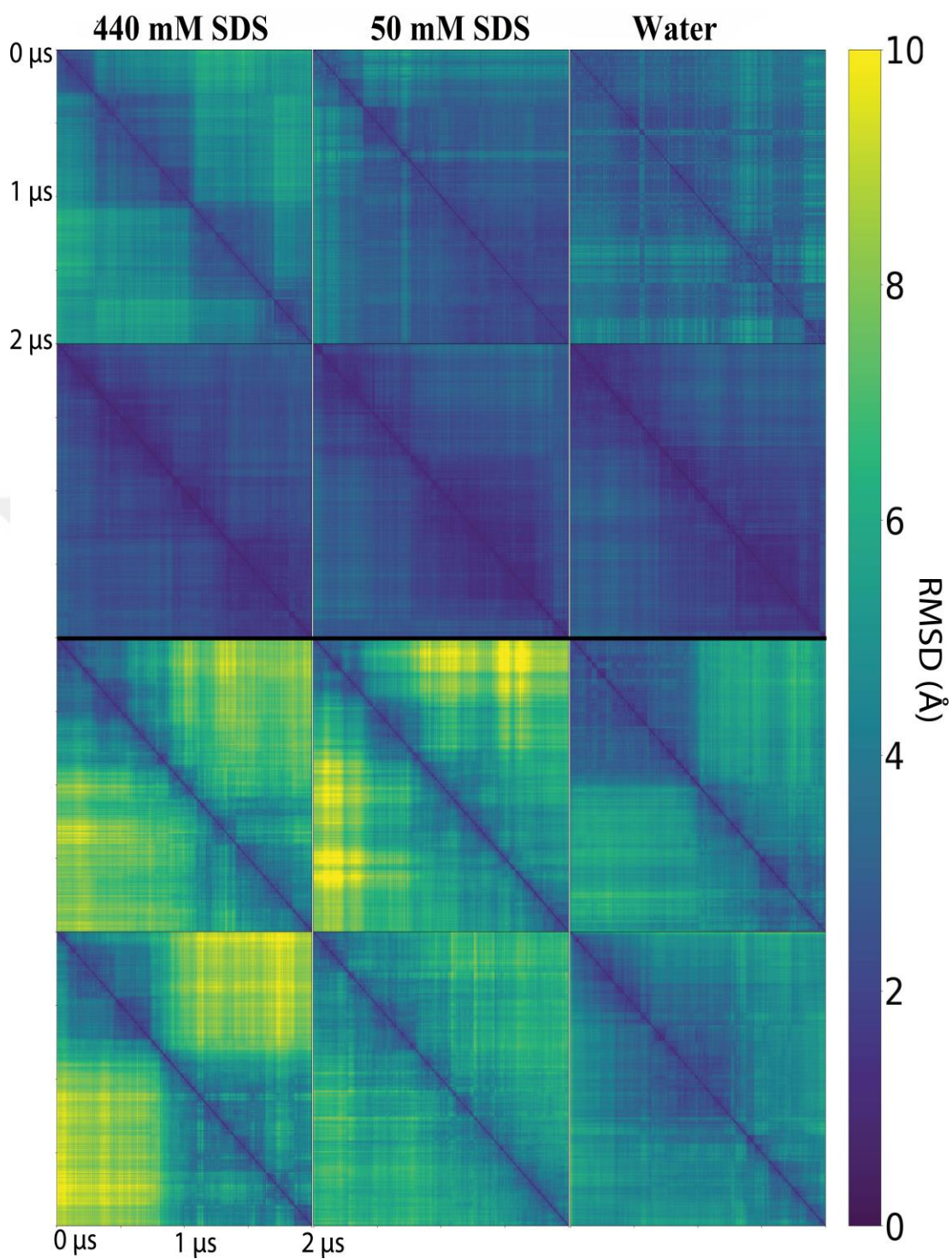


Figure 45. All-to-all RMSD plots of lipase backbone atoms in different SDS concentrations. For both subfigures, top and bottom panels show close and open conformations, respectively.

4.3.2 Compactness of lipase structure in SDS

Despite being limited to only lid domain, interfacial activation also causes notable changes in the overall lipase geometry and surface area (66). The closed conformation adopts a more globular shape with around 160 nm² of exposed surface area than the open conformation which has an increased surface area of 180 nm².

To probe the effects of SDS and/or high temperature on the compactness of the lipase structures, the radius of gyration (Rg) and solvent accessible surface area (SASA) were monitored throughout 2 μ s (**Figure 46**). Consistent with the measurements of the static structures, both Rg and SASA values were slightly higher for the open conformation than the closed conformation. In line with RMSD plots, Rg analysis suggested that the compactness of the lipase structures did not get affected by SDS at 298 K. However, we observed that SDS, particularly when supplied at a high concentration slightly increased the SASA of both conformations at 298 K. At this point, we reported that the trends in the Rg often mirrored by trends in SASA such that a change in the Rg, even a subtle one, is reflected in the SASA measurement.

Nevertheless, SASA measurements were more sensitive to SDS presence or high temperature. Measurements from the closed conformation particularly shows this sensitivity. For the closed lipase at 373 K and in 180-SDS containing system, the Rg values rose from 2.0 to 2.4 Å while for the same period of 2 μ s, SASA rose from 160 to 245 nm². Overall, the compactness and surface area of the closed conformation was more affected by SDS presence and/or high temperature than was the open conformation.

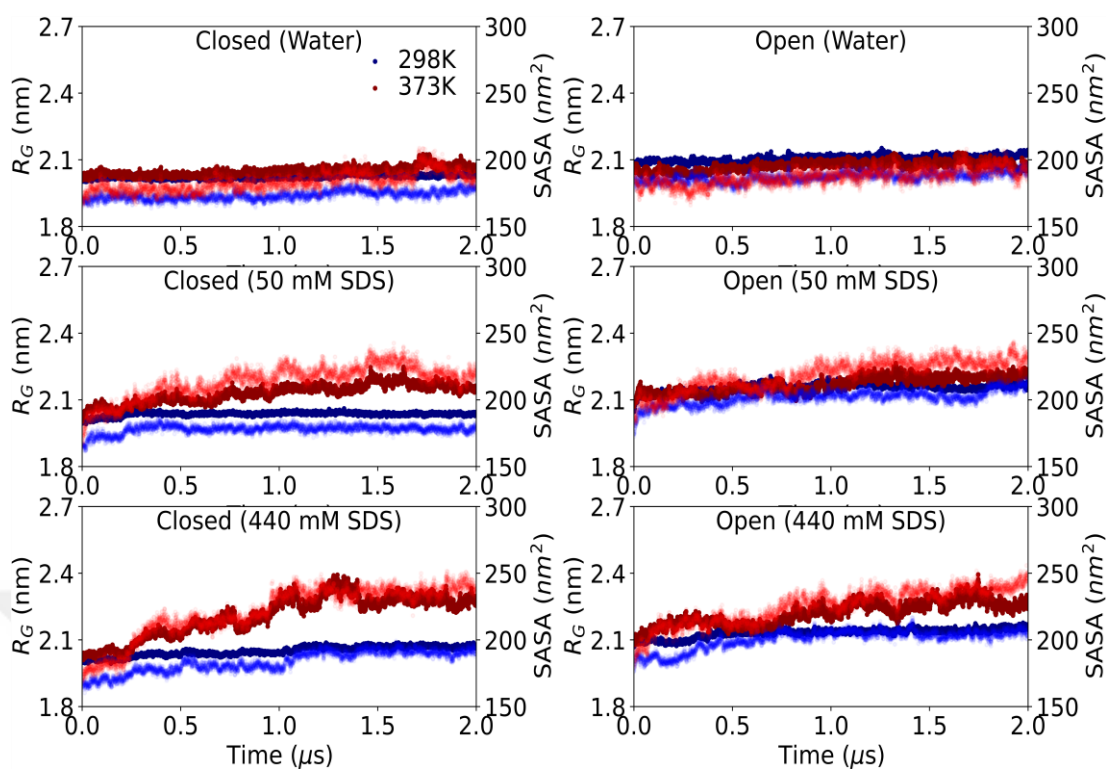


Figure 46. R_g (solid lines, left y axis) and SASA (dotted lines, right y axis) (blue-298 K, red-373 K) analyses of all systems.

4.3.3 Investigation of lipase dynamics in SDS

To identify the lipase regions that were specially mobilized by SDS presence and high temperature, C-alpha fluctuations and essential dynamics of the systems were analyzed (**Figure 47-48**). For the latter, residue contributions to the first principal components (pc1 and pc2) and the scree plots showing the variance explained by the first 5 pcs were plotted (**Figure 49**). Comparison of the flexibility profiles obtained from the first 2 pcs and RMSF analysis suggested an agreement almost for all of the regions. Probably, one exception to this agreement is the N-terminal loop whose RMSF trend were captured by the first 2 pcs at 298 K but not at 373 K. This discrepancy is due to the appearance of other highly mobile regions due to increased kinetic energy dominating the first 2 pcs.

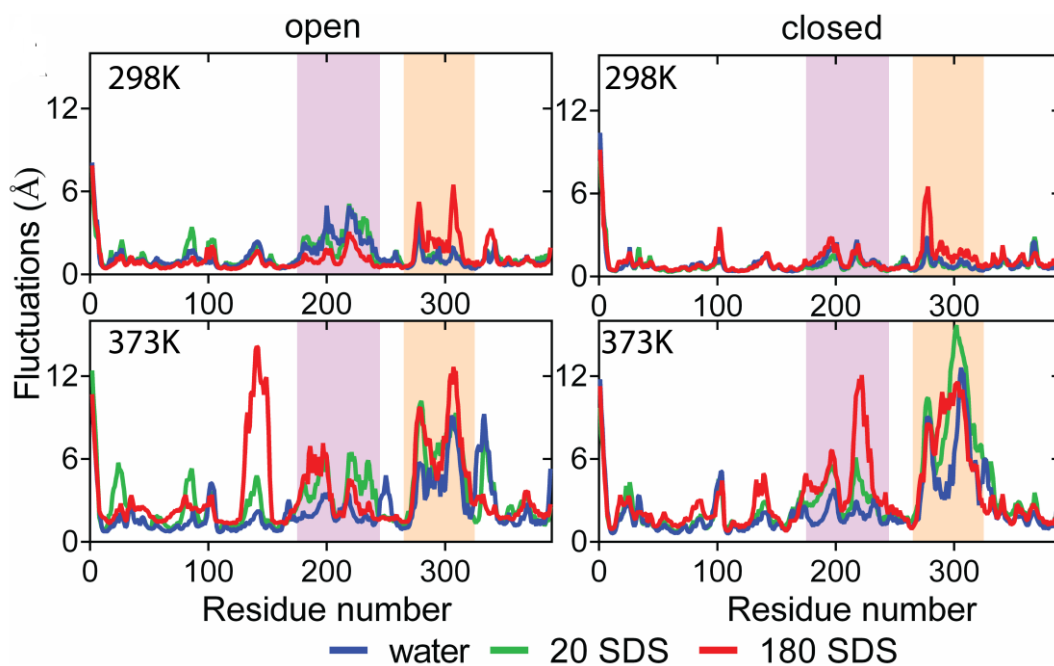


Figure 47. RMSF analysis based on $C\alpha$ fluctuations throughout 2 μ s. The lid domain and its neighboring β -flap is shaded by purple and orange respectively.

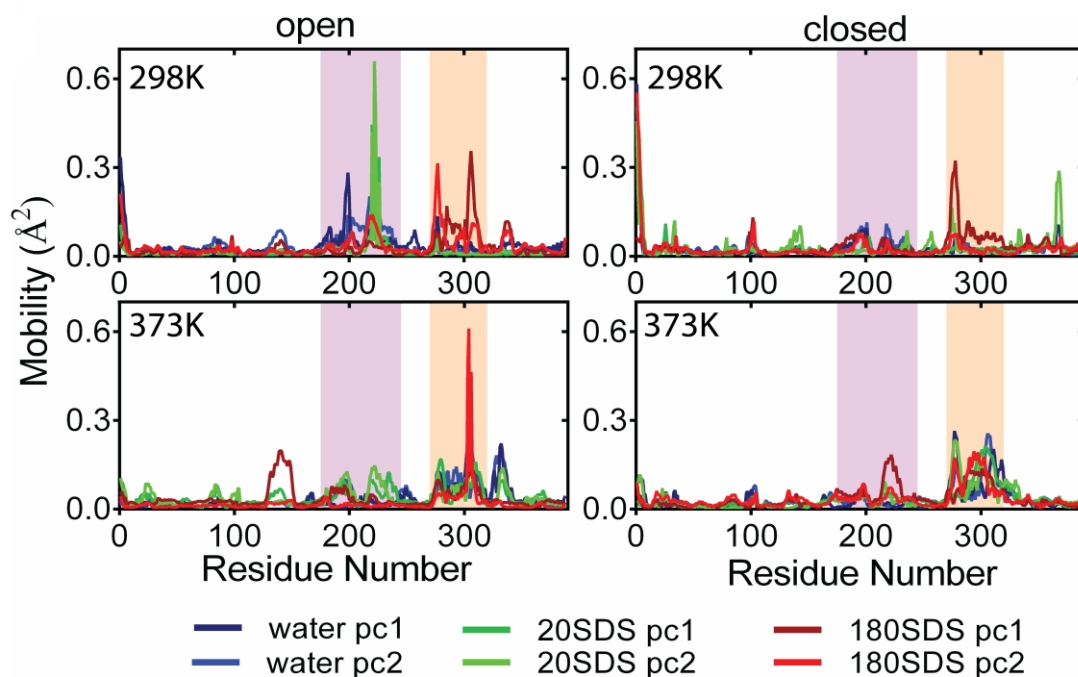


Figure 48. Residue loading onto the first two principal components (pcs) obtained from PCA. The lid domain and its neighboring β -flap is shaded by purple and orange respectively.

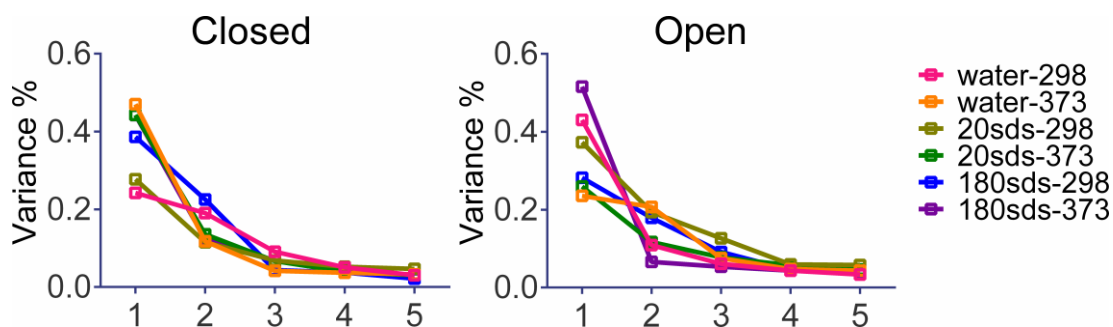


Figure 49. Scree plots showing the variance explained by the first 5 pcs for all systems.

Other than the N-terminal loop, we focused on 3 more regions that fluctuated more than 5 Å. Our first focus is the lid domain spanning the residues from 169 to 239 and the second one is the region composed of a β -flap flanked by short sparse helices covering the residues from 270 to 320. The reduced trajectories of these two surface regions were illustrated in **Figure 45**. The lid fluctuations were found to be specific particularly for the SDS containing systems at high temperature simulations. Otherwise, neither SDS presence nor increased kinetic energy alone increased lid fluctuations (**Figure 47-48**). Whilst lid fluctuations were specific only to the SDS containing and high temperature simulations, either one of the factors, SDS presence or increased kinetic energy was sufficient to mobilize the β -ap and its flanking sparse short helices (**Figure 47-48**). Especially at high SDS concentration and at high temperature enhanced fluctuations of this flap eventually led to unfolding (**Figure 50**).

The third region that showed enhanced fluctuations was observed only for the open conformation at high SDS concentration and high temperature (**Figure 47-49**). This region spanning the residues from 118 to 148 is another surface region formed by short sparse helices which is closely located to the nucleophilic elbow harboring the catalytic serine at the 114th position. Enhanced flexibility of this close neighbor of catalytic site was likely to be associated with the specific interactions between SDS and open cleft. Otherwise, the same conditions of SDS or high temperature did not induce fluctuations of this region in the closed conformation.

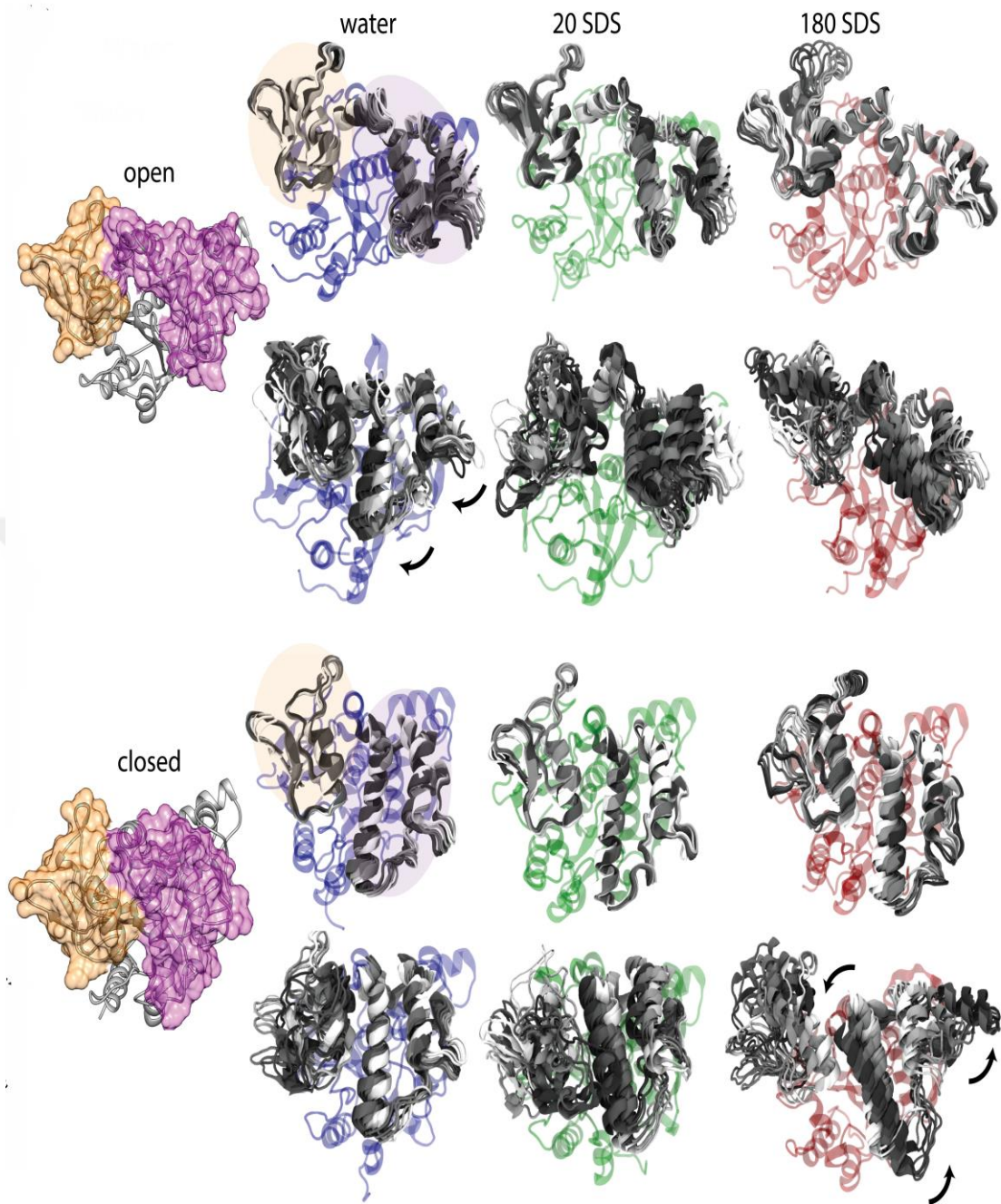


Figure 50. Reduced trajectory of the highly fluctuating two regions that are shaded in purple (the lid domain) and in orange (β -flap domain). The time dependence of the trajectory is color-scaled; 0-white, 2 μ s-black. The crystal structures are illustrated with the two highly fluctuating regions in surface representation. Top two rows indicate the open lipase systems and the bottom two show the closed systems. Arrows used to indicate the ordered lid movements comparable to those during activation.

Given the fact that tested SDS concentrations here can experimentally denature proteins, the evolution of the overall lipase fold throughout the entire 2 μ s of simulation was shown. The changes in the first two pcs were used to extract the representative structures from the start and end of the simulations for the control and 180-SDS containing systems (**Figure 51A**). Consistently for both conformations and for every solvent tested, the lipase backbone was found to sample a limited space at 298 K than it did at 373 K (**Figure 51B**). However, SDS or increased kinetic energy or combination thereof led to a much wider pc1-pc2 plane.

Representative structures obtained from the end of simulations did not show a substantial unfolding (**Figure 51C**). Despite the fact that the overall lipase fold including its core and lid domain stayed intact, unfolding of the surface structures with short secondary structures interconnected by loops was observed (**Figure 51C**). In parallel with the fluctuation analyses, the β -ap as a such surface structure became unfolded at 373 K. Furthermore, at 298 K, SDS was found not to interfere with the overall lipase structure but only with the β -flap region.

On the other hand, as marked in **Figure 50**, the lid mobility at 373 K, particularly the water simulation for the open conformation and the 180-SDS containing system for the closed conformation did not result in a significant loss of secondary structure of the lid domain.

Altogether, we appraise that SDS, even though it was supplied at a high concentration and/or accompanied with elevated temperatures did not induce a complete unfolding of thermoalkaphilic lipases. This observation was further confirmed by analysis of native contacts for which the fraction of native contacts (Q1) was found to be reduced only to 0.75 (**Figure 52**). Hence, despite unfolding of the surface structures, the lipase core stayed intact without any apparent loss of its secondary structure.

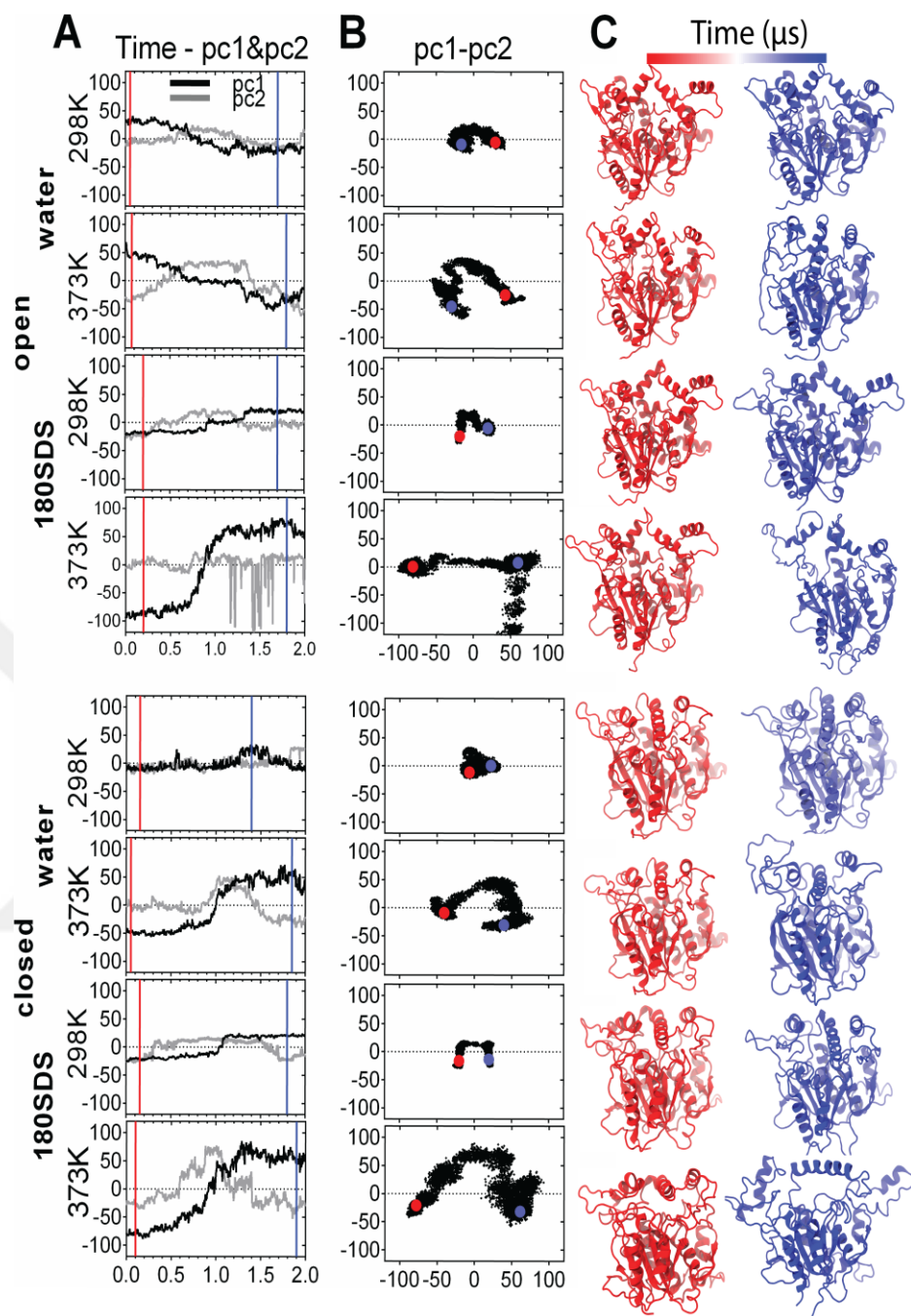


Figure 51. Time-dependent change in the first two pcs, (B) Scatterplots of the first two pcs (x,y; pc1, pc2), (C) Representative conformations showing the initial and the final conformations that were obtained as the snapshots of the time-points shown by colored vertical lines in (A) and dots in (B). Red color indicates the start of the simulation and the blue color the end of the simulation.

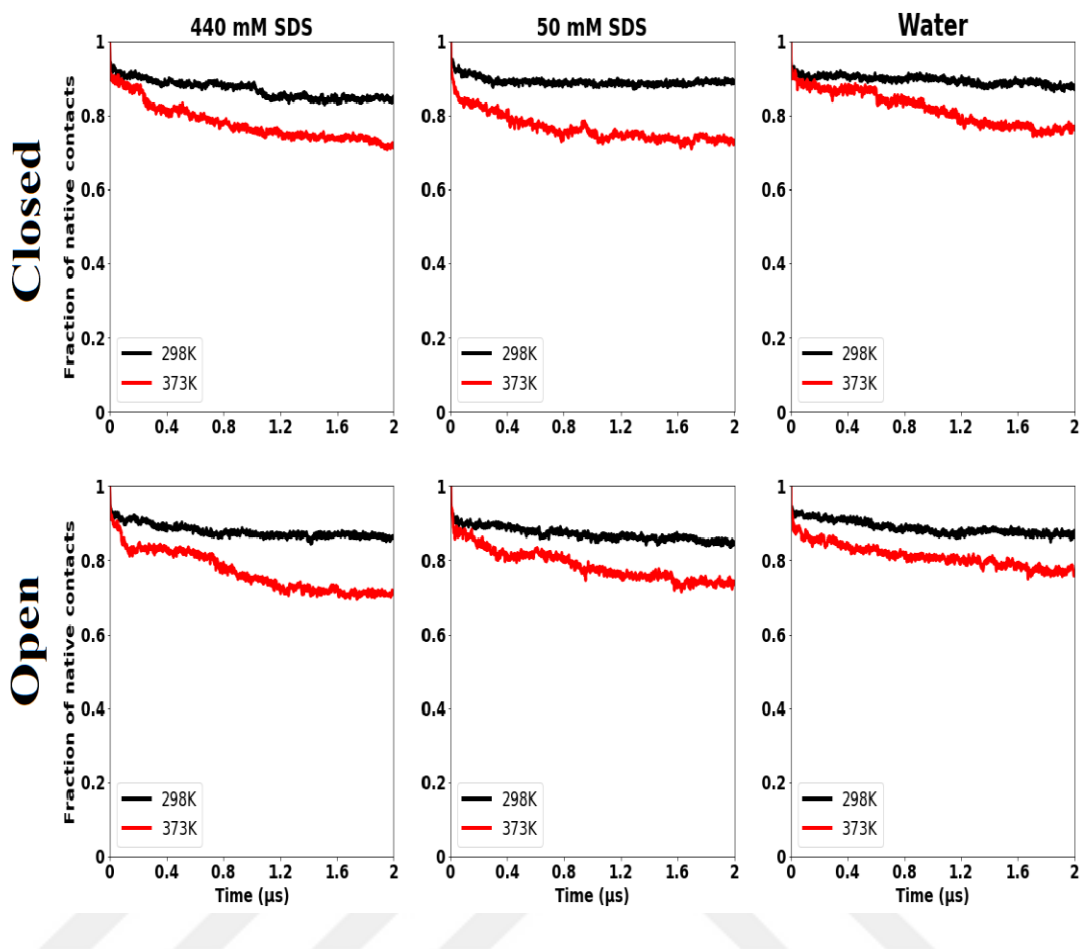


Figure 52. Fraction of native contacts analysis.

4.3.4 Investigation of SDS-induced lipase interfacial activation

To evaluate whether any of the SDS containing systems underwent an activation/deactivation process or not, the crystal structures of the closed and open conformations were compared. From closed (1KU0) to open (2W22), only the lid domain, the continuous epitope covering the residues from 169 to 239, adopts a divergent configuration with an overall change of 5.4 Å in the C-alpha RMSD while the rest of the C-alpha atoms (310 atom pairs) stayed fixed with an overall RMSD change of 0.365 Å.

In addition to the comparison of static structures, we further looked into the dynamics of the activation of this lipase family which was previously modeled by using MD simulations and another member of the same conserved lipase family (155).

In line with the static data, dynamics of the activation also suggested that the lid domain was the only flexible region that mobilized during activation in water-octane layer at 370 K. However, none of our simulations showed an isolated lid motion regardless of SDS presence or high temperatures, challenging SDS as the true activator of this lipase family.

Instead of specific lid mobility, our simulations led to a consistently highly moving β -flap, particularly in response to SDS and high temperatures. Both quantitative and structural analyses confirmed that the lid movement was always accompanied by the movement of β -flap (**Figure 47-50**). However, ignoring the flexibility of the β -flap, the lid movement particularly in two systems was found to be consistent with a plausible interfacial activation for two systems: (i) the open conformation at 373 and in water, (ii) the closed conformation at 373 K in the presence of 180-SDS molecules. Essentially these lid movements were akin to those during interfacial activation/deactivation (**Figure 50**).

To further investigate the activation process, the surface exposed tunnels of the snapshots extracted from 2 μ s of trajectories of closed conformation were analyzed (**Figure 53**). The identified tunnels were compared with those found in the open conformation. At 298 K, SDS, regardless of its concentration, led to formation of tunnels in the closed conformation overlapping with those found in the open conformation and that were maintained throughout 2 μ s while this was not the case for the water solvent. At 373 K, the tunnels were disrupted particularly toward the end of the simulation probably due to the large interference from the highly flexible β -flap (**Figure 47-48**).

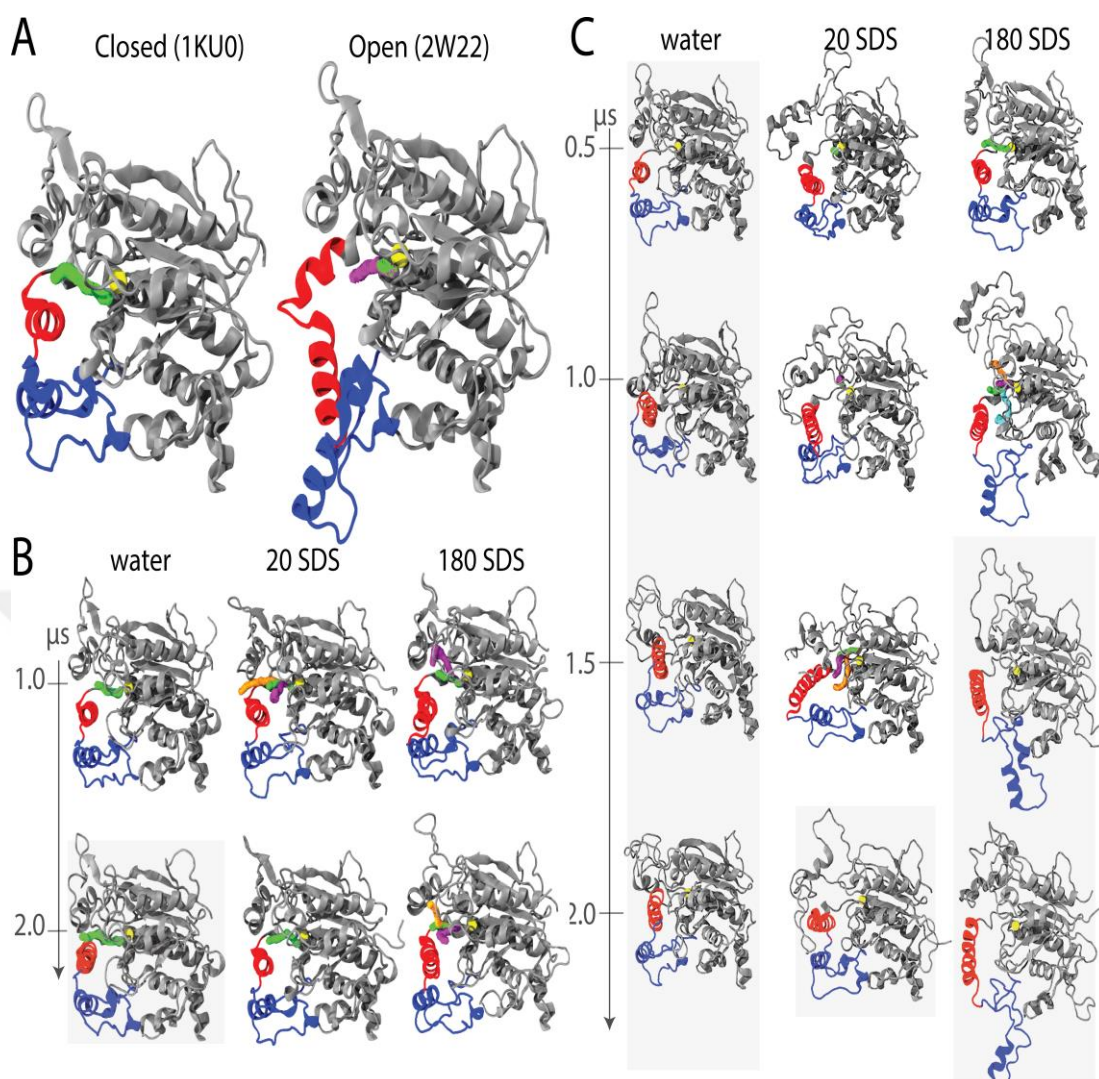


Figure 53. Catalytic Tunnels determined in (A) The Crystal structure of the open and closed conformations, (B) Simulated systems at 298K, (C) Simulated Systems at 373K. Structures showing non-catalytic tunnels were shaded in grey.

To gain more insights on the activation process, the number of SDS molecules occupied within the cleft was calculated and the catalytic triad geometry was visually analyzed (**Figure 54**). An open lipase cleft harbors 3 binding pockets and an oxyanion hole for the sn-1, sn-2 and sn-3 acyl chains and the head group of the triacylglycerol substrate respectively (66, 248). In line with the fact that this family formed by 1,3-specific lipases, two of the binding pockets for the sn-1 and sn-3 acyl chains were occupied by two Triton-X 100 in the open structure (66). Our simulations of the open conformations suggested that after 1 μ s at 298 K a single SDS molecule in the sn-1 acyl chain binding pocket was accommodated for both SDS-containing systems. These

open lipase-SDS complexes when a single SDS was inserted into their active sites had the correct orientation and shape of the catalytic machinery. First, the catalytic triad formed by the S114, D318 and H357 were ideally superimposed with the open crystal structure (**Figure 54**). Second, the side chain of F17 which is the only amino acid in the catalytic cleft that adopts a different side chain rotamer with around 100° change in its dihedral angle during interfacial activation maintained its open conformation. Lastly, the SDS molecules that were spotted in the open conformations were docked to the binding pocket for the sn-1 chain which ideally overlaps with one of the Triton-X 100 moieties present in the open crystal structure (**Figure 54**).

Altogether these observations suggest that SDS, similar to non-ionic surfactants, can keep the lipase in the active state by binding to correct acyl-binding pockets that also accommodate substrates and/or substrate analogs.

For the closed structure, SDS molecules were spotted inside the cleft for only the 180 SDS containing system. The spotted 2 SDS molecules were in fact accommodated by the binding pockets for the sn-1 and sn-2 acyl chains (**Figure 54**). Furthermore, the rotamer of the F17's side-chain changed in the closed conformation, adapting the open conformation. Another notable point was that the head group of one of the SDS molecules was inserted toward the catalytic S114 which performs the nucleophilic attack on the carboxylic ester bond.

Taken together with the tunnel analysis that confirmed the closed lipase cleft were transformed to an open-like configuration in the presence of SDS, these results suggested that SDS not only maintain open lipase conformation but also to some extent induce activation of the thermoalkalophilic lipases (**Figure 53**). When temperature increased to 373 K, SDS almost invaded the active site reaching the number as high as four to six per lipase for 20- and 180- containing systems, respectively. Considering that the open lipase cleft can accommodate up to 3 acyl-chains in 3 distinct pockets, the catalytic machinery was inspected and the catalytic triad were found to be loosened at 373 K regardless of SDS concentration or lipase conformation. This observation was coincident with the particularly high flexibility of the β -flap which holds one of

the triad residues (D318) (**Figure 47-48**). Although the central β -fold of the lipases were not affected by increased kinetic energy and SDS presence, close-inspection of the catalytic machinery of the lipases revealed that SDS at high temperature may interfere with the lipase function through unfolding of the β -flap (**Figure 51**). These observations particularly highlight the role of the structural integrity of the surface β -flap for the lipase activity and the possible SDS interference with the structural integrity of this flap.

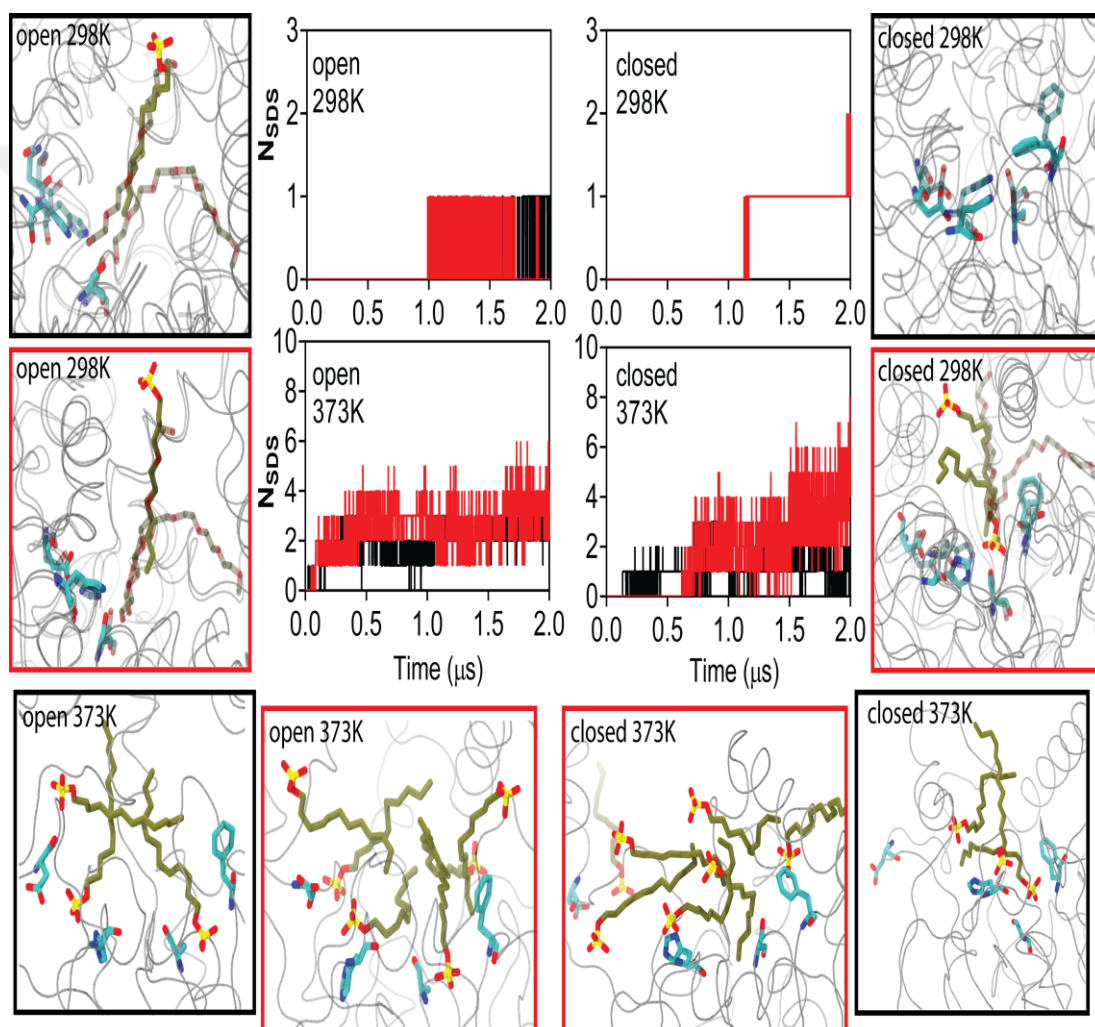


Figure 54. Number of SDS molecules occupied within the catalytic cleft.

4.3.5 Investigation of lipase-SDS interactions

To gain further insights on the stability and activation of lipase in SDS, lipase and SDS interactions were quantitatively and visually investigated (**Figure 55-56**). Lipase-SDS contacts were increased with the increasing temperature for both conformations. For the 180-SDS containing systems, although the number of contacts were much higher than those in the 20-SDS containing systems, ~75 SDS molecules out of 180 came in close contact ($< 5 \text{ \AA}$) with protein, while almost all SDS molecules had come in close contact with the lipases for the 20-SDS containing systems.

SDS interactions with the lipase lid and the β -flap were also analyzed. At 298 K, SDS selected the open lid over the β -flap while the closed lid interacted with SDS at a comparable level with the β -flap. At 373 K, the competition SDS interactions with the lid and β -flap were at similar level, suggesting a competition between the β -flap and the open lid particularly at high temperature.

This competition was also present in the closed conformation regardless of temperature, in fact slightly higher number of SDS interacted with the lid than they did with the β -flap. These observations which were true for both temperature and conformation implied that around 75 SDS per lipase were sufficient to saturate lipase surface.

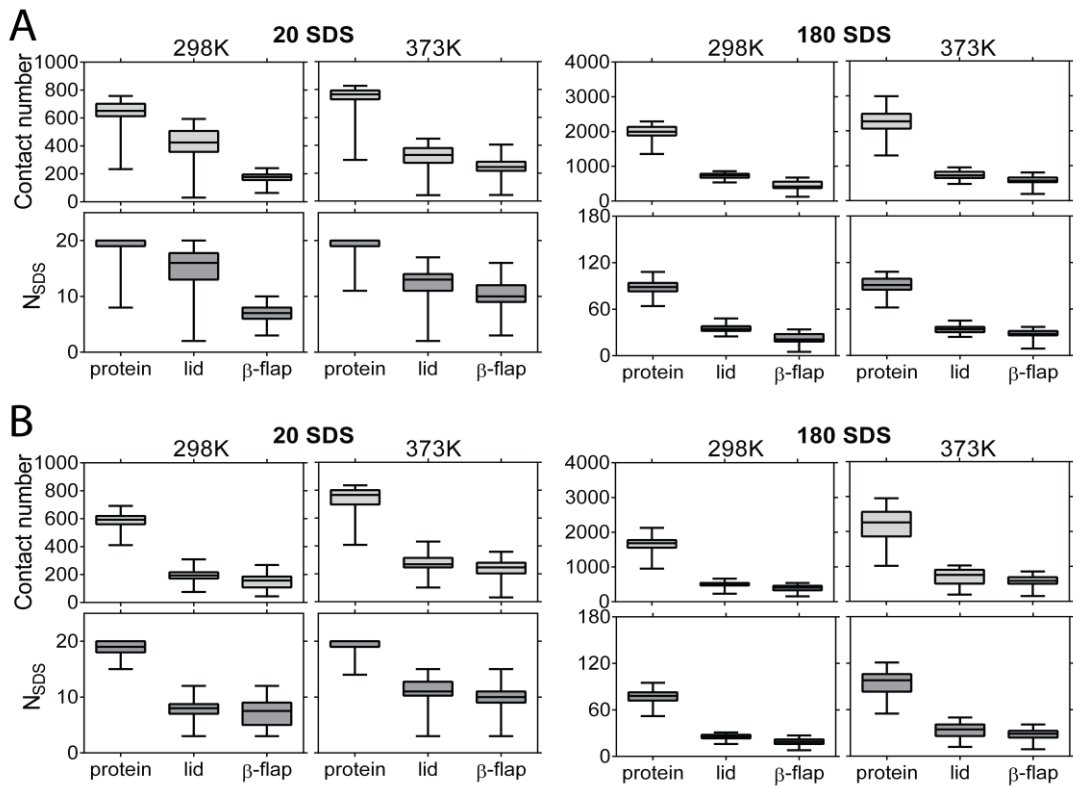


Figure 55. The distribution of the number of SDS contacts ($< 5 \text{ \AA}$) with the entire lipase, the lid domain (169-239) and the β -flap (270-320) were illustrated by box-plots for (A) the open and (B) closed conformations. For both (A) and (B), top panel shows the absolute number of SDS atom contacts and the bottom panels shows the number of SDS molecules.

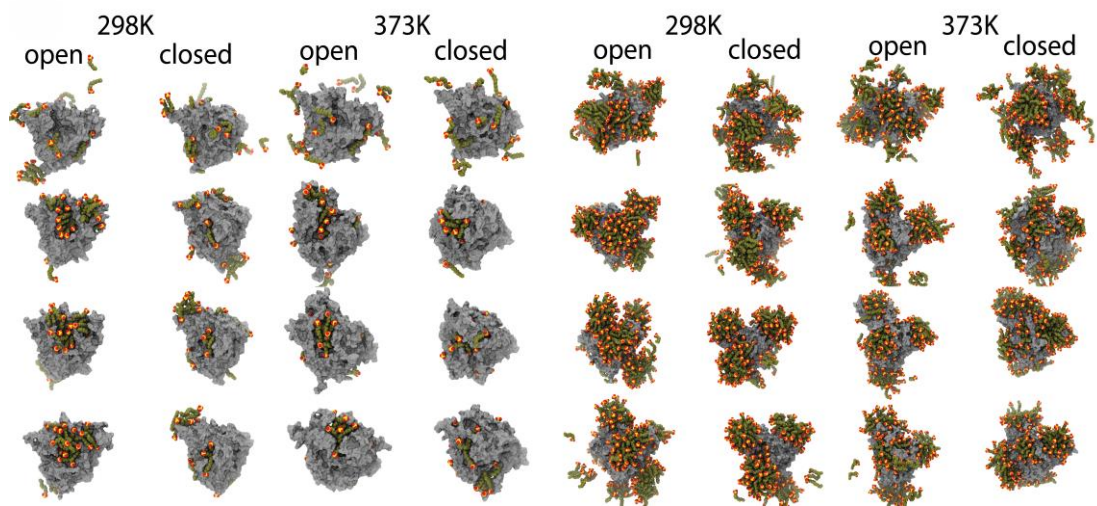


Figure 56. Structural visuals extracted from every 660 ns. Protein structures were rendered by surface views while SDS molecules were rendered by VdW spheres (C: tan, S: yellow, O: red)

The contributions of both charged head and the hydrophobic tail of SDS to lipase-SDS interactions were further analyzed (**Figure 57**). SDS tail was found to be more involved with lipase interactions, particularly lid interactions were dominantly made by the SDS tails. These quantitative results were structurally visualized (**Figure 58-59**).

The surface of the lipases was largely covered by assembled SDS for the 180-SDS containing systems whilst only specific surface regions were occupied by SDS for the 20-SDS containing systems. As such the competition between the lid and β -flap was notable particularly at 298 K. Unless the lid was in the open conformation SDS preferred to interact with the β -flap.

Visually, SDS molecules were stabbed into the open cleft as their head groups mostly pointed toward the solvent. This particular observation was true for both SDS containing systems. At high concentration, SDS formed large self-assemblies while at low SDS concentration such assemblies were absent, rather SDS were mostly engaged with the lipase; in the open conformation with the lid and in the closed conformation both the lid and the β -flap. SDS assemblies were further analyzed in the absence of lipase for 500 ns from which 6 snapshots were obtained. Regardless of lipase presence, SDS was noted to form assemblies similar to the spherical micelles which in the presence of lipase interacted with the lipase surface (**Figure 58**).

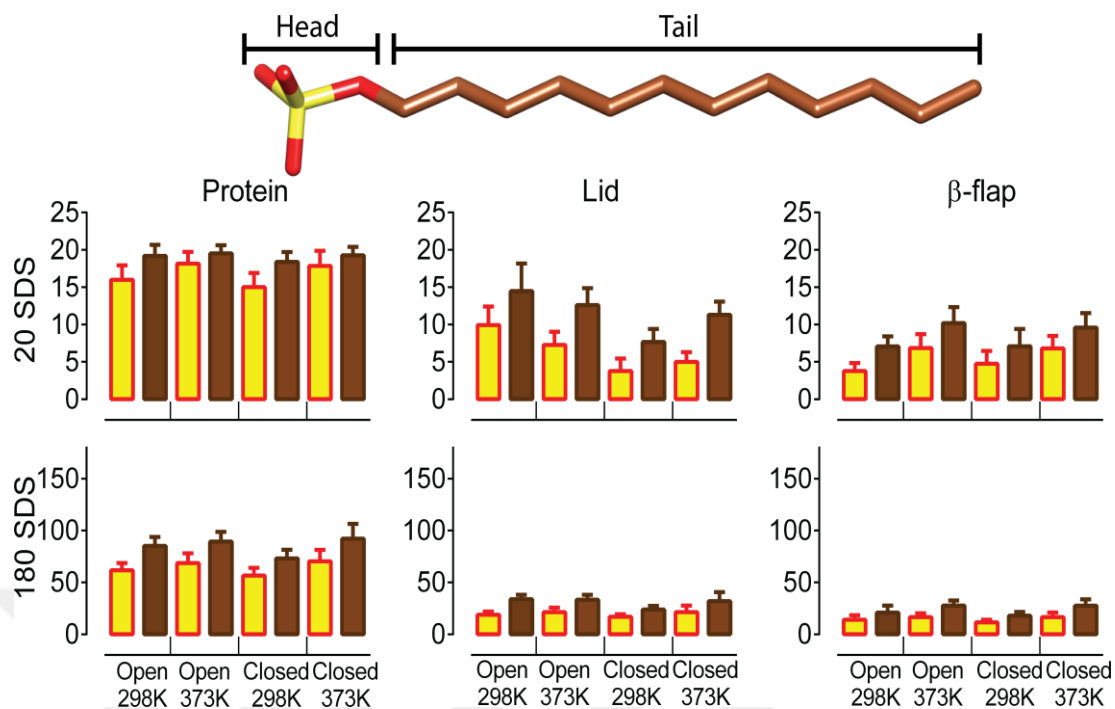


Figure 57. Number of SDS contacts with protein. Bars in yellow show number of SDS head contacts; bars in brown shows SDS tail contacts.

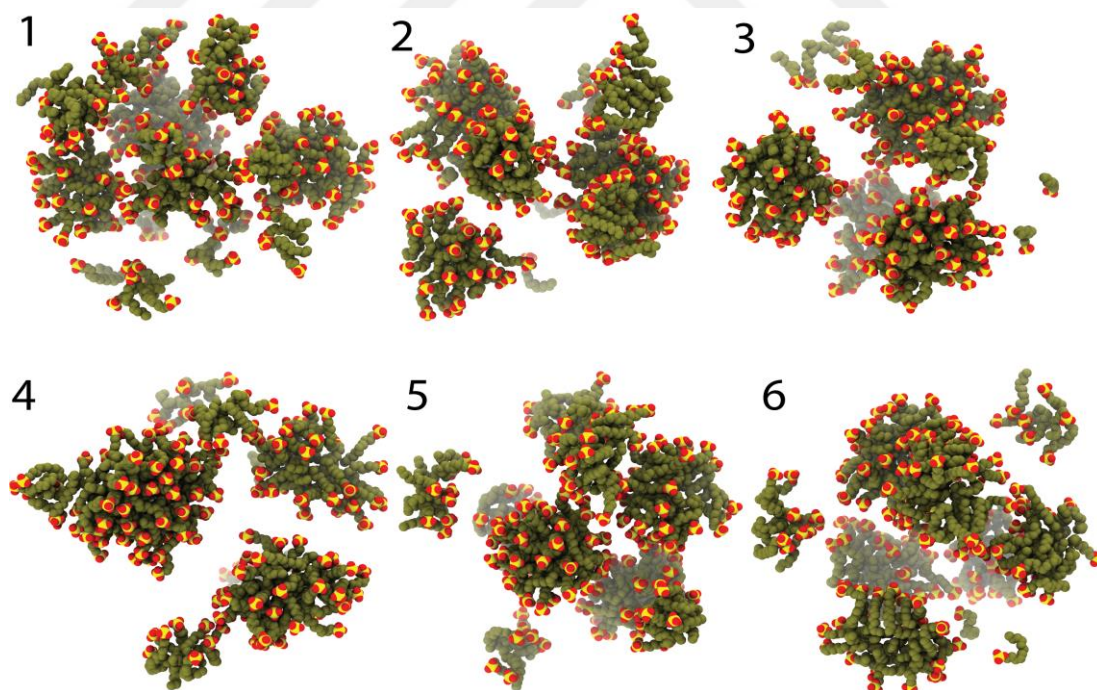


Figure 58. Snapshots of SDS assemblies from SDS simulations at 373K in the absence of lipase

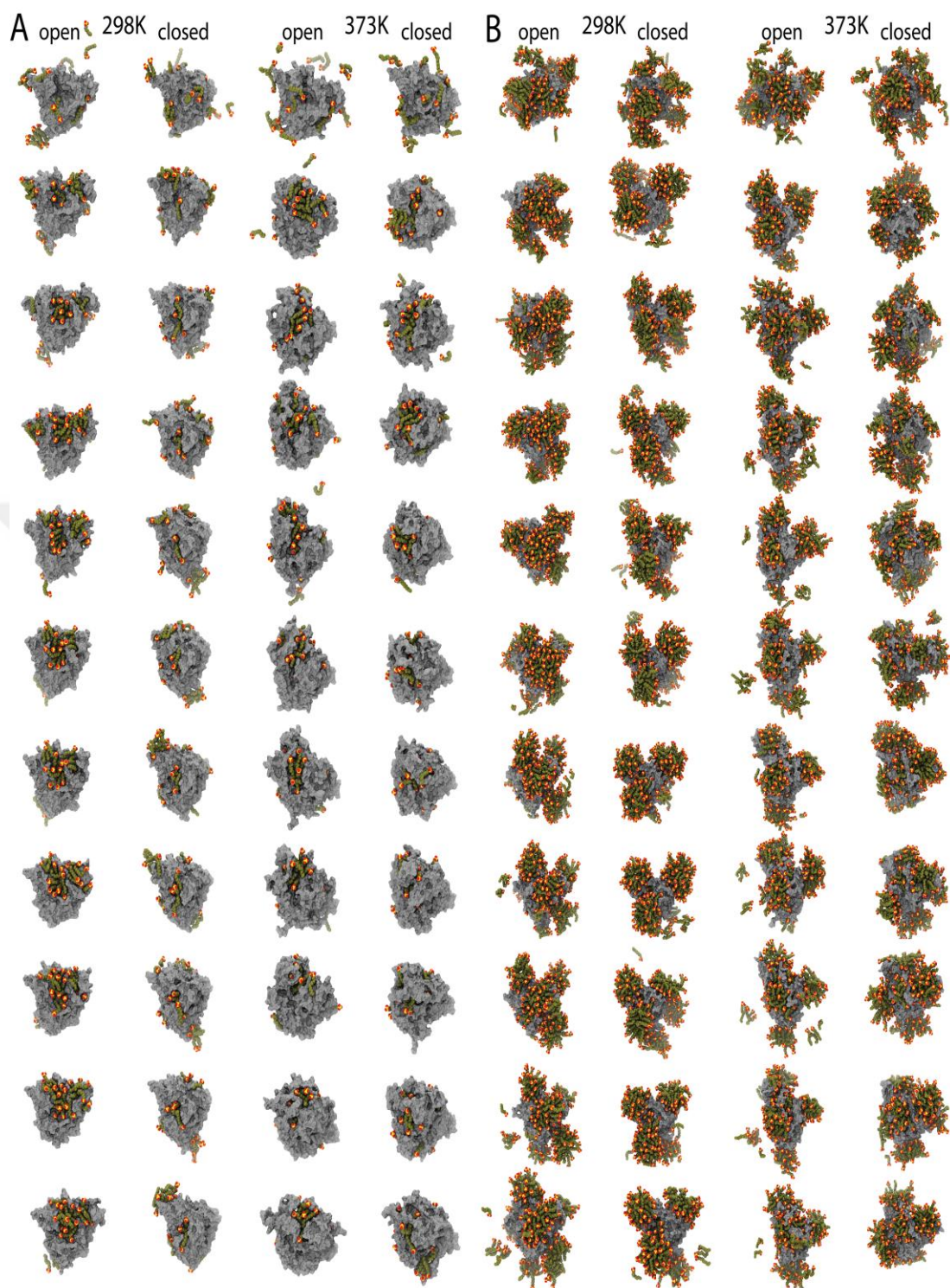


Figure 59. Snapshots from every 200 ns of simulations of (A) 20-SDS and (B) 180-SDS containing systems were visualized. Lipase structures were rendered by surface representation, SDS molecules were shown by its headgroup (S: yellow, O: red) and tail (C: tan). For clarity waters and ions were not shown.

To further investigate the lipase-SDS interactions, COM-RDFs between lipase and SDS were computed (**Figure 60**). COM-RDFs indicated that the probability of SDS and lipase contacts was higher at low SDS concentration than it was at high concentration. With the increasing in temperature, the probability of lipase-SDS contacts was increased for both SDS concentrations.

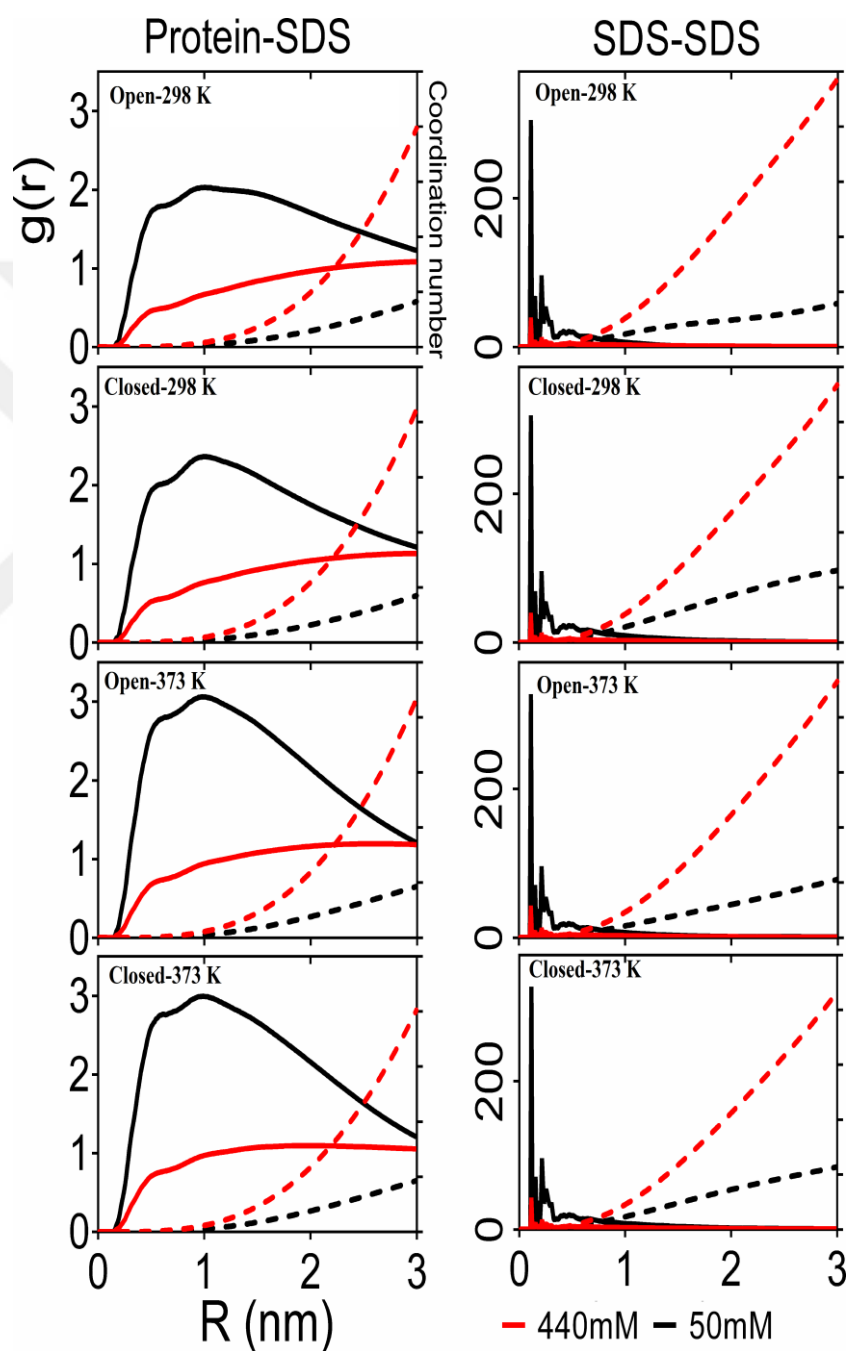


Figure 60. COM-RDF analysis of protein and SDS (left) and SDS-SDS (right).

The intermolecular hydrogen bonds formed between lipase and SDS were also quantified (**Figure 61**). Higher number of hydrogen bonds was reported for the 180-SDS containing systems than 20-SDS systems when raw counts were considered, while normalized counts suggested otherwise such that 20-SDS containing systems showed higher number of hydrogen bonds per SDS molecule. At high temperature, hydrogen bonds formed were found to increase for all conditions whilst no significant differences were observed in the hydrogen bonding profiles of the open and closed conformations.



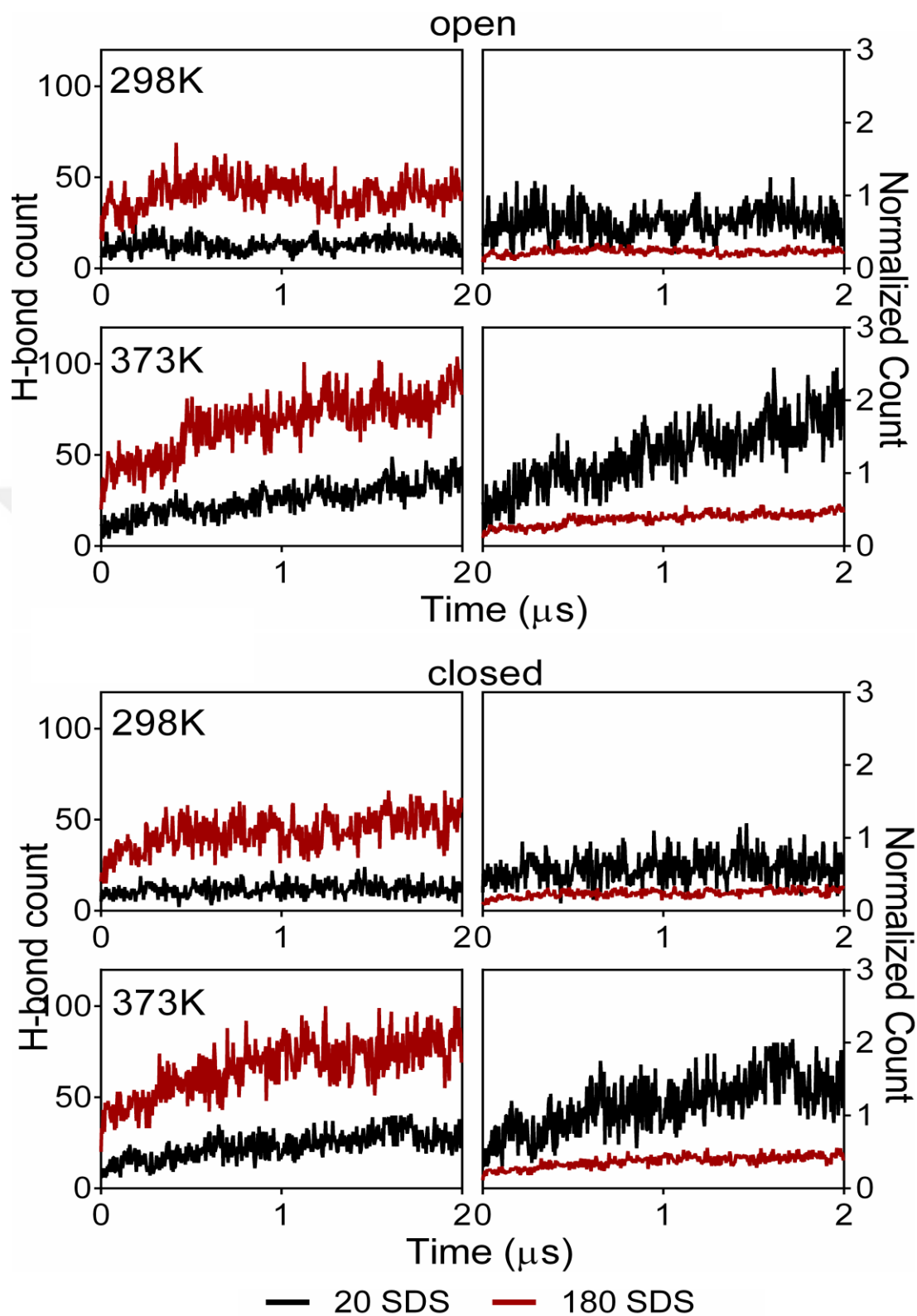


Figure 61. Analysis of hydrogen bonds formed between SDS and lipase; left Y-axis shows raw count of hydrogen bonds while right Y-axis shows normalized hydrogen bonds count

Altogether RDF and H-bond analyses showed that thermoalkalophilic lipase and SDS interactions, regardless of the lid conformation were saturated at high SDS concentration wherein SDS-SDS interactions were more favorable than lipase-SDS interactions. On the other hand, at low SDS concentration, although SDS molecules interacted through the same lipase surface as they did at high concentration, they did not form self-assemblies, suggesting more favorable lipase-SDS interactions than SDS-SDS interactions.

4.3.6 Effect structural dimerization on lipase stability in SDS

The closed conformation of lipase was crystallized as homodimer in which the β -flap domain is located at the interface between the lipase subunits. In order to investigate whether the extra movement of the β -flap domain is due to the absence of the dimeric structure in our simulation or because of a partial unfolding of lipase, MD simulation of the lipase dimeric form was performed at high temperature.

Comparing the backbone flexibility of the monomer and dimeric structures of lipase showed a significant decrease in the β -flap region fluctuations in case of dimer simulation suggesting that the dimeric structure of lipase potentiates lipase stability especially at high temperature (**Figure 62**).

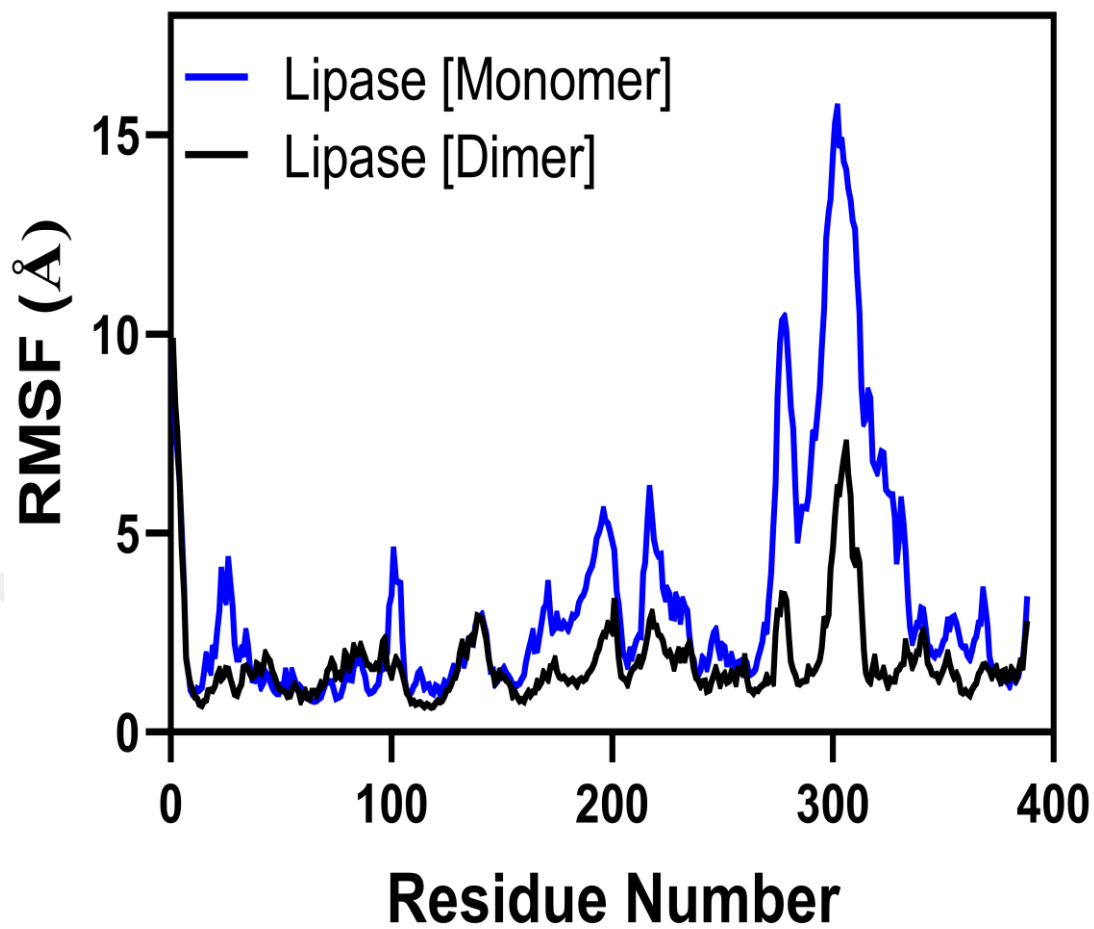


Figure 62. RMSF analysis of chain A of 1KU0 lipase in monomeric state simulation (black) and in dimeric state simulation (blue).

5 DISCUSSION

5.1 Lipase in Organic Solvents

Organic solvents was introduced as an alternative reaction media in lipase reactions for the first time by Klibanov and Zaks in 1984 (5). Their studies showed that lipases can operate and remain stable for hours in organic solvent at 100 °C. Following this seminal work, lipase catalysis and stability in organic media have been extensively studied by a plethora of experimental and computational studies (151-159). Aiming to delineate the molecular effects of different organic solvents on the dynamical equilibrium and structural stability of lipases, the stability and dynamics of the open (2W22) and the closed (1KU0) conformers of thermoalkalophilic lipases were extensively studied by a combination of computational and experimental approaches (235).

Initially, molecular dynamics (MD) simulations of the two conformers were carried out at low temperature in different polar and non-polar solvents. No lipase denaturation was observed in any of the solvents. Furthermore, enhanced lipase dynamics were noted in polar solvents compared to the non-polar ones. The difference in lipase dynamics between the non-polar and polar solvents is thermodynamically anticipated, because transferring a folded globular lipase from aqueous media to less polar environment like methanol or ethanol results in burial of some of the lipase surface polar groups leading to an increased solvation free energy (ΔG) (249). On the other hand, transferring lipase from water to hydrophobic environment such as toluene or cyclohexane leads to very high solvation free energy (ΔG) (249). This is mainly because of the burial of all the lipase surface groups in order to avoid the unfavourable hydrophobic environment. This behaviour was clearly seen in the Rg and SASA profiles in which lipase showed significantly lower Rg and SASA values in non-polar solvents compared to the polar ones (**Figure 6A and 7A**). Additionally, PCA and DCCM plots also indicated reduced dynamics of lipase in non-polar solvents compared to the polar ones (**Figure 8 and 9**).

In order to evaluate the impact of the chemical nature of the solvent on lipase thermostability, MD simulations were also performed at elevated temperature. In contrast to low temperature simulations, elevated temperature simulations showed a strong correlation between lipase thermostability and the nature of the solvents. Both of the lipase conformers were found to unfold in polar solvents while this was not the case for the non-polar solvents (**Figure 3B and 7B**). Interestingly, lipase structure was found to be highly rigid in non-polar solvents even at such very elevated temperature (**Figure 6B**). Notably, ethanol was an intermediate case between the two solvent groups such that lipase structures showed properties which are characteristic to both non-polar and polar solvents. This is possibly because despite being a polar solvent, ethanol has more hydrophobic character than water and methanol rendering it act in some cases like non-polar solvents.

Apart from the large structural changes induced by the bulk solvents, the interactions between the individual molecules of the solvents and lipase were evaluated by COM-RDFs (**Figure 14**). Small solvents molecules such as acetone and methanol were found to diffuse to the lipase hydrophobic core while no diffusion was observed for the non-polar solvent molecules. This effect was observed for both of the lipase structures in both low and high temperature simulations. A diffusion of small polar molecules to the hydrophobic core of lipase can inhibit and significantly disturb the overall fold of lipase. Examples of enzymes inhibition due to interactions of small alcohols with their active sites have been already documented (144).

Altogether, these theoretical insights suggest that polar organic solvent improve lipase dynamics at low temperature which could be useful for lipase catalysis at ambient temperatures where structural dynamics are naturally low. On the other hand, these observations also underscore the critical role of structural rigidity imparted to lipase by non-polar solvents in potentiating lipase stability at high temperatures.

Experiments were conducted at low and high temperature to validate these theoretical observations (**Figure 16**). Generally, all the solvents were found to enhance the activity of lipase at low temperature (**Figure 16A**). Lipase activity was found to be

higher in polar solvents than the non-polar ones at low temperature. Indeed, this is expected since a degree of flexibility is needed for lipase to function at low temperature where the natural fluctuations are low due to the limited kinetic energy. This is consistent with our low temperature simulations which showed improved lipase structural fluctuations particularly at the lid domain in polar solvents (**Figure 4A**).

In general, lipase activation in all organic solvents was found to be up to a particular concentration after which lipase is either partially inactivated or totally inhibited (**Figure 16A**). Several examples of this behaviour have been already reported in literature for different enzymes. For instance, Toshi et al. noted that low concentrations of organic solvents enhanced hemoglobin stability, while it was denatured at high concentrations of the same solvents. Indeed, such a diminished activation of lipase at very high concentrations of organic solvents is mainly because of chemical reasons rather than structural ones. For instance, inactivation of lipase at very high solvent concentration is anticipated because high organic solvent concentration shifts the thermodynamical equilibrium of the hydrolysis reaction toward esterification reaction. Moreover, inhibition of lipase in high concentrations of solvents like methanol and acetone is expected since both of these solvents are known to reduce protein solubility and often used to precipitate proteins (244).

Experiments were also performed at high temperature to validate our high temperature simulations. For these experiments lipase activity was measured upon incubation in three different solvents, water, cyclohexane, and ethanol. Lipase activity was found to be higher in both of the organic solvents than in water (**Figure 16B**). The highest lipase activity was observed in 25% (v/v) ethanol while no activity was noted beyond this concentration. The stability of lipase in ethanol at high temperature was predicted by our high temperature simulations which indicated that the catalytic machinery of lipase was stable in ethanol (**Figure 11B and 12**). The inhibition of lipase at high ethanol concentrations could be due to an extra-flexibility-induced lipase unfolding resulting from combining two sources of flexibility, ethanol and increased kinetic energy at high temperature.

On the other hand, cyclohexane was found to improve lipase stability and activity at concentration as high as 70% (v/v) (**Figure 16B**). The improved stability here is possibly because of the burial of lipase polar surface residues inside the protein protecting its globular form. Harpaz et al. studied the contribution of surface residues burial the overall stability of 108 different enzymes (250). Their data indicated that that burial of proteins surface residues contributes to protein stability more than the non-polar residues. This behaviour was explicitly seen in our 450 K simulations which showed that the SASA and Rg values of lipase were significantly diminished in non-polar solvents despite the very elevated temperature (**Figure 6B and 7B**).

Overall, our results provide molecular insights that can be useful for a better medium engineering approaches in lipase reaction in organic solvents. Moreover, it paves the way for the rational design of organic solvent stable lipase variants that can function at extreme industrial conditions. These observations can also be adapted to other lipases especially particularly the member of family I.5 and other enzyme groups.

5.2 Lipase in Deep Eutectic Solvents

Over the past decades, developing green solvents for enzymatic reactions have been a major focus of several studies to reduce the environmental burden associated with using organic solvents (164). DESs, a subclass of ionic liquid, stand out as a strong alternative to organic media in enzymatic reactions because of their promising green characteristics (166). Hitherto, several successful examples of lipase-catalyzed reactions in DESs have been documented, albeit the theoretical investigation of lipase stability in DESs is limited only to two studies and none of them studied the effect of water content in DESs on lipase structural stability (15, 189). Given the recent reports showing how the hydration of DESs changes their nanostructures and reduces the yields of lipase reactions, we stress that investigating the effect of water content in DESs on lipase stability is of a great importance to potentiate lipase implementations in these promising solvents. Motivated by this necessity, we utilized MD simulations to delineate the effect of water content in DESs on the stability and dynamics of thermoalkalophilic lipases. To validate our MD simulations, a collaboration was

constructed with experimentalists to evaluate the effects of different reline formulations on lipase activity and stability (242).

MD simulation is utilized often to scrutinize the solvent stability of different lipases (148, 155, 235, 251-253). Both of the two computational studies that previously investigated the effects of DESs on lipase stability have simulated the structure (1TCA) of mesophilic *Candida antartica* lipase (CALB) (15, 189). Yet they used two different DESs formulations; particularly, Nian et al used the naturally occurring betaine:xylitol and chloride:glycerol DESs while Monhemi et al. used choline chloride:urea based DESs which is commonly known as reline. Indeed, employing CALB in their studies was a strategic selection because it is commonly used in industry and widely available in commercial formulations (254). Thermoalkalophilic lipases employed in our study similarly have high potential for industrial applications, but they are highly stable enzymes compared to other lipases such as CALB (255).

Consistent with the results of the previous investigations, our MD simulations showed that lipase structure is highly stabilized in pure DES. This high stability was reflected in a decreased flexibility and increased compactness of lipase structure in pure DES (**Figure 20-22**). Increasing the hydration level of reline was resulted in a less ordered nano-structure of the solvent, in agreements with the previous experimental reports in literature (187). On the other hand, coherent with the improved flexibility of the lid domain in hydrated reline, experiments showed that hydrated reline improved the interfacial activation of lipase (242). This experimental observation is valid for incubation of lipase at low and high temperatures. Notably, very low hydration level was needed to activate lipase at high temperature (242). Indeed, these observations are also in agreement with the results of Nian et al. despite the difference in the lipase structure studied and the DES formulation used (189).

In aqueous media, lipases adapt the closed/inactive conformation by covering the catalytic site under the lid region. At the oil-water interface, the lid domain is adsorbed to the hydrophobic phase and they adapt the open/active conformer (256). Therefore, it was necessary to recruit both of lipase conformers to our simulations to investigate

how aqueous media and water in DES may affect this dynamical equilibrium. Our MD simulations coherently showed that regardless of the solvent and the simulation temperature, the closed form of thermoalkalophilic lipases is more stable than the open conformation. The higher stability of the closed form was reflected in reduced fluctuations, SASA, and Rg values compared with the open form (**Figure 20-22**).

Temperature is one of the factors required for the activation of thermoalkalophilic lipases (16, 155). However, alone temperature is not enough to achieve a complete activation of lipases. Indeed, the interfacial activation at the oil/water interface of another thermoalkalophilic lipase, T1 lipase, was studied by MD simulations which indicated that the interfacial activation occurred only at high temperature (155). Our simulations also indicated that high temperature alone was not enough to induce specific fluctuations of the closed lid domain which would suggest lipase activations. However, enhanced fluctuations of the closed lid were observed in hydrated reline at high temperature, a result that suggest activation of lipase in hydrated reline when combined with high temperature (**Figure 27**).

On the other hand, increased flexibility of the antiparallel β -flap domain of the closed form was also observed in hydrated reline and water (**Figure 27**). This could be due to the fact that thermoalkalophilic lipases are known to adapt a dimeric structure in the closed form wherein this domain is at the dimer interface, implying that this domain is not exposed to the solvent in the closed form (257). Moreover, this domain is also rich of the hydrophobic residues, therefore, it is not a surprise to be less stable in hydrated solvents.

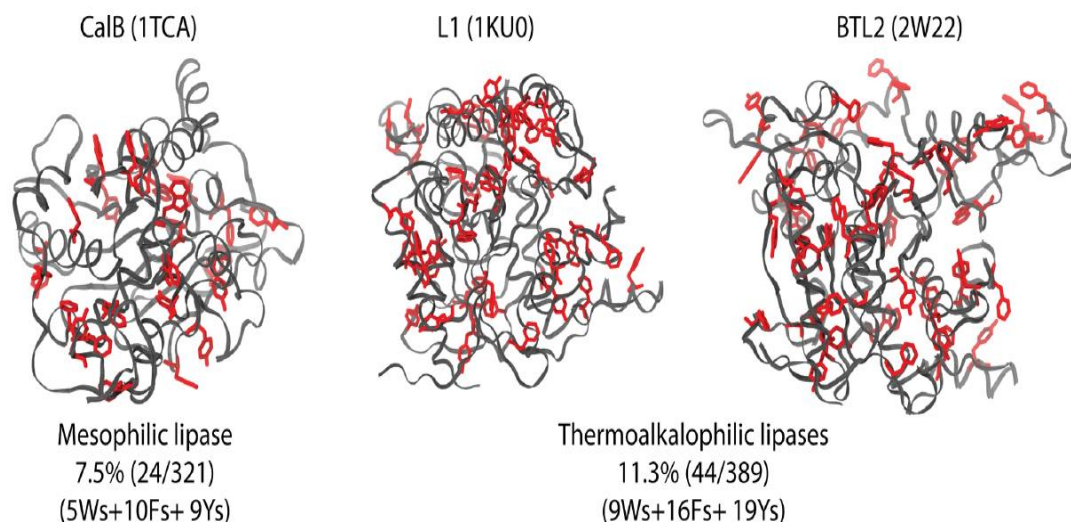


Figure 63. Comparison of hydrophobic content of bulky amino acids (W, F, Y) between CALB and thermoalkalophilic lipase structures.

A decrease in the number of hydrogen bond formed between lipase and reline which reported to improve lipase stability was observed in hydrated reline and water (15) (**Figure 43**). Thus, unfavorable interaction, other than hydrogen bonding, between the β -flap domain and water may partially account for the increased fluctuation of this domain in water and hydrated reline. Increased mobility of the β -flap flanking helices was observed in water, urea, and highly hydrated reline (**Figure 20-43**). Taken into consideration that one of the catalytic triad D318 is harbored by this domain, one would expect that these increased mobility might lead to lipase destabilization and in turn inhibition. Coherent with these expectations, experiments showed that incubation of lipase in water or hydrated reline solutions at high temperature led to a detrimental effect on lipase activity (242).

In the previous investigations, CALB was found to completely unfold in 8M urea in high temperature simulations (15). However, apart from a partial loss of secondary structure, neither of the lipase conformers unfolded in the same conditions in our simulations (**Figure 29**). Such a contradicting results from the two studies are expected since the lipases simulated in our study are thermophilic, while CALB is not (258). However, surprisingly, neither increased fluctuations nor secondary structure denaturation of CLAB was observed in water at high temperature (15). The maximum

fluctuations of CALB were up to 4 Å in water at 373K, while our thermostable lipases fluctuated up to 10 Å at the same simulation conditions (**Figure 20**). In agreement with our results, experiments showed a severe decrease in the activity of lipase after incubation in water at high temperature (242).

The contradiction between the two studies is true, however, our simulations which were performed in duplicates for longer time (300ns) than those of CALB (50ns). Shorter time scales of the CALB simulations might account for such an unexpected rigidity of CALB in water at such elevated temperature. Apart from the difference in the simulations time scale, being activated by temperature, thermoalkalophilic lipases might need more fluctuations particularly at the lid domain to achieve the activation, while this fluctuation might be uniform overall the structure of CALB because it is a lidless lipase.

5.3 Lipase in Sodium Dodecyl Sulfate

One particular study in 2012 showed the complete activation of a member of thermoalkalophilic lipases in a much shorter MD time (10 ns) (155). Particularly, a water-octane layer was included in the systems leading the closed lid to open without any apparent flexibility of any other parts of the backbone. Compared with this activation model established for another member of the same lipase family, SDS was not a true activator of this lipase family as the water-octane layer, mainly because we did not observe isolated fluctuations of the lid domain but observed high fluctuations from the β -flap domain (**Figure 47 and 48**) (155). However, before assessing SDS as being a lipase activator, we compared the control simulations of both studies which were expected to produce parallel outcomes because both studies have simulated the closed lipase structure under similar conditions, i.e in the aqueous media and at high temperature, either at 370 K in their study or at 373 K in our study. Particularly, the most flexible region in our control simulations at 373 K is the β -flap, albeit this particular surface region did not show any peaked flexibility in the previous analysis (**Figure 47 and 48**) (155).

We focused on the differences between the closed structures utilized by two studies. For the closed structure we have used 1KU0 while they have utilized 2DSN. We had to note slight differences in the qualities of the crystals in favor of 2DSN which had a slightly higher resolution and lower R-factor than 1KU0 (16, 259). However, they share almost identical sequences (~ 95%).

In other words, the same β -flap exists in both structures with almost the exactly the same surroundings. Still, 2DSN simulations in aqueous media at 370 K produced an almost rigid β -flap, in contrast to the highly mobile β -flap in our simulations performed under similar conditions.

Comparison of the crystals interestingly confirmed the β -flap as one of the most flexible regions in both structures, while it is more flexible in 1KU0 than in 2DSN (**Figure 64**). Therefore, despite discrepancies between fluctuations of the β -flap from simulations, we underscore the agreement of the crystallographic temperature factors obtained from both 1KU0 and 2DSN structures with high fluctuations of the β -flap from our simulations.

Differences in the MD application such as the MD algorithm and forces fields may also lead to differences in the fluctuations of the β -flap. We have utilized NAMD method along with CHARMM36 ff, while Rahman et al. have used YASARA Dynamics and AMBER03 ff (260-262).

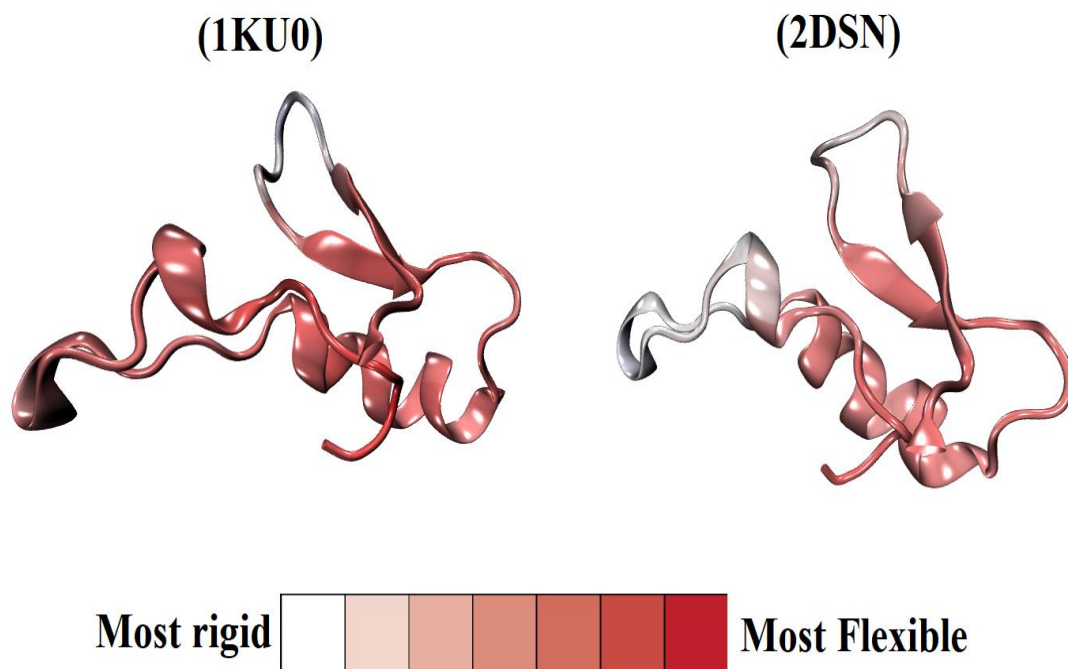


Figure 64. Comparison of the β -flap domain flexibility in 1KU0 and 2DSN lipases.

Another point is that we have sampled a single simulation per system which was indeed a limitation of this study. Nevertheless, we stress that having investigated this lipase family in other studies which also applied MD simulations, this was not the first time we encountered peaked fluctuations for β -flap region. In fact, our previous simulations on this lipase in organic and deep eutectic solvents similarly suggested that albeit not as high as SDS enhanced fluctuations for this particular region.

Apart from all the distinctions between two MD studies exploiting the same lipase conformation, we emphasize the difference in the MD time scales such that the duration of the simulations greatly differed between this and previous study (155). Here we have run almost 200 times longer MD simulations than Rahman et al. and almost 10 times longer than our previous longest simulations (155). The longer the simulation lasted, the higher the fluctuations were reached by this β -flap. Essentially, all-to-all RMSD plots show an abrupt change in the backbone displacement of both open and closed conformations after 1 μ s which was associated with the relatively high level of the β -flap flexibility (**Figure 45**).

Overall, we underscore that the discrepancy between the control simulations of our and Rahman et al. studies, particularly the higher flexibility of the β -flap is less likely to be resulted from differences in the MD parameters and or subtle structural difference or any errors in either of the studies, but the much longer MD time scales could have granted us an access to distinct lipase conformations which are failed to be sampled in shorter MD time.

Aiming to delineate the mechanism of protein unfolding in SDS, a plethora of experimental studies proposed several models of protein-SDS complex including flexible helix model, necklace-and-beads model, and rigid rods model (17, 263-272). One the other hand, molecular dynamics (MD) simulations have been also used to investigate the dynamics of protein unfolding in SDS (273-276). Albeit an unequivocal mechanism of SDS-induced protein unfolding has not been established yet.

In our simulations, we did not observe a complete denaturation of lipase in SDS, however, the anti-parallel β -flap was denatured by almost the same unfolding mechanism described recently for Titin I27 domain (246). In this mechanism, the unfolding was initiated by direct insertion of either the polar headgroup or the hydrophobic tail of an individual SDS molecule between the protein secondary structure paving the way for SDS micelle to wedge the protein secondary structure apart. However, in our simulations, the unfolding was initiated by interactions with SDS assemblies rather than individual molecules and lipase did not show any apparent unfolding of the core domain as the denaturation was limited only to the surface regions such as the β -flap domain. The localization of the unfolding at this β -flap is because it is a highly flexible domain by nature. Moreover, it is neighboring the lid region which is a main target for SDS molecules and where large structural rearrangements occur upon activation. Another reason for the strong destabilization of the β -flap domain is due to the absence of the dimeric/oligomeric state of lipase which contributes to the stability of this domain as described earlier.

6 CONCLUSION

Given the versatility of lipase catalyzed reactions, they have been widely used in several industrial applications. In the vast majority of these applications, lipases are exposed to non-aqueous environments either as a reaction media or substrates. Therefore, understanding lipases stability mechanisms in non-aqueous environments is of great importance to potentiate their large-scale industrial applications. Motivated by this necessity, we combined molecular dynamics (MD) simulations with experiments to study the behavior of the highly stable thermoalkalophilic lipases in different non-aqueous environments. To evaluate how different non-aqueous environments affect lipase activation, both the open/active and closed/inactive conformers of thermoalkalophilic lipases were included in all of our studies.

Firstly, we investigated the effect of organic solvents polarity on the structural stability of thermoalkalophilic lipases at both low and high temperatures. Despite the hazardous associated with applying organic solvents in enzymatic reactions, they are still the most utilized solvents in industrial applications. Our MD simulations showed that at low temperature, polar solvents improved lipase fluctuations particularly at the lid domain, while non-polar solvents led to a frozen lipase structure. On the other hand, polar solvents were found to denature lipase at high temperature. In contrast, non-polar solvents were found to have significant stabilizing effects such that lipase overall fold remained intact despite the very elevated simulation temperature. Consistent with these results, our experiments showed that all organic solvents enhanced lipase activity at low temperature, while at high temperature, lipase was significantly stabilized only in non-polar solvents.

DESs have been introduced as green and environmentally friendly alternative reaction media for lipase reactions. Given the increasing reports on the effects of the DESs hydration level on the yield of lipase-catalyzed reactions, in the second part of this thesis, we applied molecular dynamics (MD) simulations to evaluate the effect of DES (reline) hydration level on the dynamics and stability of thermoalkalophilic lipase.

Our simulation at both low and high temperatures showed that lipase structure was highly stabilized in reline. Slightly hydrating reline was found to improve lipase dynamics specifically at the lid domain. On the other hand, a less ordered reline nanostructure was observed at high hydration level. Notably, no denaturation was observed in any of the solvents including the very aggressive 8M urea solution, implying the extreme stability of this lipase family. Experimental results, on the other hand, were consistent with these theoretical insights such that slightly hydrated reline led to the highest lipase activity, while highly hydrated completely inactivated lipase.

The activation of lipases involves a large conformational change triggered by the lipid interface. Surfactants, as they mimic lipase substrates, are often used to induce lipase activation. Thus, studying lipase-surfactants interactions is of a great importance to understand their catalytic mechanism. Therefore, in the third part of this thesis, we report the effects of the anionic surfactant sodium dodecyl sulfate (SDS) on the activation and dynamics of thermoalkalophilic lipases. Despite a long history of research in protein-SDS interactions, lipase-SDS interaction and how SDS activates lipases have not been investigated at the molecular level yet. On the grounds of this, we applied extensive molecular dynamics MD simulations to study the molecular impact of SDS on thermoalkalophilic lipases. Our computational results have suggested that; first, SDS activates lipase regardless of the simulation temperature; second, as SDS concentration increases, it forms micelles and ceases to engage with lipase activation; third, lipase doesn't denature in SDS even at elevated temperature and lastly the dimeric structure of lipase potentiates lipase stability especially at high temperature.

Altogether, we surmise that these results provide a valuable contribution to our understanding of lipase behavior in non-aqueous media. Based on the insights gained from this work, future studies will be centred on engineering lipase variants for optimal operation at aggressive condition of solvents, detergents, and temperature as well as modelling lipase stability in different solvents detergent groups.

7 REFERENCES

1. Illanes A, Cauerhff A, Wilson L, Castro GR. Recent trends in biocatalysis engineering. *Bioresour Technol.* 2012;115:48-57.
2. Stepankova V, Bidmanova S, Koudelakova T, Prokop Z, Chaloupkova R, Damborsky J. Strategies for stabilization of enzymes in organic solvents. *ACS Catalysis.* 2013;3(12):2823-36.
3. Schmid A, Dordick J, Hauer B, Kiener A, Wubbolts M, Witholt B. Industrial biocatalysis today and tomorrow. *Nature.* 2001;409(6817):258-68.
4. Serdakowski AL, Dordick JS. Enzyme activation for organic solvents made easy. *Trends Biotechnol.* 2008;26(1):48-54.
5. Zaks A, Klivanov AM. Enzymatic catalysis in organic media at 100 degrees C. *Science.* 1984;224(4654):1249-51.
6. Gotor-Fernández V, Brieva R, Gotor V. Lipases: Useful biocatalysts for the preparation of pharmaceuticals. *J Mol Catal B: Enzym.* 2006;40(3-4):111-20.
7. Plechkova NV, Seddon KR. Applications of ionic liquids in the chemical industry. *Chem Soc Rev.* 2008;37(1):123-50.
8. Durand E, Lecomte J, Baréa B, Dubreucq E, Lortie R, Villeneuve P. Evaluation of deep eutectic solvent–water binary mixtures for lipase-catalyzed lipophilization of phenolic acids. *Green Chem.* 2013;15(8):2275-82.
9. Abbott AP, Capper G, Davies DL, Munro HL, Rasheed RK, Tambyrajah V. Preparation of novel, moisture-stable, Lewis-acidic ionic liquids containing quaternary ammonium salts with functional side chains. *ChemComm.* 2001(19):2010-1.
10. Gorke JT, Sreenc F, Kazlauskas RJ. Hydrolase-catalyzed biotransformations in deep eutectic solvents. *Chem Commun.* 2008(10):1235-7.
11. Durand E, Lecomte J, Baréa B, Piombo G, Dubreucq E, Villeneuve P. Evaluation of deep eutectic solvents as new media for *Candida antarctica* B lipase catalyzed reactions. *Process Biochem.* 2012;47(12):2081-9.
12. Kleiner B, Schörken U. Native lipase dissolved in hydrophilic green solvents: A versatile 2-phase reaction system for high yield ester synthesis. *Eur J Lipid Sci Technol.* 2015;117(2):167-77.
13. Durand E, Lecomte J, Baréa B, Villeneuve P. Towards a better understanding of how to improve lipase-catalyzed reactions using deep eutectic solvents based on choline chloride. *Eur J Lipid Sci Technol.* 2014;116(1):16-23.
14. Guajardo N, Domínguez de María P, Ahumada K, Schrebler RA, Ramírez-Tagle R, Crespo FA, et al. Water as Cosolvent: Nonviscous Deep Eutectic Solvents for Efficient Lipase-Catalyzed Esterifications. *ChemCatChem.* 2017;9(8):1393-6.
15. Monhemi H, Housaindokht MR, Moosavi AA, Bozorgmehr MR. How a protein can remain stable in a solvent with high content of urea: insights from molecular dynamics simulation of *Candida antarctica* lipase B in urea: choline chloride deep eutectic solvent. *PCCP.* 2014;16(28):14882-93.

16. Jeong S-T, Kim H-K, Kim S-J, Chi S-W, Pan J-G, Oh T-K, et al. Novel zinc-binding center and a temperature switch in the *Bacillus stearothermophilus* L1 lipase. *J Biol Chem*. 2002;277(19):17041-7.
17. Andersen KK, Oliveira CL, Larsen KL, Poulsen FM, Callisen TH, Westh P, et al. The role of decorated SDS micelles in sub-CMC protein denaturation and association. *J Mol Biol*. 2009;391(1):207-26.
18. Nielsen MM, Andersen KK, Westh P, Otzen DE. Unfolding of β -sheet proteins in SDS. *Biophys J*. 2007;92(10):3674-85.
19. Otzen DE, Oliveberg M. Burst-phase expansion of native protein prior to global unfolding in SDS. *J Mol Biol*. 2002;315(5):1231-40.
20. Pedersen JN, Lyngsø J, Zinn T, Otzen DE, Pedersen JS. A complete picture of protein unfolding and refolding in surfactants. *Chem Sci*. 2020;11(3):699-712.
21. Otzen DE. Protein unfolding in detergents: effect of micelle structure, ionic strength, pH, and temperature. *Biophys J*. 2002;83(4):2219-30.
22. Otzen DE, Oliveberg M. A simple way to measure protein refolding rates in water. *J Mol Biol*. 2001;313(3):479-83.
23. Martinelle M, Holmquist M, Hult K. On the interfacial activation of *Candida antarctica* lipase A and B as compared with *Humicola lanuginosa* lipase. *Biochim Biophys Acta, Lipids Lipid Metab*. 1995;1258(3):272-6.
24. Hughes G, Lewis JC. Introduction: biocatalysis in industry. *Chem Rev*. 2018;118(1):1-3.
25. Straathof AJ, Adlercreutz P. *Applied biocatalysis*: CRC Press; 2000.
26. Grunwald P. *Biocatalysis: biochemical fundamentals and applications*: World Scientific; 2009.
27. Sheldon RA, Woodley JM. Role of biocatalysis in sustainable chemistry. *Chem Rev*. 2018;118(2):801-38.
28. Whittall J, Sutton PW. *Practical methods for biocatalysis and biotransformations*: John Wiley & Sons; 2009.
29. Tao JA, Kazlauskas RJ. *Biocatalysis for green chemistry and chemical process development*: John Wiley & Sons; 2011.
30. Choi J-M, Han S-S, Kim H-S. Industrial applications of enzyme biocatalysis: Current status and future aspects. *Biotechnol Adv*. 2015;33(7):1443-54.
31. Sheldon RA, Pereira PC. Biocatalysis engineering: the big picture. *Chem Soc Rev*. 2017;46(10):2678-91.
32. Huisman GW, Collier SJ. On the development of new biocatalytic processes for practical pharmaceutical synthesis. *Curr Opin Chem Biol*. 2013;17(2):284-92.
33. Tao J, Xu J-H. Biocatalysis in development of green pharmaceutical processes. *Curr Opin Chem Biol*. 2009;13(1):43-50.
34. Zheng G-W, Xu J-H. New opportunities for biocatalysis: driving the synthesis of chiral chemicals. *Curr Opin Biotechnol*. 2011;22(6):784-92.
35. Hoyos P, Pace V, J Hernaiz M, R Alcantara A. Biocatalysis in the pharmaceutical industry. A greener future. *Curr Green Chem*. 2014;1(2):155-81.

36. Patel RN. Biocatalysis in the pharmaceutical and biotechnology industries: CRC press; 2006.
37. Sheldon RA, Pereira PC. Biocatalysis engineering: the big picture. *Chem Soc Rev.* 2017;46(10):2678-91.
38. Bornscheuer UT, Kazlauskas RJ. Catalytic promiscuity in biocatalysis: using old enzymes to form new bonds and follow new pathways. *Angew Chem Int Ed.* 2004;43(45):6032-40.
39. Tracewell CA, Arnold FH. Directed enzyme evolution: climbing fitness peaks one amino acid at a time. *Curr Opin Chem Biol.* 2009;13(1):3-9.
40. Turner NJ. Directed evolution drives the next generation of biocatalysts. *Nat Chem Biol.* 2009;5(8):567-73.
41. Reetz MT. Directed evolution of enantioselective enzymes: an unconventional approach to asymmetric catalysis in organic chemistry. *J Org Chem.* 2009;74(16):5767-78.
42. Luetz S, Giver L, Lalonde J. Engineered enzymes for chemical production. *Biotechnol Bioeng.* 2008;101(4):647-53.
43. Woodley JM. Protein engineering of enzymes for process applications. *Curr Opin Chem Biol.* 2013;17(2):310-6.
44. Bommaris AS, Blum JK, Abrahamson MJ. Status of protein engineering for biocatalysts: how to design an industrially useful biocatalyst. *Curr Opin Chem Biol.* 2011;15(2):194-200.
45. Sheldon RA, van Pelt S. Enzyme immobilisation in biocatalysis: why, what and how. *Chem Soc Rev.* 2013;42(15):6223-35.
46. Hold C, Billerbeck S, Panke S. Forward design of a complex enzyme cascade reaction. *Nat Commun.* 2016;7(1):1-8.
47. MarketsandMarkets™. Enzymes Market Size, Share & Trends Analysis Report By Application (Industrial Enzymes, Specialty Enzymes), By Product (Carbohydrase, Proteases, Lipases), By Source, By Region, And Segment Forecasts, 2020 - 2027 2020 [Available from: <https://www.grandviewresearch.com/industry-analysis/enzymes-industry>].
48. Schmid RD, Verger R. Lipases: interfacial enzymes with attractive applications. *Angew Chem Int Ed.* 1998;37(12):1608-33.
49. Jaeger K-E, Eggert T. Lipases for biotechnology. *Curr Opin Biotechnol.* 2002;13(4):390-7.
50. Casas-Godoy L, Duquesne S, Bordes F, Sandoval G, Marty A. Lipases: an overview. *Lipases and phospholipases.* 2012:3-30.
51. Björkling F, Godtfredsen SE, Kirk O. The future impact of industrial lipases. *Trends Biotechnol.* 1991;9(1):360-3.
52. Bornscheuer U, Reif O-W, Lausch R, Freitag R, Scheper T, Kolisis FN, et al. Lipase of *Pseudomonas cepacia* for biotechnological purposes: purification, crystallization and characterization. *Biochim Biophys Acta Gen Subj.* 1994;1201(1):55-60.
53. Mukherjee KD. Lipase-catalyzed reactions for modification of fats and other lipids. *Biocatal Biotransformation.* 1990;3(4):277-93.
54. Sharma R, Chisti Y, Banerjee UC. Production, purification, characterization, and applications of lipases. *Biotechnol Adv.* 2001;19(8):627-62.

55. Kazlauskas RJ. Enhancing catalytic promiscuity for biocatalysis. *Curr Opin Chem Biol.* 2005;9(2):195-201.
56. Dwivedee BP, Soni S, Sharma M, Bhaumik J, Laha JK, Banerjee UC. Promiscuity of lipase-catalyzed reactions for organic synthesis: a recent update. *ChemistrySelect.* 2018;3(9):2441-66.
57. Bisen PS, Sanodiya BS, Thakur GS, Baghel RK, Prasad G. Biodiesel production with special emphasis on lipase-catalyzed transesterification. *Biotechnol Lett.* 2010;32(8):1019-30.
58. Reetz MT. Lipases as practical biocatalysts. *Curr Opin Chem Biol.* 2002;6(2):145-50.
59. Brady L, Brzozowski AM, Derewenda ZS, Dodson E, Dodson G, Tolley S, et al. A serine protease triad forms the catalytic centre of a triacylglycerol lipase. *Nature.* 1990;343(6260):767-70.
60. Nardini M, Dijkstra BW. α/β Hydrolase fold enzymes: the family keeps growing. *Curr Opin Struct Biol.* 1999;9(6):732-7.
61. Holmquist M. Alpha beta-hydrolase fold enzymes structures, functions and mechanisms. *Curr Protein Pept Sci.* 2000;1(2):209-35.
62. Lenfant N, Hotelier T, Velluet E, Bourne Y, Marchot P, Chatonnet A. ESTHER, the database of the α/β -hydrolase fold superfamily of proteins: tools to explore diversity of functions. *Nucleic Acids Res.* 2012;41(D1):D423-D9.
63. Kapoor M, Gupta MN. Lipase promiscuity and its biochemical applications. *Process Biochem.* 2012;47(4):555-69.
64. Kim KK, Song HK, Shin DH, Hwang KY, Suh SW. The crystal structure of a triacylglycerol lipase from *Pseudomonas cepacia* reveals a highly open conformation in the absence of a bound inhibitor. *Structure.* 1997;5(2):173-85.
65. Winkler FK, D'Arcy A, Hunziker W. Structure of human pancreatic lipase. *Nature.* 1990;343(6260):771-4.
66. Carrasco-López C, Godoy C, de Las Rivas B, Fernández-Lorente G, Palomo JM, Guisán JM, et al. Activation of bacterial thermoalkalophilic lipases is spurred by dramatic structural rearrangements. *J Biol Chem.* 2009;284(7):4365-72.
67. Hjorth A, Carriere F, Cudrey C, Woldike H, Boel E, Lawson DM, et al. A structural domain (the lid) found in pancreatic lipases is absent in the guinea pig (phospho) lipase. *Biochemistry.* 1993;32(18):4702-7.
68. Pleiss J, Fischer M, Schmid RD. Anatomy of lipase binding sites: the scissile fatty acid binding site. *Chem Phys Lipids.* 1998;93(1-2):67-80.
69. Klibanov AM. Enzymatic catalysis in anhydrous organic solvents. *Trends Biochem Sci.* 1989;14(4):141-4.
70. Bora L, Gohain D, Das R. Recent advances in production and biotechnological applications of thermostable and alkaline bacterial lipases. *J Chem Technol Biotechnol.* 2013;88(11):1959-70.
71. Ghasemi S, Heidary M, Faramarzi MA, Habibi Z. Immobilization of lipase on Fe₃O₄/ZnO core/shell magnetic nanoparticles and catalysis of Michael-type addition to chalcone derivatives. *J Mol Catal B: Enzym.* 2014;100:121-8.
72. Aouf C, Durand E, Lecomte J, Figueroa-Espinoza M-C, Dubreucq E, Fulcrand H, et al. The use of

lipases as biocatalysts for the epoxidation of fatty acids and phenolic compounds. *Green Chem.* 2014;16(4):1740-54.

73.Sarda L, Desnuelle P. Action of pancreatic lipase on emulsified esters. *Biochim Biophys Acta.* 1958;30:513-21.

74.Cygler M, Schrag JD. Structure as basis for understanding interfacial properties of lipases. *Meth Enzymol.* 1997;284:3-27.

75.Verger R, De Haas GH. Interfacial enzyme kinetics of lipolysis. *Annu Rev Biophys Bioeng.* 1976;5(1):77-117.

76.Labourdenne S, Cagna A, Delorme B, Esposito G, Verger R, Rivière C. Oil-drop tensiometer: Applications for studying the kinetics of lipase action. *Meth Enzymol.* 1997;286:306-26.

77.Holmquist M, Martinelle M, Clausen IG, Patkar S, Svendsen A, Hult K. Trp89 in the lid of *Humicola lanuginosa* lipase is important for efficient hydrolysis of tributyrin. *Lipids.* 1994;29(9):599-603.

78.Joerger RD, Haas MJ. Alteration of chain length selectivity of a *Rhizopus delemar* lipase through site-directed mutagenesis. *Lipids.* 1994;29(6):377-84.

79.Peters GH, van Aalten D, Svendsen A, Bywater R. Essential dynamics of lipase binding sites: the effect of inhibitors of different chain length. *Protein Eng* 1997;10(2):149-58.

80.Yang J, Koga Y, Nakano H, Yamane T. Modifying the chain-length selectivity of the lipase from *Burkholderia cepacia* KWI-56 through in vitro combinatorial mutagenesis in the substrate-binding site. *Protein Eng.* 2002;15(2):147-52.

81.Barriuso J, Vaquero ME, Prieto A, Martínez MJ. Structural traits and catalytic versatility of the lipases from the *Candida rugosa*-like family: A review. *Biotechnol Adv.* 2016;34(5):874-85.

82.Wang J-b, Li G, Reetz MT. Enzymatic site-selectivity enabled by structure-guided directed evolution. *Chem Commun.* 2017;53(28):3916-28.

83.Ghattas N, Abidi F, Galai S, Marzouki MN, Salah AB. Monoolein production by triglycerides hydrolysis using immobilized *Rhizopus oryzae* lipase. *Int J Biol Macromol.* 2014;68:1-6.

84.Yan Q, Duan X, Liu Y, Jiang Z, Yang S. Expression and characterization of a novel 1, 3-regioselective cold-adapted lipase from *Rhizomucor endophyticus* suitable for biodiesel synthesis. *Biotechnol Biofuels.* 2016;9(1):1-13.

85.Brígida AI, Amaral PF, Coelho MA, Goncalves LR. Lipase from *Yarrowia lipolytica*: Production, characterization and application as an industrial biocatalyst. *J Mol Catal B: Enzym.* 2014;101:148-58.

86.Bueso F, Moreno L, Cedeño M, Manzanarez K. Lipase-catalyzed biodiesel production and quality with *Jatropha curcas* oil: exploring its potential for Central America. *J Biol Eng.* 2015;9(1):1-7.

87.Watanabe Y, Sato S, Sera S, Sato C, Yoshinaga K, Nagai T, et al. Enzymatic Analysis of Positional Distribution of Fatty Acids in Solid Fat by 1, 3-Selective Transesterification with *Candida antarctica* Lipase B. *J Am Oil Chem Soc.* 2014;91(8):1323-30.

88.Sarkar P, Yamasaki S, Basak S, Bera A, Bag PK. Purification and characterization of a new alkali-thermostable lipase from *Staphylococcus aureus* isolated from *Arachis hypogaea* rhizosphere. *Process Biochem.* 2012;47(5):858-66.

89.Horchani H, Aissa I, Ouertani S, Zarai Z, Gargouri Y, Sayari A. Staphylococcal lipases:

- biotechnological applications. *J Mol Catal B: Enzym.* 2012;76:125-32.
- 90.Ota Y, Sawamoto T, Hasuo M. Tributyrin specifically induces a lipase with a preference for the sn-2 position of triglyceride in *Geotrichum* sp. FO401B. *Biosci, Biotechnol.* 2000;64(11):2497-9.
- 91.Krishna SH, Manohar B, Divakar S, Prapulla S, Karanth N. Optimization of isoamyl acetate production by using immobilized lipase from *Mucor miehei* by response surface methodology. *Enzyme Microb Technol.* 2000;26(2-4):131-6.
- 92.Jensen RG. Characteristics of the lipase from the mold, *Geotrichum candidum*: A review. *Lipids.* 1974;9(3):149-57.
- 93.Pleiss J, Scheib H, Schmid RD. The His gap motif in microbial lipases: a determinant of stereoselectivity toward triacylglycerols and analogs. *Biochimie.* 2000;82(11):1043-52.
- 94.Rogalska E, Cudrey C, Ferrato F, Verger R. Stereoselective hydrolysis of triglycerides by animal and microbial lipases. *Chirality.* 1993;5(1):24-30.
- 95.Matteis V. Temperature and solvent effects on enzyme stereoselectivity: inversion temperature in kinetic resolutions with lipases. *Chem Commun.* 2000(23):2351-2.
- 96.Ferreira-Dias S, Sandoval G, Plou F, Valero F. The potential use of lipases in the production of fatty acid derivatives for the food and nutraceutical industries. *Electron J Biotechnol.* 2013;16(3):12-.
- 97.Chaurasia S, Bhandaria K, Sharma A, Dalai A. A review on lipase catalysed synthesis of DHA rich glyceride from fish oils. *Int J Res Sci Innov.* 2016;3:9-19.
- 98.Miguel AM, Martins-Meyer TS, Figueiredo E, Lobo BWP, Dellamora-Ortiz GM. Enzymes in bakery: current and future trends. *J Food Ind.* 2013:278-321.
- 99.Houde A, Kademi A, Leblanc D. Lipases and their industrial applications. *Appl Biochem Biotechnol.* 2004;118(1):155-70.
- 100.Lailaja V, Chandrasekaran M. Detergent compatible alkaline lipase produced by marine *Bacillus smithii* BTMS 11. *World J Microbiol Biotechnol.* 2013;29(8):1349-60.
- 101.Zhang HY, Wang X, Ching CB, Wu JC. Experimental optimization of enzymic kinetic resolution of racemic flurbiprofen. *Biotechnol Appl Biochem.* 2005;42(1):67-71.
- 102.Hasan F, Shah AA, Hameed A. Industrial applications of microbial lipases. *Enzyme Microb Technol.* 2006;39(2):235-51.
- 103.Muralidhar R, Chirumamilla R, Ramachandran V, Marchant R, Nigam P. Racemic resolution of RS-baclofen using lipase from *Candida cylindracea*. *Meded Rijksuniv Gent Fak Landbouwk Toegep Biol Wet.* 2001;66(3a):227-32.
- 104.Rasor JP, Voss E. Enzyme-catalyzed processes in pharmaceutical industry. *Appl Catal A: Gen.* 2001;221(1-2):145-58.
- 105.Patel RN. Microbial/enzymatic synthesis of chiral drug intermediates. *Adv Appl Microbiol.* 2000.
- 106.Joseph B, Ramteke PW, Thomas G. Cold active microbial lipases: some hot issues and recent developments. *Biotechnol Adv.* 2008;26(5):457-70.
- 107.Iding H, Siegert P, Mesch K, Pohl M. Application of α -keto acid decarboxylases in biotransformations. *BBA-PROTEIN STRUCT M.* 1998;1385(2):307-22.
- 108.Gerhartz W. Industrial uses of enzymes. VCH publishers, Germany; 1990. p. 77-92.

109. Maugard T, Rejasse B, Legoy MD. Synthesis of water-soluble retinol derivatives by enzymatic method. *Biotechnol Prog.* 2002;18(3):424-8.
110. Lott JA, Lu CJ. Lipase isoforms and amylase isoenzymes: assays and application in the diagnosis of acute pancreatitis. *Clin Chem.* 1991;37(3):361-8.
111. Nouredini H, Gao X, Philkana R. Immobilized *Pseudomonas cepacia* lipase for biodiesel fuel production from soybean oil. *Bioresour Technol.* 2005;96(7):769-77.
112. Tan T, Lu J, Nie K, Deng L, Wang F. Biodiesel production with immobilized lipase: a review. *Biotechnol Adv.* 2010;28(5):628-34.
113. Bajpai P. Application of enzymes in the pulp and paper industry. *Biotechnol Prog.* 1999;15(2):147-57.
114. Demirjian DC, Moris-Varas F, Cassidy CS. Enzymes from extremophiles. *Curr Opin Chem Biol.* 2001;5(2):144-51.
115. Schmidt-Dannert C, Sztajer H, Stöcklein W, Menge U, Schmid RD. Screening, purification and properties of a thermophilic lipase from *Bacillus thermocatenulatus*. *Biochim Biophys Acta, Lipids Lipid Metab.* 1994;1214(1):43-53.
116. Cho A-R, Yoo S-K, Kim E-J. Cloning, sequencing and expression in *Escherichia coli* of a thermophilic lipase from *Bacillus thermoleovorans* ID-1. *FEMS Microbiol Lett.* 2000;186(2):235-8.
117. Jaeger K, Dijkstra B, Reetz M. Bacterial biocatalysts: molecular biology, three-dimensional structures, and biotechnological applications of lipases. *Annu Rev Microbiol.* 1999;53(1):315-51.
118. Rosenstein R, Götz F. Staphylococcal lipases: biochemical and molecular characterization. *Biochimie.* 2000;82(11):1005-14.
119. Simons JWF, van Kampen MD, Riel S, Götz F, Egmond MR, Verheij HM. Cloning, purification and characterisation of the lipase from *Staphylococcus epidermidis*: Comparison of the substrate selectivity with those of other microbial lipases. *Eur J Biochem.* 1998;253(3):675-83.
120. Oh B-C, Kim H-K, Lee J-K, Kang S-C, Oh T-K. *Staphylococcus haemolyticus* lipase: biochemical properties, substrate specificity and gene cloning. *FEMS Microbiol Lett.* 1999;179(2):385-92.
121. Schmidt-Dannert C, Rua ML, Atomi H, Schmid RD. Thermoalkalophilic lipase of *Bacillus thermocatenulatus*. I. Molecular cloning, nucleotide sequence, purification and some properties. *Biochim Biophys Acta, Lipids Lipid Metab.* 1996;1301(1-2):105-14.
122. Herbert RA. A perspective on the biotechnological potential of extremophiles. *Trends Biotechnol.* 1992;10:395-402.
123. Jaeger K-E, Ransac S, Dijkstra BW, Colson C, van Heuvel M, Misset O. Bacterial lipases. *FEMS Microbiol Rev.* 1994;15(1):29-63.
124. Zaks A, Klivanov AM. Enzyme-catalyzed processes in organic solvents. *Proc Nat Acad Sci* 1985;82(10):3192-6.
125. Zaks A, Klivanov AM. Enzymatic catalysis in nonaqueous solvents. *J Biol Chem.* 1988;263(7):3194-201.
126. Klivanov AM. Improving enzymes by using in organic solvents. *Nature.* 2001;409(6817):241-6.
127. Carrea G, Ottolina G, Riva S. Role of solvents in the control of enzyme selectivity in organic media.

Trends Biotechnol. 1995;13(2):63-70.

128.Li C, Wang P, Zhao D, Cheng Y, Wang L, Wang L, et al. Enantioselective enzymatic hydrolysis of racemic glycidyl butyrate by lipase from *Bacillus subtilis* with improved catalytic properties. *J Mol Catal B: Enzym.* 2008;55(3-4):152-6.

129.Hansen TV, Waagen V, Partali V, Anthonsen HW, Anthonsen T. Co-solvent enhancement of enantioselectivity in lipase-catalysed hydrolysis of racemic esters. A process for production of homochiral C-3 building blocks using lipase B from *Candida antarctica*. *Tetrahedron: Asymmetry.* 1995;6(2):499-504.

130.Raminelli C, Comasseto JV, Andrade LH, Porto AL. Kinetic resolution of propargylic and allylic alcohols by *Candida antarctica* lipase (Novozyme 435). *Tetrahedron: Asymmetry.* 2004;15(19):3117-22.

131.Ammazzalorso A, Amoroso R, Bettoni G, De Filippis B, Fantacuzzi M, Giampietro L, et al. *Candida rugosa* lipase-catalysed kinetic resolution of 2-substituted-aryloxyacetic esters with dimethylsulfoxide and isopropanol as additives. *Chirality.* 2008;20(2):115-8.

132.Tsuzuki W, Ue A, Nagao A. Polar organic solvent added to an aqueous solution changes hydrolytic property of lipase. *Biosci, Biotechnol, Biochem.* 2003;67(8):1660-6.

133.Du C, Zhao B, Li C, Wang P, Wang Z, Tang J, et al. Improvement of the enantioselectivity and activity of lipase from *Pseudomonas* sp. via adsorption on a hydrophobic support: kinetic resolution of 2-octanol. *Biocatal Biotransformation.* 2009;27(5-6):340-7.

134.Mohapatra SC, Hsu JT. Optimizing lipase activity, enantioselectivity, and stability with medium engineering and immobilization for β -blocker synthesis. *Biotechnol Bioeng.* 1999;64(2):213-20.

135.Cheng Y-C, Tsai S-W. Enantioselective esterification of (RS)-2-(4-chlorophenoxy) propionic acid via *Carica papaya* lipase in organic solvents. *Tetrahedron: Asymmetry.* 2004;15(18):2917-20.

136.Xia X, Wang Y-H, Yang B, Wang X. Wheat germ lipase catalyzed kinetic resolution of secondary alcohols in non-aqueous media. *Biotechnol Lett.* 2009;31(1):83-7.

137.Xu K, Klibanov AM. pH control of the catalytic activity of cross-linked enzyme crystals in organic solvents. *J Am Chem Soc.* 1996;118(41):9815-9.

138.Kirchner G, Scollar MP, Klibanov AM. Resolution of racemic mixtures via lipase catalysis in organic solvents. *J Am Chem Soc.* 1985;107(24):7072-6.

139.Zaks A, Dodds DR. Application of biocatalysis and biotransformations to the synthesis of pharmaceuticals. *Drug Discov Tod.* 1997;2(12):513-31.

140.Gutman AL, Meyer E, Kalerin E, Polyak F, Sterling J. Enzymatic resolution of racemic amines in a continuous reactor in organic solvents. *Biotechnol Bioeng.* 1992;40(7):760-7.

141.Carrea G, Riva S. Properties and synthetic applications of enzymes in organic solvents. *Angew Chem Int Ed.* 2000;39(13):2226-54.

142.Akkara JA, Ayyagari MS, Bruno FF. Enzymatic synthesis and modification of polymers in nonaqueous solvents. *Trends Biotechnol.* 1999;17(2):67-73.

143.Stepankova V, Damborsky J, Chaloupkova R. Hydrolases in non-conventional media: implications for industrial biocatalysis. *Industrial biocatalysis* Pan Stanford Publishing Ltd, Germany. 2015:583-630

144. Alam M, Tadasa K, Maeda T, Kayahara H. Correlation of inhibition of thermolysin by water-miscible alcoholic solvents with their physicochemical parameters and the status of monoalcoholic character of water in the peptide synthesis of Z-Phe-Phe-OMe in water organic one-phase reaction system. *Biotechnol Lett.* 1997;19(11):1129-33.
145. Hudson EP, Eppler RK, Clark DS. Biocatalysis in semi-aqueous and nearly anhydrous conditions. *Curr Opin Biotechnol.* 2005;16(6):637-43.
146. Peters G, Van Aalten D, Edholm O, Toxvaerd S, Bywater R. Dynamics of proteins in different solvent systems: analysis of essential motion in lipases. *Biophys J.* 1996;71(5):2245-55.
147. Ramakrishnan SK, Krishna V, Kumar V, Lakshmi B, Anishetty S, Gautam P. Molecular dynamics simulation of lipases. *Int J Integr Biol.* 2008;2(3):204-13.
148. Trodler P, Pleiss J. Modeling structure and flexibility of *Candida antarctica* lipase B in organic solvents. *BMC Struct Biol.* 2008;8(1):1-10.
149. Rehm S, Trodler P, Pleiss J. Solvent-induced lid opening in lipases: A molecular dynamics study. *Protein Sci.* 2010;19(11):2122-30.
150. Kulschewski T, Sasso F, Secundo F, Lotti M, Pleiss J. Molecular mechanism of deactivation of *C. antarctica* lipase B by methanol. *J Biotechnol.* 2013;168(4):462-9.
151. Li C, Tan T, Zhang H, Feng W. Analysis of the conformational stability and activity of *Candida antarctica* lipase B in organic solvents: insight from molecular dynamics and quantum mechanics/simulations. *J Biol Chem.* 2010;285(37):28434-41.
152. Park HJ, Park K, Yoo YJ. Understanding the effect of tert-butanol on *Candida antarctica* lipase B using molecular dynamics simulations. *Mol Simul.* 2013;39(8):653-9.
153. Barbe S, Lafaquiere V, Guieysse D, Monsan P, Remaud-Siméon M, Andre I. Insights into lid movements of *Burkholderia cepacia* lipase inferred from molecular dynamics simulations. *Proteins.* 2009;77(3):509-23.
154. Artham T, Mohanalakshmi N, Paragi-Vedanthi PP, Doble M. Mechanistic investigations of lipase-catalyzed degradation of polycarbonate in organic solvents. *Enzyme Microb Technol.* 2011;48(1):71-9.
155. Rahman MZA, Salleh AB, Rahman RNZRA, Rahman MBA, Basri M, Leow TC. Unlocking the mystery behind the activation phenomenon of T1 lipase: a molecular dynamics simulations approach. *Protein Sci.* 2012;21(8):1210-21.
156. Mathpati AC, Bhanage BM. Combined docking and molecular dynamics study of lipase catalyzed kinetic resolution of 1-phenylethanol in organic solvents. *J Mol Catal B: Enzym.* 2016;133:S119-S27.
157. Park HJ, Joo JC, Park K, Kim YH, Yoo YJ. Prediction of the solvent affecting site and the computational design of stable *Candida antarctica* lipase B in a hydrophilic organic solvent. *J Biotechnol.* 2013;163(3):346-52.
158. Jiang Y, Li L, Zhang H, Feng W, Tan T. Lid closure mechanism of *Yarrowia lipolytica* lipase in methanol investigated by molecular dynamics simulation. *J Chem Inf Model.* 2014;54(7):2033-41.
159. Graber M, Irague R, Rosenfeld E, Lamare S, Franson L, Hult K. Solvent as a competitive inhibitor for *Candida antarctica* lipase B. *Biochim Biophys Acta, Proteins Proteomics.* 2007;1774(8):1052-7.
160. Castillo E, Casas-Godoy L, Sandoval G. Medium-engineering: a useful tool for modulating lipase

- activity and selectivity. *Biocatalysis*. 2016;1(1):178-88.
161. Berglund P. Controlling lipase enantioselectivity for organic synthesis. *Biomol Eng*. 2001;18(1):13-22.
162. Cui H, Zhang L, Eltoukhy L, Jiang Q, Korkunç SKb, Jaeger K-E, et al. Enzyme Hydration Determines Resistance in Organic Cosolvents. *ACS Catal*. 2020;10(24):14847-56.
163. Cui H, Eltoukhy L, Zhang L, Markel U, Jaeger KE, Davari MD, et al. Less Unfavorable Salt Bridges on the Enzyme Surface Result in More Organic Cosolvent Resistance. *Angew Chem Int Ed*. 2021;60(20):11448-56.
164. Sheldon RA. Biocatalysis and biomass conversion in alternative reaction media. *Chem Eur J*. 2016;22(37):12984-99.
165. Durand E, Lecomte J, Baréa B, Dubreucq E, Lortie R, Villeneuve P. Evaluation of deep eutectic solvent–water binary mixtures for lipase-catalyzed lipophilization of phenolic acids. *Green Chem*. 2013;15(8):2275-82.
166. Pätzold M, Siebenhaller S, Kara S, Liese A, Syltatk C, Holtmann D. Deep eutectic solvents as efficient solvents in biocatalysis. *Trends Biotechnol*. 2019;37(9):943-59.
167. Liu P, Hao J-W, Mo L-P, Zhang Z-H. Recent advances in the application of deep eutectic solvents as sustainable media as well as catalysts in organic reactions. *RSC Adv*. 2015;5(60):48675-704.
168. Pena-Pereira F, Namieśnik J. Ionic liquids and deep eutectic mixtures: sustainable solvents for extraction processes. *ChemSusChem*. 2014;7(7):1784-800.
169. Hammond OS, Bowron DT, Edler KJ. Liquid structure of the choline chloride-urea deep eutectic solvent (reline) from neutron diffraction and atomistic modelling. *Green Chem*. 2016;18(9):2736-44.
170. Hayyan M, Hashim MA, Hayyan A, Al-Saadi MA, AlNashef IM, Mirghani ME, et al. Are deep eutectic solvents benign or toxic? *Chemosphere*. 2013;90(7):2193-5.
171. Wen Q, Chen J-X, Tang Y-L, Wang J, Yang Z. Assessing the toxicity and biodegradability of deep eutectic solvents. *Chemosphere*. 2015;132:63-9.
172. Abbott AP, Capper G, Davies DL, Rasheed RK, Tambyrajah V. Novel solvent properties of choline chloride/urea mixtures. *Chem Commun*. 2003(1):70-1.
173. Zhang Q, Wang Q, Zhang S, Lu X, Zhang X. Electrodeposition in ionic liquids. *ChemPhysChem*. 2016;17(3):335-51.
174. Bubalo MC, Tušek AJ, Vinković M, Radošević K, SrLek VG, Redovniković IR. Cholinium-based deep eutectic solvents and ionic liquids for lipase-catalyzed synthesis of butyl acetate. *J Mol Catal B: Enzym*. 2015;122:188-98.
175. Zhao H, Zhang C, Crittle TD. Choline-based deep eutectic solvents for enzymatic preparation of biodiesel from soybean oil. *J Mol Catal B: Enzym*. 2013;85:243-7.
176. Zhao H, Baker GA, Holmes S. New eutectic ionic liquids for lipase activation and enzymatic preparation of biodiesel. *Org Biomol Chem*. 2011;9(6):1908-16.
177. Zhang Y, Xia X, Duan M, Han Y, Liu J, Luo M, et al. Green deep eutectic solvent assisted enzymatic preparation of biodiesel from yellow horn seed oil with microwave irradiation. *J Mol Catal B: Enzym*. 2016;123:35-40.

178. Merza F, Fawzy A, AlNashef I, Al-Zuhair S, Taher H. Effectiveness of using deep eutectic solvents as an alternative to conventional solvents in enzymatic biodiesel production from waste oils. *Energy Rep.* 2018;4:77-83.
179. Kleiner B, Fleischer P, Schörken U. Biocatalytic synthesis of biodiesel utilizing deep eutectic solvents: A two-step-one-pot approach with free lipases suitable for acidic and used oil processing. *Process Biochem.* 2016;51(11):1808-16.
180. Domínguez de María P, Guajardo N, Kara S. Enzyme catalysis: In DES, with DES, and in the presence of DES. *Deep Eutectic Solvents: Synthesis, Properties, and Applications.* 2019:257-71.
181. Siebenhaller S, Muhle-Goll C, Luy B, Kirschhöfer F, Brenner-Weiss G, Hiller E, et al. Sustainable enzymatic synthesis of glycolipids in a deep eutectic solvent system. *J Mol Catal B: Enzym.* 2016;133:S281-S7.
182. González Martínez D, Gotor Santamaría VM, Gotor Fernández V. Application of deep eutectic solvents in promiscuous lipase-catalysed aldol reactions. *Eur J Org Chem.* 2016.
183. Borse B, Borude V, Shukla S. Synthesis of novel dihydropyrimidin-2 (1H)-ones derivatives using lipase and their antimicrobial activity. *Curr Chem Lett.* 2012;1(2):59-68.
184. Shah D, Mjalli FS. Effect of water on the thermo-physical properties of Reline: An experimental and molecular simulation based approach. *PCCP.* 2014;16(43):23900-7.
185. Sapir L, Harries D. Restructuring a deep eutectic solvent by water: The nanostructure of hydrated choline chloride/urea. *J Chem Theory Comput.* 2020;16(5):3335-42.
186. Kaur S, Gupta A, Kashyap HK. How hydration affects the microscopic structural morphology in a deep eutectic solvent. *J Phys Chem.* 2020;124(11):2230-7.
187. Hammond OS, Bowron DT, Edler KJ. The effect of water upon deep eutectic solvent nanostructure: An unusual transition from ionic mixture to aqueous solution. *Angew Chem Int Ed.* 2017;56(33):9782-5.
188. Gabriele F, Chiarini M, Germani R, Tiecco M, Spreti N. Effect of water addition on choline chloride/glycol deep eutectic solvents: Characterization of their structural and physicochemical properties. *J Mol Liq.* 2019;291:111301.
189. Nian B, Cao C, Liu Y. How *Candida antarctica* lipase B can be activated in natural deep eutectic solvents: experimental and molecular dynamics studies. *J Chem Technol Biotechnol.* 2020;95(1):86-93.
190. Ortiz C, Ferreira M, Barbosa O, Dos Santos J, Rodrigues R, Berenguer-Murcia Á, et al. Novozym435: The “perfect” lipase immobilized biocatalyst? *Catal Sci Technol.* 2019;9(2380):10.1039.
191. Derewenda ZS, Sharp AM. News from the interface: the molecular structures of triacylglyceride lipases. *Trends Biochem Sci.* 1993;18(1):20-5.
192. Delorme V, Dhouib R, Canaan S, Fotiadu F, Carrière F, Cavalier J-F. Effects of surfactants on lipase structure, activity, and inhibition. *Pharm Res.* 2011;28(8):1831-42.
193. Mateos-Díaz E, Amara S, Roussel A, Longhi S, Cambillau C, Carrière F. Probing conformational changes and interfacial recognition site of lipases with surfactants and inhibitors. *Methods Enzymol.* 2017;583:279-307.

194. Mogensen JE, Sehgal P, Otzen DE. Activation, inhibition, and destabilization of *Thermomyces lanuginosus* lipase by detergents. *Biochemistry*. 2005;44(5):1719-30.
195. Skagerlind P, Jansson M, Bergenståhl B, Hult K. Binding of *Rhizomucor miehei* lipase to emulsion interfaces and its interference with surfactants. *Colloids Surf B Biointerfaces*. 1995;4(3):129-35.
196. Canioni P, Julien R, Rathelot J, Sarda L. Inhibition of sheep pancreatic lipase activity against emulsified tributyrin by non-ionic detergents. *Biochimie*. 1976;58(6):751-3.
197. Skagerlind P, Folmer B, Jha B, Svensson M, Holmberg K. Lipase-surfactant interactions. *The Colloid Science of Lipids*: Springer; 1998. p. 47-57.
198. Fletcher PD, Robinson BH, Freedman RB, Oldfield C. Activity of lipase in water-in-oil microemulsions. *J Chem Soc Faraday Trans*. 1985;81(11):2667-79.
199. Jenta TRJ, Batts G, Rees GD, Robinson BH. Kinetic studies of *Chromobacterium viscosum* lipase in AOT water in oil microemulsions and gelatin microemulsion-based organogels. *Biotechnol Bioeng*. 1997;54(5):416-27.
200. Holmberg K, Lassen B, Stark MB. Enzymatic glycerolysis of a triglyceride in aqueous and nonaqueous microemulsions. *J Am Oil Chem Soc*. 1989;66(12):1796-800.
201. Polizelli PP, Tiera MJ, Bonilla-Rodriguez GO. Effect of surfactants and polyethylene glycol on the activity and stability of a lipase from oilseeds of *Pachira aquatica*. *J Am Oil Chem Soc*. 2008;85(8):749-53.
202. Diaz JM, Cordova J, Baratti J, Carriere F, Abousalham A. Effect of nonionic surfactants on *Rhizopus homothallicus* lipase activity. *Mol Biotechnol*. 2007;35(3):205.
203. Domínguez A, Deive FJ, Sanromán MA, Longo MA. Effect of lipids and surfactants on extracellular lipase production by *Yarrowia lipolytica*. *J Chem Technol Biotechnol* 2003;78(11):1166-70.
204. Magalhaes SS, Alves L, Sebastiao M, Medronho B, Almeida ZL, Faria TQ, et al. Effect of ethyleneoxide groups of anionic surfactants on lipase activity. *Biotechnol Prog*. 2016;32(5):1276-82.
205. Jutila A, Zhu K, Patkar SA, Vind J, Svendsen A, Kinnunen PK. Detergent-induced conformational changes of *Humicola lanuginosa* lipase studied by fluorescence spectroscopy. *Biophys J*. 2000;78(3):1634-42.
206. Goswami D. Lipase catalysis in presence of nonionic surfactants. *Appl Biochem Biotechnol*. 2020;191(2):744-62.
207. Syed MN, Iqbal S, Bano S, Khan AB, Ali-ul-Qader S, Azhar A. Purification and characterization of 60 kD lipase linked with chaperonin from *Pseudomonas aeruginosa* BN-1. *Afr j biotechnol*. 2010;9(45):7724-32.
208. Wu H-Y, Xu J-H, Liu Y-Y. A practical enzymatic method for preparation of (S)-ketoprofen with a crude *Candida rugosa* lipase. *Synth Commun*. 2001;31(22):3491-6.
209. Dutta S, Ray L. Production and characterization of an alkaline thermostable crude lipase from an isolated strain of *Bacillus cereus* C 7. *Appl Biochem Biotechnol*. 2009;159(1):142-54.
210. Prazeres JNd, Cruz JAB, Pastore GM. Characterization of alkaline lipase from *Fusarium oxysporum* and the effect of different surfactants and detergents on the enzyme activity. *Braz J Microbio*

2006;37:505-9.

211.Helistö P, Korpela T. Effects of detergents on activity of microbial lipases as measured by the nitrophenyl alkanoate esters method. *Enzyme Microb Technol.* 1998;23(1-2):113-7.

212.Lai DT, O'Connor CJ. Synergistic effects of surfactants on kid pregastric lipase catalyzed hydrolysis reactions. *Langmuir.* 2000;16(1):115-21.

213.Fendri A, Frikha F, Mosbah H, Miled N, Zouari N, Bacha AB, et al. Biochemical characterization, cloning, and molecular modelling of chicken pancreatic lipase. *Arch Biochem Biophys.* 2006;451(2):149-59.

214.Savelli G, Spreti N, Di Profio P. Enzyme activity and stability control by amphiphilic self-organizing systems in aqueous solutions. *Curr Opin Colloid Interface Sci* 2000;5(1-2):111-7.

215.Reis P, Holmberg K, Watzke H, Leser M, Miller R. Lipases at interfaces: a review. *Adv Colloid Interface Sci.* 2009;147:237-50.

216.Creighton TE. *Proteins: structures and molecular properties*: Macmillan; 1993.

217.Folmer B, Holmberg K, Svensson M. Interaction of *Rhizomucor miehei* lipase with an amphoteric surfactant at different pH values. *Langmuir.* 1997;13(22):5864-9.

218.Peters GH. The dynamic response of a fungal lipase in the presence of charged surfactants. *Colloids Surf B Biointerfaces.* 2002;26(1-2):84-101.

219.Das S, Balasubramanian S. pH-Induced Rotation of Lidless Lipase LipA from *Bacillus subtilis* at Lipase–Detergent Interface. *J Phys Chem.* 2018;122(18):4802-12.

220.Kübler D, Bergmann A, Weger L, Ingenbosch KN, Hoffmann-Jacobsen K. Kinetics of detergent-induced activation and inhibition of a minimal lipase. *J Phys Chem.* 2017;121(6):1248-57.

221.Luo M, Dommer AC, Schiffer JM, Rez DJ, Mitchell AR, Amaro RE, et al. Surfactant charge modulates structure and stability of lipase-embedded monolayers at marine-relevant aerosol surfaces. *Langmuir.* 2019;35(27):9050-60.

222.Martínez L, Andrade R, Birgin EG, Martínez JM. PACKMOL: a package for building initial configurations for molecular dynamics simulations. *J Comput Chem.* 2009;30(13):2157-64.

223.Humphrey W, Dalke A, Schulten K. VMD: visual molecular dynamics. *J Mol Graphics.* 1996;14(1):33-8.

224.Pastor RW, Brooks BR, Szabo A. An analysis of the accuracy of Langevin and molecular dynamics algorithms. *Mol Phys.* 1988;65(6):1409-19.

225.Phillips JC, Braun R, Wang W, Gumbart J, Tajkhorshid E, Villa E, et al. Scalable molecular dynamics with NAMD. *J Comput Chem.* 2005;26(16):1781-802.

226.MacKerell Jr AD, Bashford D, Bellott M, Dunbrack Jr RL, Evanseck JD, Field MJ, et al. All-atom empirical potential for molecular modeling and dynamics studies of proteins. *J Phys Chem.* 1998;102(18):3586-616.

227.Huang J, MacKerell Jr AD. CHARMM36 all-atom additive protein force field: Validation based on comparison to NMR data. *J Comput Chem.* 2013;34(25):2135-45.

228.Brooks BR, Brooks III CL, Mackerell Jr AD, Nilsson L, Petrella RJ, Roux B, et al. CHARMM: the biomolecular simulation program. *J Comput Chem.* 2009;30(10):1545-614.

- 229.Jorgensen WL, Chandrasekhar J, Madura JD, Impey RW, Klein ML. Comparison of simple potential functions for simulating liquid water. *J Chem Phys.* 1983;79(2):926-35.
- 230.Darden T, York D, Pedersen L. Particle mesh Ewald: An $N \cdot \log(N)$ method for Ewald sums in large systems. *J Chem Phys.* 1993;98(12):10089-92.
- 231.Michaud-Agrawal N, Denning EJ, Woolf TB, Beckstein O. MDAAnalysis: a toolkit for the analysis of molecular dynamics simulations. *J Comput Chem.* 2011;32(10):2319-27.
- 232.Grant BJ, Rodrigues AP, ElSawy KM, McCammon JA, Caves LS. Bio3d: an R package for the comparative analysis of protein structures. *Bioinformatics.* 2006;22(21):2695-6.
- 233.McGibbon RT, Beauchamp KA, Harrigan MP, Klein C, Swails JM, Hernández CX, et al. MDTraj: a modern open library for the analysis of molecular dynamics trajectories. *Biophys J.* 2015;109(8):1528-32.
- 234.Stourac J, Vavra O, Kokkonen P, Filipovic J, Pinto G, Brezovsky J, et al. Caver Web 1.0: identification of tunnels and channels in proteins and analysis of ligand transport. *Nucleic Acids Res.* 2019;47(W1):W414-W22.
- 235.Shehata M, Timucin E, Venturini A, Sezerman OU. Understanding thermal and organic solvent stability of thermoalkalophilic lipases: insights from computational predictions and experiments. *J Mol Model.* 2020;26(6):1-12.
- 236.Bradford MM. A rapid and sensitive method for the quantitation of microgram quantities of protein utilizing the principle of protein-dye binding. *Anal Biochem.* 1976;72(1-2):248-54.
- 237.Huang X, Zhou H-X. Similarity and difference in the unfolding of thermophilic and mesophilic cold shock proteins studied by molecular dynamics simulations. *Biophys J.* 2006;91(7):2451-63.
- 238.Merkley ED, Parson WW, Daggett V. Temperature dependence of the flexibility of thermophilic and mesophilic flavoenzymes of the nitroreductase fold. *Protein Eng Des Sel.* 2010;23(5):327-36.
- 239.Purmonen M, Valjakka J, Takkinen K, Laitinen T, Rouvinen J. Molecular dynamics studies on the thermostability of family 11 xylanases. *Protein Eng Des Sel.* 2007;20(11):551-9.
- 240.Fic E, Kedracka-Krok S, Jankowska U, Pirog A, Dziedzicka-Wasylewska M. Comparison of protein precipitation methods for various rat brain structures prior to proteomic analysis. *Electrophoresis.* 2010;31(21):3573-9.
- 241.Leron RB, Li M-H. High-pressure density measurements for choline chloride: Urea deep eutectic solvent and its aqueous mixtures at $T=(298.15$ to $323.15)$ K and up to 50 MPa. *J Chem Thermodyn* 2012;54:293-301.
- 242.Shehata M, Unlu A, Sezerman U, Timucin E. Lipase and Water in a Deep Eutectic Solvent: Molecular Dynamics and Experimental Studies of the Effects of Water-In-Deep Eutectic Solvents on Lipase Stability. *J Phys Chem.* 2020;124(40):8801-10.
- 243.Stefanovic R, Ludwig M, Webber GB, Atkin R, Page AJ. Nanostructure, hydrogen bonding and rheology in choline chloride deep eutectic solvents as a function of the hydrogen bond donor. *PCCP.* 2017;19(4):3297-306.
- 244.Gapsys V, de Groot BL. On the importance of statistics in molecular simulations for thermodynamics, kinetics and simulation box size. *Elife.* 2020;9:e57589.

245. Rubin RW, Warren RW. Quantitation of microgram amounts of protein in SDS-mercaptoethanol-Tris electrophoresis sample buffer. *Anal Biochem.* 1977;83(2):773-7.
246. Winogradoff D, John S, Aksimentiev A. Protein unfolding by SDS: the microscopic mechanisms and the properties of the SDS-protein assembly. *Nanoscale.* 2020;12(9):5422-34.
247. Jafari M, Mehrnejad F, Rahimi F, Asghari SM. The molecular basis of the sodium dodecyl sulfate effect on human ubiquitin structure: a molecular dynamics simulation study. *Sci Rep.* 2018;8(1):1-15.
248. Nardini M, Lang DA, Liebeton K, Jaeger K-E, Dijkstra BW. Crystal structure of *Pseudomonas aeruginosa* lipase in the open conformation: the prototype for family I. 1 of bacterial lipases. *J Biol Chem.* 2000;275(40):31219-25.
249. Nick Pace C, Trevino S, Prabhakaran E, Martin Scholtz J. Protein structure, stability and solubility in water and other solvents. *Philos Trans R Soc Lond B Biol Sci.* 2004;359(1448):1225-35.
250. Harpaz Y, Gerstein M, Chothia C. Volume changes on protein folding. *Structure.* 1994;2(7):641-9.
251. Micaelo NM, Soares CM. Modeling hydration mechanisms of enzymes in nonpolar and polar organic solvents. *FEBS J.* 2007;274(9):2424-36.
252. Sasso F, Kulschewski T, Secundo F, Lotti M, Pleiss J. The effect of thermodynamic properties of solvent mixtures explains the difference between methanol and ethanol in *C. antarctica* lipase B catalyzed alcoholysis. *J Biotechnol.* 2015;214:1-8.
253. Wedberg R, Abildskov J, Peters GnH. Protein dynamics in organic media at varying water activity studied by molecular dynamics simulation. *J Phys Chem.* 2012;116(8):2575-85.
254. Ortiz C, Ferreira ML, Barbosa O, dos Santos JC, Rodrigues RC, Berenguer-Murcia Á, et al. Novozym 435: the “perfect” lipase immobilized biocatalyst? *Catal Sci Technol.* 2019;9(10):2380-420.
255. Arpigny JL, JAEGER K-E. Bacterial lipolytic enzymes: classification and properties. *Biochem J.* 1999;343(1):177-83.
256. Brzozowski A, Derewenda U, Derewenda Z, Dodson G, Lawson D, Turkenburg J, et al. A model for interfacial activation in lipases from the structure of a fungal lipase-inhibitor complex. *Nature.* 1991;351(6326):491-4.
257. Tyndall JD, Sinchaikul S, Fothergill-Gilmore LA, Taylor P, Walkinshaw MD. Crystal structure of a thermostable lipase from *Bacillus stearothermophilus* P1. *J Mol Biol.* 2002;323(5):859-69.
258. Eom GT, Lee SH, Song BK, Chung K-W, Kim Y-W, Song JK. High-level extracellular production and characterization of *Candida antarctica* lipase B in *Pichia pastoris*. *J Biosci Bioeng.* 2013;116(2):165-70.
259. Matsumura H, Yamamoto T, Leow TC, Mori T, Salleh AB, Basri M, et al. Novel cation- π interaction revealed by crystal structure of thermoalkalophilic lipase. *Proteins.* 2008;70(2):592-8.
260. Krieger E, Koraimann G, Vriend G. Increasing the precision of comparative models with YASARA NOVA—a self-parameterizing force field. *Proteins: Struct, Funct, Bioinf.* 2002;47(3):393-402.
261. Krieger E, Darden T, Nabuurs SB, Finkelstein A, Vriend G. Making optimal use of empirical energy functions: force-field parameterization in crystal space. *Proteins: Struct, Funct, Bioinf.* 2004;57(4):678-83.

262. Duan Y, Wu C, Chowdhury S, Lee MC, Xiong G, Zhang W, et al. A point-charge force field for molecular mechanics simulations of proteins based on condensed-phase quantum mechanical calculations. *J Comput Chem*. 2003;24(16):1999-2012.
263. Reynolds JA, Tanford C. Binding of dodecyl sulfate to proteins at high binding ratios. Possible implications for the state of proteins in biological membranes. *Proc Nat Acad Sci*. 1970;66(3):1002-7.
264. Jones MN, Wilkinson A. The interaction between β -lactoglobulin and sodium n-dodecyl sulphate. *Biochem J*. 1976;153(3):713-8.
265. Chen S-H, Teixeira J. Structure and fractal dimension of protein-detergent complexes. *Phys Rev Lett*. 1986;57(20):2583.
266. Guo X, Zhao N, Chen S, Teixeira J. Small-angle neutron scattering study of the structure of protein/detergent complexes. *Biopolymers*. 1990;29(2):335-46.
267. Rasmussen HØ, Enghild JJ, Otzen DE, Pedersen JS. Unfolding and partial refolding of a cellulase from the SDS-denatured state: From β -sheet to α -helix and back. *Biochim Biophys Acta, Gen Subj*. 2020;1864(1):129434.
268. Parker W, Song P-S. Protein structures in SDS micelle-protein complexes. *Biophys J*. 1992;61(5):1435-9.
269. Das TK, Mazumdar S, Mitra S. Characterization of a partially unfolded structure of cytochrome c induced by sodium dodecyl sulphate and the kinetics of its refolding. *Eur J Biochem*. 1998;254(3):662-70.
270. Gelamo E, Silva C, Imasato H, Tabak M. Interaction of bovine (BSA) and human (HSA) serum albumins with ionic surfactants: spectroscopy and modelling. *Biochim Biophys Acta, Protein Struct Mol Enzymol*. 2002;1594(1):84-99.
271. Reynolds JA, Tanford C. The gross conformation of protein-sodium dodecyl sulfate complexes. *J Biol Chem*. 1970;245(19):5161-5.
272. Saha D, Ray D, Kohlbrecher J, Aswal VK. Unfolding and refolding of protein by a combination of ionic and nonionic surfactants. *ACS omega*. 2018;3(7):8260-70.
273. Braun R, Engelman DM, Schulten K. Molecular dynamics simulations of micelle formation around dimeric glycoporphin A transmembrane helices. *Biophys J*. 2004;87(2):754-63.
274. Krishnamani V, Lanyi JK. Molecular dynamics simulation of the unfolding of individual bacteriorhodopsin helices in sodium dodecyl sulfate micelles. *Biochemistry*. 2012;51(6):1061-9.
275. Dominguez H. Interaction of the interleukin 8 protein with a sodium dodecyl sulfate micelle: A computer simulation study. *J Mol Model*. 2017;23(7):1-7.
276. Roussel G, Caudano Y, Matagne A, Sansom MS, Perpète EA, Michaux C. Peptide-surfactant interactions: A combined spectroscopic and molecular dynamics simulation approach. *Spectrochim Acta, Part A*. 2018;190:464-70.

8 CURRICULUM VITAE

